CALIFORNIA INSTITUTE OF TECHNOLOGY

EARTHQUAKE ENGINEERING RESEARCH LABORATORY
Center for Research on the Prevention of Natural Disasters

RESEARCH PAPERS SUBMITTED TO FIFTH WORLD CONFERENCE ON EARTHQUAKE ENGINEERING ROME, ITALY 25-29 JUNE 1973

EERL 73-02

A Report on Research Conducted under Grants
from the National Science Foundation and
the Earthquake Research Affiliates Program
at the California Institute of Technology

Pasadena, California
March, 1973

CALIFORNIA INSTITUTE OF TECHNOLOGY

EARTHQUAKE ENGINEERING RESEARCH LABORATORY

RESEARCH PAPERS
SUBMITTED TO
FIFTH WORLD CONFERENCE ON
EARTHQUAKE ENGINEERING
ROME, ITALY 25-29 JUNE 1973

Report No. EERL 73-02

A Report on Research Conducted under Grants
from the National Science Foundation and
the Earthquake Research Affiliates Program
at the California Institute of Technology

Pasadena, California

March, 1973

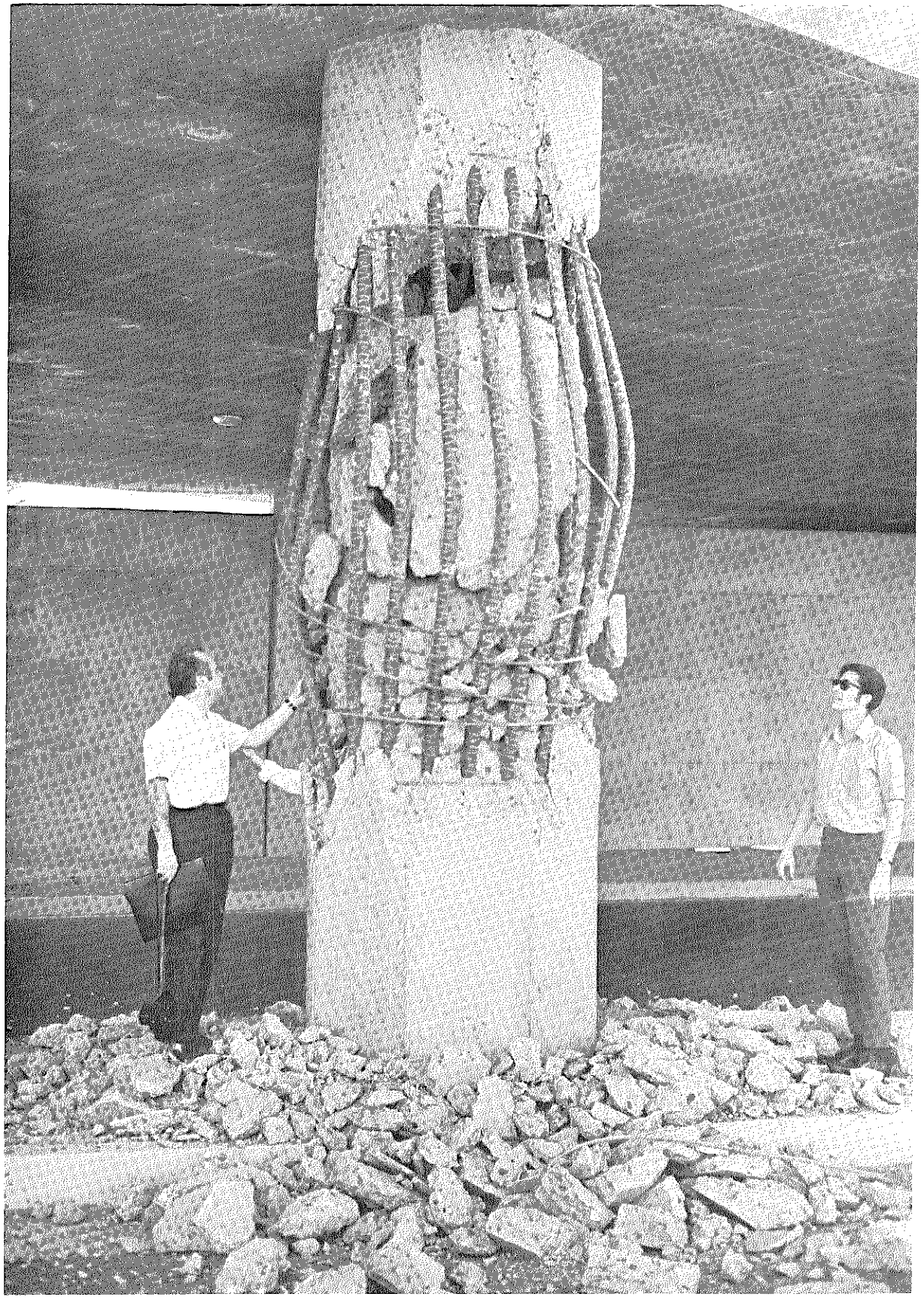

Frontispiece — Damage to concrete column of freeway overpass bridge during the San Fernando, California earthquake of 9 February 1971.
(see paper "The San Fernando, California Earthquake of 9 February 1971.")

TABLE OF CONTENTS

		Page
1.	Problems in Seismic Zoning, by G. W. Housner and P. C. Jennings	1
2.	Local Distribution of Strong Earthquake Ground Motions, by D. E. Hudson and F. E. Udwadia	11
3.	Standard Data Processing of Strong-Motion Accelerograms, by A. G. Brady and D. E. Hudson.	21
4.	Recent Developments in Data Processing and Accuracy Evaluations of Strong-Motion Acceleration Measurements, by M. D. Trifunac, F. E. Udwadia and A. G. Brady.	25
5.	A Model for the Dynamic Analysis of Deteriorating Structures, by W. D. Iwan.	35
6.	Earthquake-Induced Earth Pressures on Retaining Walls, by R. F. Scott.	45
7.	Ambient Vibration Tests of Full-Scale Structures, by F. E. Udwadia and M. D. Trifunac.	55
8.	Characterization of Response Spectra by Parameters Governing the Gross Nature of Earthquake Source Mechanisms, by M. D. Trifunac.	65
9.	Computation of Individual Fourier Spectrum Ordinates, by P. C. Jennings.	69
10.	The Role of Earthquake Ground Motions in Earthquake Engineering, by G. W. Housner.	73
11.	The San Fernando, California, Earthquake of February 9, 1971, by P. C. Jennings and G. W. Housner	83

*

*

FOREWORD

The papers in this report were prepared for presentation at the Fifth World Conference on Earthquake Engineering (5WCEE) and will, in due course, appear in the Proceedings of that conference. Because of requests for copies of the papers, they have been printed in this Caltech report form.

PROBLEMS IN SEISMIC ZONING

by

G. W. Housner[I] and P. C. Jennings[II]

SYNOPSIS

The paper analyzes the problems of seismic zoning for engineering design and makes recommendations for future practice. The degree of data and judgment that are present in seismic zoning maps of different types is reviewed and the characteristics of the different forms of data are examined. A brief section is devoted to an assessment of micro-zoning and the theoretical calculation of surface motions.

It is concluded that a good seismic zoning map for engineering use should be simple, with broad zones, and should not be overly dependent on individual past earthquakes. In the writers' judgment, seismic zoning maps specifying design criteria should be drawn by knowledgeable engineers in each particular field, using more general scientific maps for data and guidance. It is concluded also that microzoning and the theoretical calculation of surface motions are not yet reliable methods for determining ground motions for design calculations; it is more appropriate to determine such motions by direct extrapolation from comparable recorded accelerograms.

INTRODUCTION

A seismic zoning map for engineering use is a map that specifies the levels of forces or motions for earthquake-resistant design, and thus it differs from a seismicity map that provides information only about the occurrence of earthquakes. Seismic zoning maps are practical tools in earthquake-resistant design because they provide useful guidance when it is not feasible to make thorough studies of the earthquake hazard at particular locations. Such studies can, in general, only be justified for large projects such as major dams, nuclear power plants, etc. It must be realized, however, that the forces specified by a seismic zoning map are only a part of the overall earthquake-resistant design procedure; to assess the true level of earthquake resistance implied by a design technique it is necessary to know the allowable stresses, strains, deflections, damping, ductility, etc., used in the design process.

The construction of seismic zoning maps is made difficult by the lack of adequate data, by the conflict between the needs for safety and economy, and by a lack of knowledge of the occurrence of earthquakes and the detailed character of potentially damaging earthquake motions. This lack of

[I] Professor of Civil Engineering and Applied Mechanics, California Institute of Technology, Pasadena, California.

[II] Professor of Applied Mechanics, California Institute of Technology, Pasadena, California.

important knowledge is, of course, one of the major reasons for having seismic zoning maps, as it is unreasonable under these conditions to expect engineers specializing in design to make judgments about the earthquake hazards of a particular site. It is better for experts to apply the required judgment by making zoning maps. A map representing the compilation of the best available data and judgment of knowledgeable geologists, seismologists, earthquake engineers and design engineers is a practical necessity.

The undertaking of individual assessments of earthquake hazards at particular sites is an alternative to the use of a zoning map which is logically attractive and which has been used, for example, in California for determining recommended design forces for school buildings. Such investigations are not as thorough as those required for a nuclear power plant or a major dam and the results tend to be markedly inconsistent because of the combination of lack of basic data and different viewpoints and backgrounds of those making the assessments. A seismic zoning ma that is based on all available information and which considers consistent the various features for a particular application would be better for the public as well as the design engineer.

The first seismic zoning map used in the United States was compile by the U. S. Coast and Geodetic Survey in 1948 (1), revised in 1949 (2), (reflecting the 1949 earthquake near Olympia, Washington, and downgrad the region near Charleston, South Carolina from Zone 3 to Zone 2), and officially withdrawn in 1952 (3). The 1949 map, shown in Figure 1, was adopted, however, into the Uniform Building Code in 1949 and was retained there until 1970 (4), when it was replaced by the revised "Seismic Risk Map" developed by ESSA/Coast and Geodetic Survey in 1969 (5), shown in Figure 2. The maps now used by the Uniform Building Code (UBC) of the United States and the National Building Code of Canada are shown together in Figure 3. The maps are for the same purpose, but have been prepared by different groups. The maps are thought to be fair examples of the state of seismic zoning. Although the maps match at their common boundary in broad features, it is clear that seismic zoning, particularly in areas of moderate to low seismicity, is not yet a precise science.

The methods used to prepare both of the maps in Figure 3 are explained in papers published in the Proceedings of the 4WCEE. They are constructed on different principles, for example, the frequency of occurrence of earthquakes was not included as a factor in preparing the map adopted by the UBC, even though this is a very important factor for engineering purposes.

TYPES OF SEISMIC ZONING MAPS

A wide variety of seismicity maps, seismic zoning maps, etc., hav been prepared, depending on whether the purpose of the map is to prese basic data, to present data augmented by judgment, or to specify criter for design; and it is important to distinguish among these different maps

Within the last category there can be major differences depending on the application for which a map was prepared, as well as on the relative emphasis given to economy and safety. These maps can be categorized by the extent to which they portray a mixture of data and judgment.

Seismicity Maps. The simplest seismicity map is a plot of magnitude-rated epicenters of historical earthquakes and judgment enters only to the extent of interpreting the pre-instrumental history of the region, if included. Epicentral locations alone can be quite misleading, for they do not give information on the areal extent of strong shaking for large earthquakes. Because of this, seismicity maps are sometimes drawn on the basis of the Modified Mercalli Intensity Scale, or similar scales. Although such maps give a better indication of the areal effects of strong shaking, the interpretation of the intensity scales is highly judgmental, and maps based on intensities contain a much higher ratio of judgment to data than maps of epicenters. For regions in which the recorded seismic data is scanty, the Modified Mercalli "epicentral intensity" is often used in place of magnitude to rate epicenters plotted on a map, and such maps reflect the imprecision associated with the epicentral intensities, which may be very great.

If data were available adequate to define the frequency of occurrence vs. magnitude of earthquakes over a region, an earthquake probability map could be constructed. In most parts of the world, data is insufficient for this purpose, and much estimation must be employed.

An alternate method of presenting seismicity data that is sometimes used is to plot the distribution of strain energy density associated with historical earthquakes, resulting, for example, in a contour map of cumulative strain-energy density. The disadvantage of maps of this type from an engineering viewpoint, is that individual earthquakes are not identified, and the smooth variation of the contour plots may be misleading as to future ground shaking to be expected.

Fault Maps, Seismotectonic Maps and Seismic Probability Maps. Seismic fault maps are intended to show all faults on which movement has taken place within certain specified periods of time, e.g., in historic times or in the last 10,000 years. An example of a map of this type is shown for southern California in Figure 4(6). A great deal of judgment is involved in the preparation of such a map, even for historic earthquakes in readily accessible locations. Differences of professional opinion arise over the length of fault rupture, the differentiation of faulting from effects of slides, and over the inferred characteristics of subsurface faults. The difficulties are similar in the assessment of faults that have moved within recent geologic time, but the differences of professional judgment can arise over more major features and may revolve, for example, over whether a certain fault is active in the prescribed sense. Even if the fault is judged to be active, the probability of earthquakes of various magnitudes occurring on the fault can only be estimated imprecisely, so that the use of a fault map must be based on a very large measure of judgment.

We use the name "seismotectonic map" to describe a map which is essentially a fault map augmented by other geologic information, such as inferred tectonic processes, local geology, etc. There is a considerable

variety in the information that can be included in such maps and there is clearly a major component of judgment in the selection and presentation the material.

A seismic probability map is sometimes constructed from a fault m by assigning probabilities of occurrence of earthquakes of different mag tudes to each active fault, and assigning areal distributions of intensity earthquakes of different magnitudes. By this procedure a map is con- structed that shows a probability of intensity of shaking. Large compon of judgment and estimation are required to construct such a map.

Engineering Maps. The previously discussed maps present basic data c bined with professional seismological and geological judgment, and are erally not directly useful to the engineers,whose need is for quantitative guidance regarding seismic loads to be resisted within certain allowabl stresses, strains, etc. Maps prepared for engineering use can vary sig ficantly depending both upon the intended applications and the interests the individuals constructing the map. For example, a seismic zoning n for high-rise buildings might differ from one appropriate for short-per structures; a seismic zoning map for nuclear power plants might differ from one for single-family dwellings; and a map for use in southern Ca fornia might logically differ in character from a map for use in India. A the need for some equipment to be portable or the requirements of man facture may dictate a different type of seismic zoning map for special a plications. An example might be equipment for elevators, for which un formity of manufacture would suggest a single seismic zone for the enti western United States. An example of an engineering zoning map intenc for electrical equipment in southern California is shown in Figure 5 (6). different zones in the map are keyed to different levels of response spe and scaled accelerograms.

Dissimilarities in engineering zoning maps arising from differing i terests of the individuals preparing them are usually the result of comp mises between the requirements of economy and public safety. A map made solely from the viewpoint of public safety would be based on the strongest credible shaking, and the frequency of occurrence of the shak would not be a factor. On the other hand, a map zoned on the economics providing earthquake resistance vs. the cost of repair would be based o the probability of strong shaking, and no special design for earthquakes would be required in zones where the return period of potentially damag shaking was significantly longer than the average life of structures, reg less of the hazard to public safety should such shaking occur. It is easi recognized that most existing maps, including the U. S. map in Figure 3 a its predecessors, are compromises between these two extremes. In effe a seismic zoning map is usually a reflection of the fact that economic c siderations prevent the provision of the more complete protection other wise desirable.

The construction of a map for engineering use clearly requires maj input of judgment beyond that already embodied in the seismological an geological maps upon which they are based. We also note that factors o than technical matters have a legitimate place in the construction of sei zoning maps for engineering purposes. Jurisdictional boundaries which

affect the administration of the zoning map may suggest convenient locations of borders of zones that are ill-defined by technical information. In fact, the oddly shaped boundaries of the seismic zones in the map in Figure 1 were employed to emphasize the lack of precision in the data on which the map was based.

RELIABILITY OF THE BASIC DATA

The most important basic data for earthquake-resistant design are the strong-motion accelerograms recorded at many sites throughout the world. An eventual goal for seismic zoning would be a map keyed to collections of strong-motion records sufficient to define the seismic loading in each zone. Unfortunately, the data do not yet permit this, and this goal will not be reached for many years. The present collection of data is sufficient to produce samples of strong shaking from major earthquakes recorded under a variety of conditions, and is adequate for defining probabilities of occurrence for large areas such as California and Japan. There is not, however, enough data to define with precision the motion expected at a site or the frequency of occurrence of earthquakes in a small area, nor has the strong shaking been recorded in a great, Magnitude 8+ earthquake.

The data represented by historic accounts of earthquake damage and by seismological measurements are one step removed from the problem because it is necessary, lacking strong-motion data, to infer the strength and character of the shaking. In the case of seismological measurements it is necessary to use some relation between a seismological measure of the earthquake, such as Richter Magnitude, and engineering measures of the strength of shaking, such as spectrum intensity.

Although Intensity Scales, such as Modified Mercalli, are intended to measure the severity of shaking, they are not defined to do this effectively. The most serious weakness is a failure to separate effects on engineered structures from general effects on people, objects and nonengineered construction. The higher ratings of these scales are also well known to be overly sensitive to effects exhibited by soils which can occur under a wide range of severity of shaking. In the light of current information it appears that a given MM Intensity rating can be produced by shaking of various strengths and durations, and the Intensity ratings of a given earthquake cannot be accepted as indicative of the severity of shaking in an engineering sense without further examination.

Empirical relations between Richter Magnitude and the level of strong shaking are more reliable, but the most common of these, which relate Magnitude and epicentral distance to maximum acceleration, are known from comparisons with data to be very approximate. For example, it was observed in the San Fernando earthquake that the peak accelerations at locations equally distant varied by a factor of two(7). Furthermore, by definition, the Magnitude is the maximum response in the long-period range, measured at distances of a 100 km. or more, whereas the peak acceleration is in the short-period range and is measured at distances as short as a few kilometers. It is not surprising then, that these quantities cannot be precisely related by an empirical equation.

Use of evidence of faulting in geologically recent but prehistoric tim and other tectonic information, is another step further removed from the problem. Judgment is required to estimate the possible occurrence of earthquakes from such data and also to infer the Magnitude of potential quakes. These judgments are often stated as additions to the historic re in terms of Magnitudes or Intensities, thus reducing the engineering pro to that discussed above.

MICROZONING AND CALCULATIONS OF SURFACE MOTIONS

Several methods have recently been proposed to calculate surface m tions in earthquakes, given the occurrence of an earthquake of specified nitude on a specific fault. As shown in Figure 6, the main features from point of view of calculating surface motions are the nature of the source anism, the effect of the travel path geology upon the seismic waves, and effects of local site conditions on the surface motion. Some techniques b at the source, while others begin at the base of the local site, with bedro motion adjusted for the distance from the fault. When combined with a p abilistic estimate of the occurrence of earthquakes on the given fault, t becomes a form of seismic zoning, and such analyses have been used to estimate earthquake motions for the design of important facilities. If thi approach is carried to its logical conclusion by identifying all sources o motion over a large area, such as the State of California, and attaching p abilistic estimates to each source in a consistent manner, the results co be compared with the historic record to assess the accuracy of the proc This has not yet been done, and it is our feeling that most studies of thi type would, if done for a large area, result in probabilistic estimates fo strong shaking that are significantly higher than can be substantiated by historic seismicity.

Efforts to calculate surface motions by beginning somewhere in the source–travel path–site effects chain are useful scientific studies that h as their goal the explanation of the nature of earthquake motions. Only surface motions have been measured in strong earthquakes, however, an therefore it is not yet possible to distinguish the effects of assumptions bout the different portions of the chain. The assumptions required are q severe and, in our opinion, can involve errors exceeding those attendant directly estimating the surface motion from extrapolation of recorded m tions. Furthermore, strong-motions records obtained at El Centro (8) i cate that for firm soils, local site effects are less important than effect of different source mechanisms and travel paths. Similarly, the motion measured in Pasadena during the San Fernando earthquake showed beha inconsistent with the usual results of calculation techniques (9). Such re sults, and the present lack of measured bedrock and source motions indi that these methods are over-simplified, and are not at this time capable reliably calculating the surface motion in most practical cases.

The use of microtremors and microseisms for seismic zoning is al valid topic for scientific research, but does not yet appear to be a reliab method of seismic zoning for purposes of engineering. The principal dif culties are the observed nonstationarity of the motions (8), the unknown character of the sources of the motions, and the lack of correlation with measured characteristics of strong ground shaking.

CONCLUSIONS AND RECOMMENDATIONS

Characteristics of a Good Map. A major feature of a good seismic zoning map is that it should not change substantially after the occurrence of an earthquake: this means that, if possible, the map should not be overly dependent on any one past earthquake. This is the weakness of maps formally derived from a history which is too short to establish the seismicity of the region under study. In a practical sense, the users of a seismic zoning map really want to know what earthquake ground shaking their structures will experience. Thus, it is unavoidable that the quality of a seismic zoning map is to a large degree dependent on how well it predicts the future occurrence of ground shaking.

Another major characteristic of a good seismic map is that it not be overly elaborate. In our opinion, it is a mistake to try to draw highly detailed maps or to put a lot of information on the map. Such refinements are not justified in view of the state of the basic data, and their presence forms a barrier to understanding by those who would use the map. A map intending to specify criteria for earthquake engineering design must do so unambiguously so the user will not have to make further judgments that are out of his area of competence. A map giving expected MM Intensities or a map showing expected maximum ground acceleration are examples of maps in a form not directly useful to the engineers.

A good seismic map for use in engineering design should be adapted to the particular needs and design practices of the users. Thus, it is to be expected that a seismic zoning map for tall buildings might differ in important details from one to be used for electrical transmission facilities. It is not good practice, in general, to adopt a map and associated design criteria that were developed for a particular application directly into a different application.

Ground Motions for Design. It is our judgment that the most appropriate way to select earthquake motions for purposes of design is to assemble a group of strong-motion records recorded under as comparable conditions as possible, and to extrapolate from these records, by simple scaling, the required motions. The records used can be augmented by artificial earthquake records if necessary. This simple approach seems best suited to the present state of knowledge, and makes clear to potential users the nature of the judgments involved. The more elaborate approaches that introduce additional approximations and estimations without providing any more basic data tend to obscure the distinction between information derived from reliable data and the results provided by approximate methods of calculation.

Construction of Seismic Zoning Maps. In agreement with other authors, it is our conclusion that a number of maps should be drawn with each group of workers preparing the type of map that is within its area of competence. For example, government agencies are the logical groups to prepare large-scale maps of seismicity, faulting, and other pertinent geologic features. Such maps would form the basic data for seismic zoning maps to be used to specify forces for design. It is important that maps specifying criteria for design be updated periodically. Such updating is required because of expected increases in the knowledge of earthquake effects, and because the earthquake protection

demanded by society changes with time, increasing directly with increa urbanization and industrialization.

In view of the state of knowledge in the various disciplines that cont bute to seismic zoning for engineering design, and the large judgmental factors involved, it appears to us that the only workable way to develop a seismic zoning map for the purpose of specifying criteria for design in a particular field is to convene a group of the most knowledgeable people i the field and have them construct the map. The group would have to revi first the scientific maps and data, with advice as needed, and assess to best judgment the degree of conservatism embodied in current design pr cedures. A seismic design map drawn by such a group should represent reasonable balance of the various factors that are important to the earth quake-resistant design problems of their segment of the engineering pro sion.

REFERENCES

1. Roberts, E. B., F. P. Ulrich, "Seismological Activities of the U. S. Coast & Geodetic Survey in 1948," BSSA, 40, 195-216, 1950.
2. Roberts, E. B. and F. P. Ulrich, "Seismological Activities of the U. Coast & Geodetic Survey in 1949, "BSSA, 41, 205-220, 1951.
3. Roberts, E. B. and F. P. Ulrich, "Seismological Activities of the U. Coast & Geodetic Survey in 1951," BSSA, 43, 3, 255-268, 1953.
4. International Conference of Building Officials, "Uniform Building C 1970 Edition, Volume I," Pasadena, Calif. 1970.
5. Algermissen, S. T., "Seismic Risk Studies in the United States," Proc. Fourth World Conf. on Earthquake Eng., Vol. I, Santiago, Chile, 1969.
6. Fugro, Inc., "Seismic Risk Analysis and Aseismic Design Manual," prepared for So. Calif. Edison Co., May, 1972.
7. Hudson, D. E. (Ed.), "Strong-Motion Instrumental Data on the San Fernando Earthquake of Feb. 9, 1971," Earthquake Eng. Researc Lab., Calif. Inst. of Tech., and Seismological Field Survey, NOAA.
8. Udwadia, F. E., "Investigations of Earthquake and Microtremor Ground Motions," Earthquake Eng. Research Lab. Report 72-02, Ca Inst. of Tech., Pasadena, Calif., Sept. 1972.
9. Hudson, D. E., "Local Distribution of Strong Earthquake Ground Motion," BSSA, 62, 6, Dec. 1972.

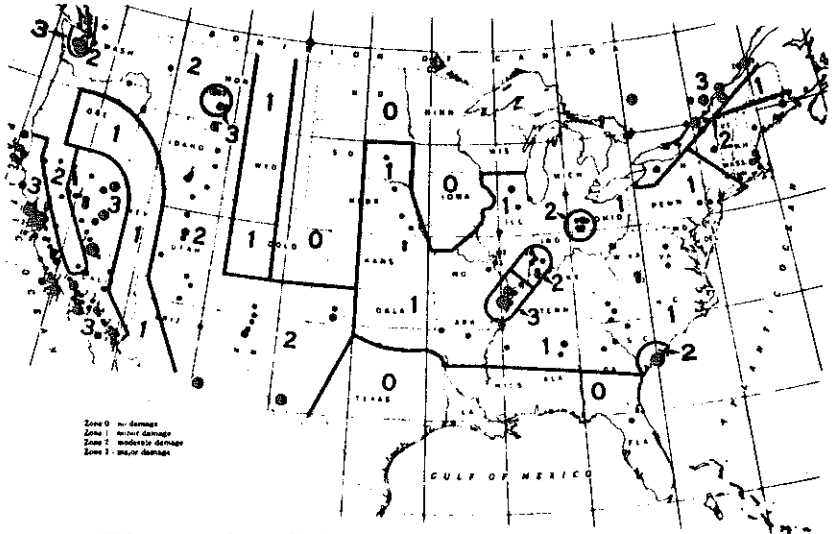

Figure 1. Seismic zoning map adopted by Uniform Building Code, 1949-1970 (2).

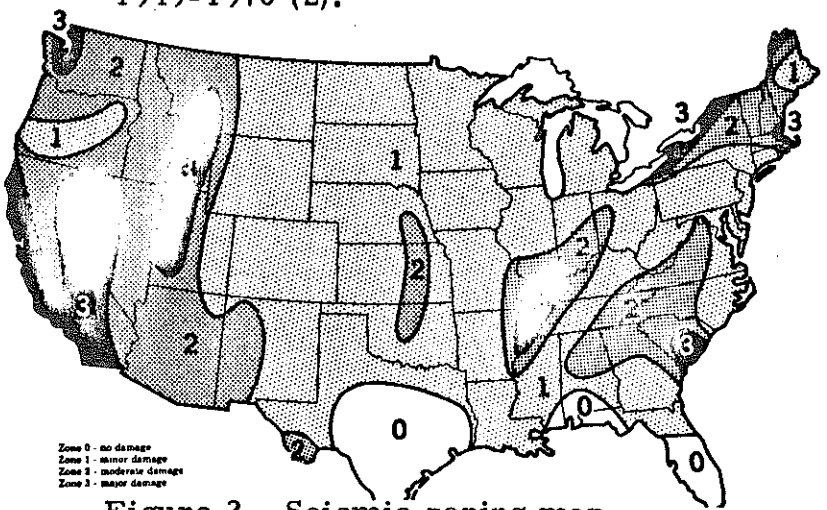

Figure 2. Seismic zoning map adopted by Uniform Building Code from 1970 to date (5).

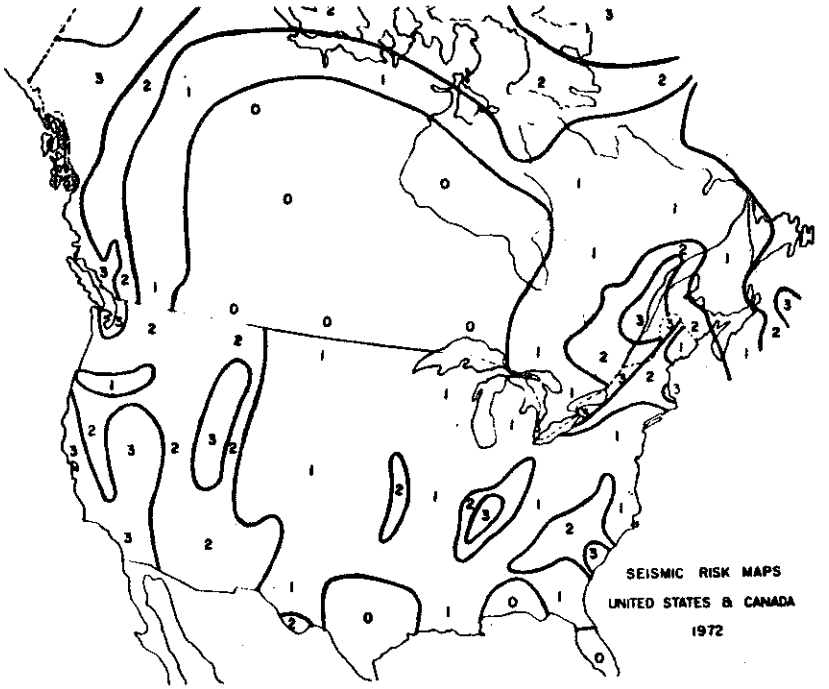

Figure 3. Comparison of seismic zoning maps now in use in building codes of Canada and U.S.

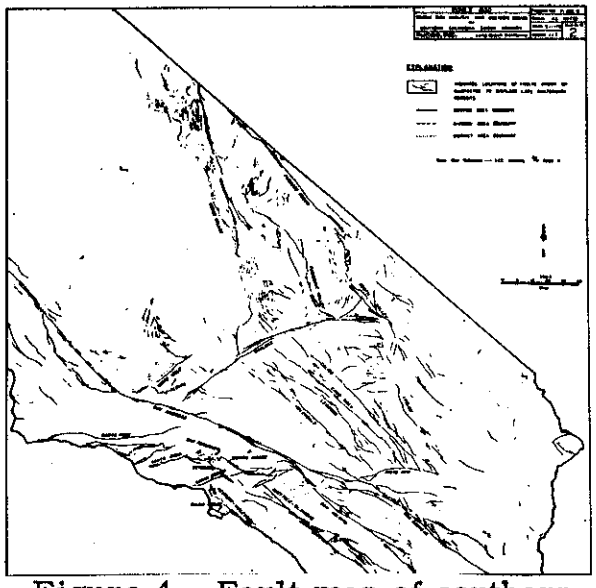

Figure 4. Fault map of southern California showing faults judged to be active within past 500,000 years (6).

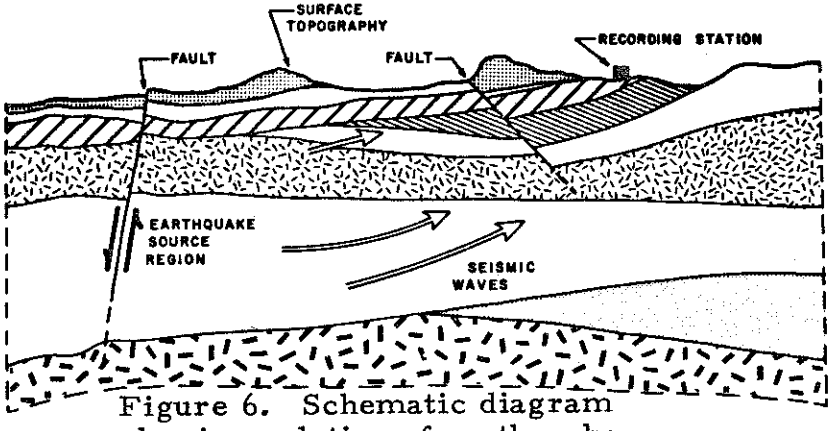

Figure 6. Schematic diagram showing relation of earthquake

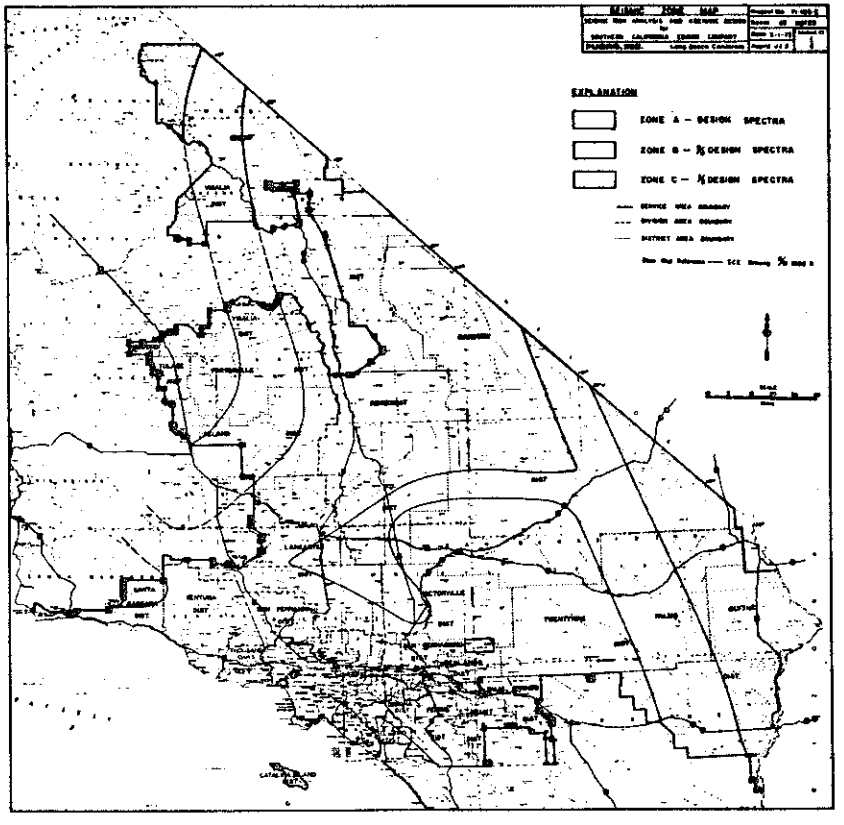

Figure 5. Seismic zoning map prepared by Fugro, Inc. for Southern California Edison Co. Intended use is for earthquake-resistant design of electrical equipment (6).

LOCAL DISTRIBUTION OF STRONG EARTHQUAKE GROUND MOTIONS

by

D. E. Hudson[I] and F. E. Udwadia[II]

SYNOPSIS

Factors influencing the ground motions at a particular site such as source mechanisms, propagation path characteristics, reflection, refraction, channeling and focusing of seismic waves, and details of local geological and soil conditions are discussed. Strong motion accelerograms from past earthquakes are analyzed to show the complexity of the problem, and it is demonstrated that no single dominating factor governs the local distribution patterns. By comparison of measured strong ground motions at selected sites, various factors can be individually studied, and in this way it is shown that local variations are largely governed by (a) source mechanisms; (b) propagation path; and (c) local geology. Considering the implications for seismic zoning, it is concluded that local site characteristics in themselves seldom offer a decisive justification for a reduced estimate of maximum ground shaking in a particular sub-zone.

INTRODUCTION

Most destructive earthquakes involve in a striking way wide variations in local destructive effects. Buildings may be heavily damaged in one small region, whereas nearby areas with apparently similar structures may escape with only minor failures. Some variations may of course be attributed to different actual resistances of the structures, and to local soil and foundation failures. In addition, however, there often seems to be a distinct pattern of local variation in the amplitude of the ground shaking itself. This is of course not surprising, in view of the enormous complexity of the whole system involving the generation of seismic waves by an extended source, and the propagation of the waves through a highly inhomogeneous anisotropic medium of complicated geometry to a site which in itself has many local irregularities.

The primary object of the present paper is to summarize the essential elements of the problem, and to illustrate, by reference to actual measurements of strong ground motion, the current state of knowledge. It is only recently that the number of measurements of strong ground shaking has become sufficiently large to clarify many aspects of the problem, and these experimental results are in turn pointing the way towards new research approaches.

[I]Professor of Mechanical Engineering and Applied Mechanics; Earthquake Engineering Research Laboratory, California Institute of Technology

[II]Research Fellow in Applied Science, Earthquake Engineering Research Laboratory, California Institute of Technology

A secondary objective is to review the implications of these local variations for the preparation of seismic risk maps. It is, of course, of great practical importance to correctly delineate regions likely to experience heavy shaking. It is clear, however, that without understanding in detail the reasons for the particular damage patterns found in past earthquakes it cannot be assumed that these same patterns will be characteristic of future earthquakes. Unless these patterns can be explained, it is also futile to attempt to predict them on the basis of measurements, such as of microtremors, at particular sites.

ELEMENTS OF THE PROBLEM

Figure 1 outlines a number of the major influences on measured surface ground motion. Assuming that the problems associated with instrumentation and data processing have been satisfactorily dealt with, the major influences may be grouped under (1) source mechanisms, (2) propagation path, and (3) local site condition. Each of these factors may be a dominant or an important item in the actual ground motion at a particular site.

If a sufficiently large number of accelerograms of strong earthquake ground motion were available for many earthquakes and for many different site conditions, comparative studies of the following kind could be made: (a) By choosing a number of different earthquakes originating near the same focal region and recorded at the same station, the effects of source mechanisms could be ascertained; (b) By recording one earthquake at many different sites, each having approximately the same local conditions, the effects of propagation paths could be studied; and (c) By comparing motions at nearby sites having differing local conditions, the effects of these local site conditions could be investigated. The existing body of strong motion accelerograms is unfortunately not large enough to completely resolve the above matters, but a careful study of existing records can certainly reveal some of the major aspects of the problem.

In the following sections, representative examples of comparisons based on measured ground accelerations will be presented by means of calculated Fourier Spectrum Curves[1]. These spectra have been computed for 40 second accelerogram time durations, using "corrected accelerograph data[2] digitized at 0.02 second intervals. The final spectrum curves have been smoothed with a triangular window having a base width of 0.4 Hz. It should be noted that this triangular window results in considerably more smoothing than the 1/4, 1/2, 1/4 running average smoothing adopted for the standard presentation of Fourier Spectra of earthquake accelerograms as given in reference (1). For the comparative purposes of the present paper, this extra smoothing is advantageous in emphasizing the major features of the frequency distribution, whereas for the standard curves it was desired to make a minimum interpretation of the basic data.

INFLUENCE OF SOURCE MECHANISM

A sequence of earthquakes recorded at El Centro, California, afford a good opportunity to illustrate the effects of source mechanisms[3]. A

that site, strong motion accelerograms have been obtained for some 15 earthquakes over the past 35 years. From seismological evidence, three of these earthquakes have been assigned the same focal location, with identical epicenters. Since propagation paths and local site conditions are identical for all three earthquakes, major differences in the spectra of ground motion would have to be attributed mainly to varying conditions at the generating source. Figure 2 shows the smoothed Fourier Spectra of these three strong motion accelerograms. It is clear that a pronounced influence of source mechanism does exist, since the spectra are in many respects significantly different. It is evident, for example, that the smaller events have relatively greater amounts of high frequency motion. It is also clear that there are few if any correlations of pronounced spectrum peaks.

LOCAL DISTRIBUTION PATTERNS

The many accelerograms recorded during the San Fernando earthquake of February 9, 1971 offer an unparalleled opportunity for the study of local distribution effects[4]. A general picture of the distribution of peak horizontal ground accelerations measured during this earthquake is given in Figure 3. Although these peak accelerations are far from being a complete description of the damaging potential of the ground shaking, in that they sample only the high-frequency end of the spectrum, they do reveal in a realistic way the complexity of the patterns. Some detailed studies of this distribution have indicated that no one factor can serve to fully explain the relative values. It has also become evident that the measured distribution of ground shaking does not in some areas agree with that previously determined on the basis of many smaller, more distant, earthquakes[5]. Some specific comparisons will now be chosen from this San Fernando data.

PROPAGATION PATH

The use of the San Fernando accelerograms to study propagation path effects is complicated by the difficulty of selecting sites with markedly different paths but with similar local site conditions, and by the fact that irregular propagating dislocations may have resulted in a radiation pattern which could account for some significant differences between particular points. In fact, for most of the strong motion sites in Southern California, little investigation of local site conditions has so far been made, and one must depend for the general picture on the area geological maps. Some approximations can be made, however, which will at least permit preliminary studies.

A comparison of the measurements at the sites Glendale (G) and Palmdale (P) will be of interest in this connection. These stations have very similar epicentral distances, G = 32 km, P = 33 km, but different azimuthal locations, G = N152° E, P = N52° E (Fig. 3). The sites are on opposites sides of the San Gabriel mountains. The Palmdale site is about 3 km north of the main trace of the San Andreas fault, on material described as "alluvium" on the California State Geological Map. The Glendale site is about 45 km south of the San Andreas on material described as "pleistocene non-marine" on the California State Geological Map and as "alluvium" on the geologic map of the Los Angeles Basin. Although the local geologic conditions cannot be described as identical,

they are perhaps as similar as may be found for any widely separated pairs of stations, given the complexity of the Los Angeles Basin geology.

From Figure 4, it can be seen that the Fourier Spectra of the groun accelerations at the G and P sites differ widely in many respects. It is of course easy to think of many reasons why these two spectra should differ. The surface topography along the travel path is markedly different, for example, not to mention the possibilities of many subsurface irregularities which no doubt also vary greatly between the two propagation paths.

LOCAL SITE CONDITIONS

The San Fernando accelerograms also permit studies of the effects of local site conditions. As a first example, Figure 5 compares spectra from two stations about 1/2 km apart at an epicentral distance of 37 km. The station marked ATH is in the basement of a 2-1/2 story reinforced concrete building, while the station marked ML is in the basement of a 9-story reinforced concrete building. Dynamic tests of the 9-story building and the adjacent site were made, and from a preliminary investigation of the result it seems likely that the basement acceleration record has not been significantly influenced by soil-structure interactions over the frequency range of interest. As far as can be ascertained, the local soil and geologic conditions are identical at the two sites. This can evidently serve as an example of the sensitivity of the ground motion to minor differences in system configuration. As far as can be determined, the propagation path and the local site conditions are indentical for the two stations and yet significant spectral differences exist.

The spectra of Figure 5 can be compared with those shown in Figure 6, which are for nearby stations. Station JPL has an epicentral distance of 29 km and is located on alluvium. Station SL, 6 km from JPL, has an epicentral distance of 34 km, and is located on a granitic rock. Although it is unlikely that there are major differences in the main features of the propagation path, the spectra do show significant differences which should perhaps be attributed to local site conditions. From the spectra, however, it would be difficult to decide which site is on the alluvium and which is on rock.

Another pair of stations of interest for comparative studies are the Lake Hughes No. 4 and No. 9 (Figure 3). Both of these stations are 29 km from the epicenter, and are 8 km apart on the same gneiss rock formation. The differences in these spectra shown in Figure 7 illustrat again the sensitivity of the surface measurements to small variations in propagation path or local conditions. The spectra of Figure 7 may also be compared with those of Figure 8, for the nearby Lake Hughes station No. 1 (31 km), 6 km from station 4 on the other side of the main trace c the San Andreas fault on granitic rock, and station No. 12 (25 km), 4 km from station No. 9 on Eocene-Paleocene marine materials. It is of special interest to note the relative absence of high-frequency components in the recorded motion at station No. 1, in spite of its location on granite. Perhaps the special characteristics of the deformed material

within the San Andreas fault zone have filtered the high-frequency signals

IMPLICATIONS FOR SEISMIC ZONING

From the historical records of earthquakes it is clear that seismic risk is far from being uniformly distributed over the earth, but is concentrated in reasonably well-defined areas. Seismic zoning involves the delineation of these risk areas, and an evaluation of the detail to which they can be divided into meaningful sub-zones from the standpoint of construction codes and regulations aimed at earthquake resistant structures. On a global basis there is an essential agreement on the approximate shape and size of three basic zones: (1) a relatively high risk area, in which provisions should be made to guard against earthquake disasters; (2) a moderate risk zone, in which damaging earthquakes may occur, but are likely to be so infrequent that economic losses can be absorbed by society with only minor protective measures; and (3) an aseismic region in which earthquakes are so rare that they can for practical purposes be ignored. The main problem for seismic zoning is the extent to which the high risk areas can be subdivided into micro-zones of lower risk. The strong motion acceleration measurements and analysis of the type discussed above suggest that a good deal of caution should be used in making such zoning judgments. There have been so many damaging ground motions measured on so many different kinds of sites, and the patterns of variation are so complicated, that the assumption that equally high amplitudes of motion could occur anywhere within the high risk zone must be seriously considered. There is no assurance that the patterns measured for one earthquake will be repeated for other earthquakes at other epicentral locations, or even at the same location. Similarly, there is no assurance that the patterns of local variation are the same for destructive earthquakes and for small, distant earthquakes, or for microtremor ground motions. In the present state of the art it is difficult to see how it would be possible to assign significantly lower risks to certain sub-regions as far as the expected level of ground shaking is concerned. On the basis of surface exploration, however, it should be possible to identify certain regions as having a higher than zone average risk for landslides, subsidences, and other potential foundation problems, in the sense that such areas might be especially vulnerable to ground shaking levels that might not adversely affect adjacent areas. It is in this direction that meaningful progress in seismic zoning must be sought for the immediate future.

BIBLIOGRAPHY

(1) Hudson, D.E., Trifunac, M.D., Udwadia, F.E., Vijayaraghavan, A. and A.G. Brady, "Analyses of Strong Motion Accelerograms, Vol. IV - Fourier Amplitude Spectra, Part A." Report EERL 72-100, Earthquake Engineering Research Laboratory, California Institute of Technology, Pasadena, 1972.

(2) Hudson, D.E., Brady, A.G., Trifunac, M.D., and A. Vijayaragha van, "Strong Motion Earthquake Accelerograms, Vol. II - Correcte Data and Integrated Ground Velocity and Displacement Curves, Part A." Report EERL 71-50, Earthquake Engineering Research Laboratory, California Institute of Technology, Pasadena, 1971. Basic data for the San Fernando sites analyzed in the present paper are in Vol. II, Parts F, G, and J.

(3) Udwadia, F.E., Investigation of Earthquake and Microtremor Ground Motions, Report EERL 72-02, Earthquake Engineering Research Laboratory, California Institute of Technology, Pasadena 1972.

(4) Hudson, D.E. (ed.), Strong Motion Instrumental Data on the San Fernando Earthquake of Feb. 9, 1971, Earthquake Engineering Research Laboratory, California Institute of Technology, and the Seismological Field Survey, National Oceanic and Atmospheric Administration, Pasadena, 1971.

(5) Hudson, D.E., "Local Distributions of Strong Earthquake Ground Shaking," Bull. Seism. Soc. Amer., vol. 62, no. 6, December, 1972.

FIGURE 1

CHARACTERISTICS OF MEASURED STRONG GROUND MOTION

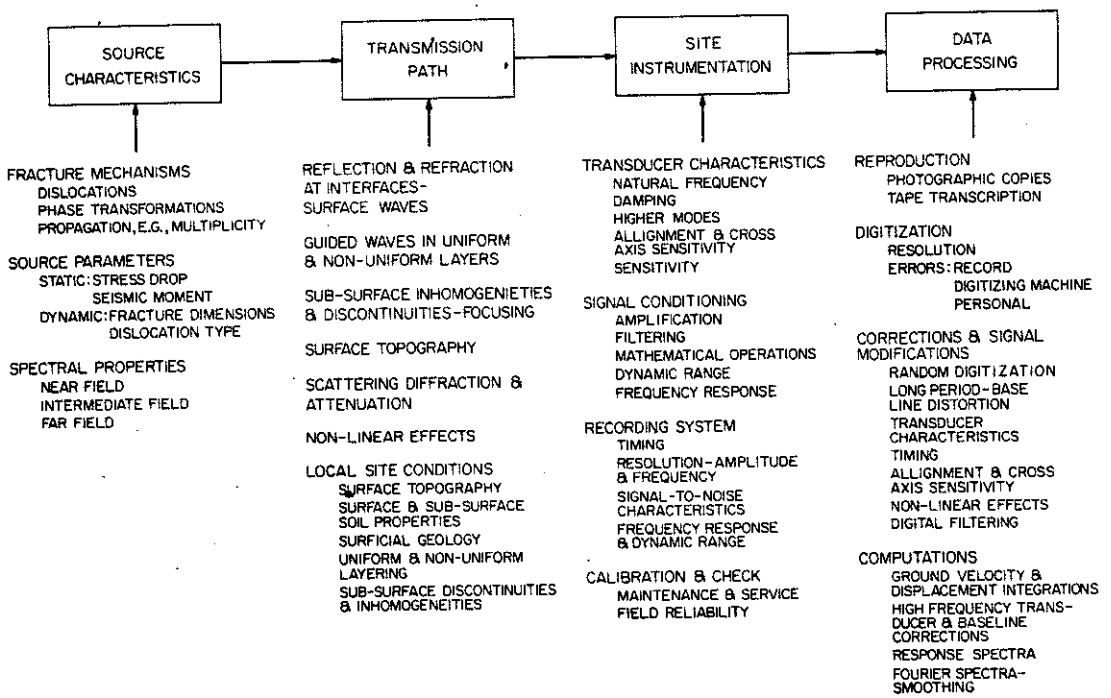

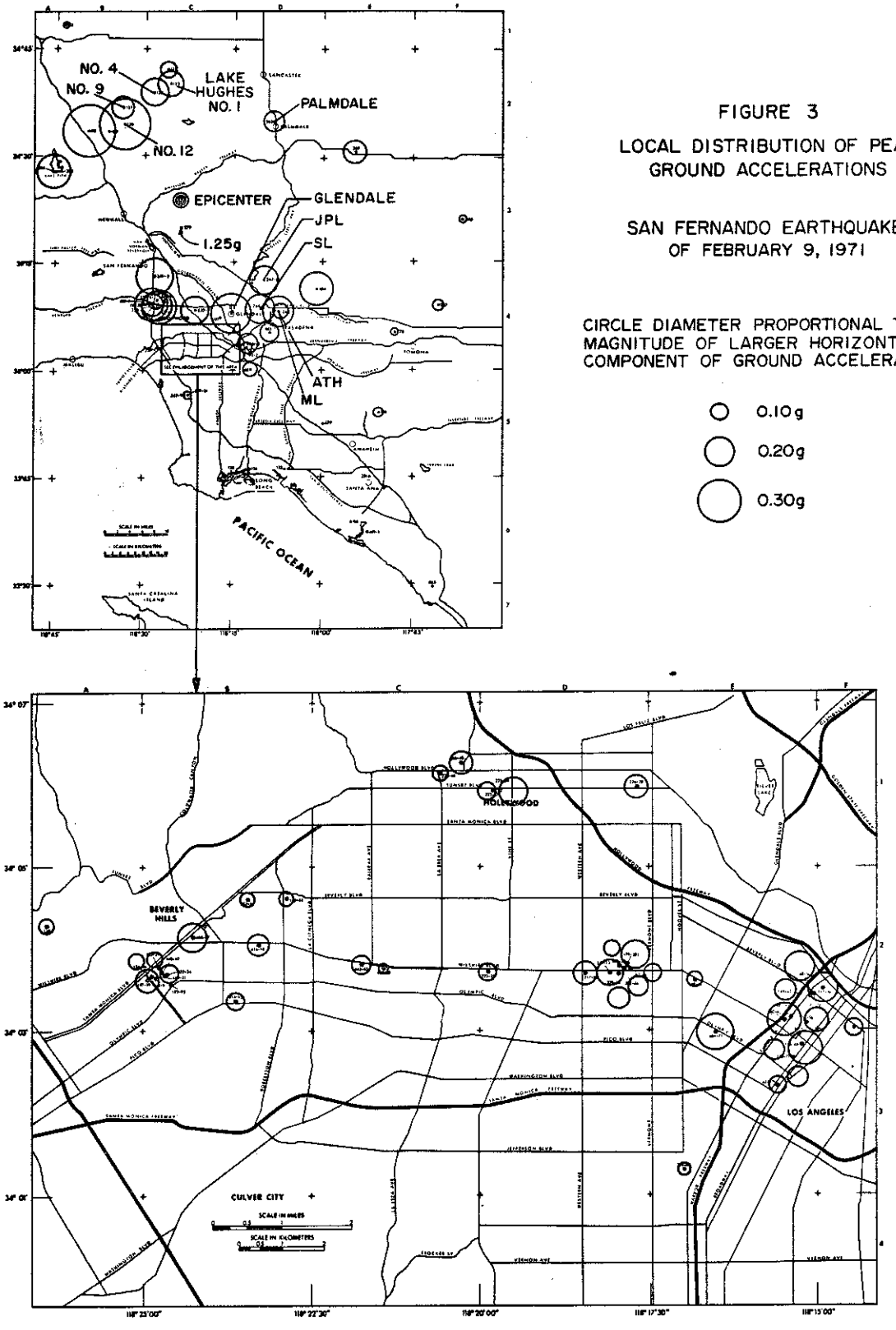

FIGURE 3

LOCAL DISTRIBUTION OF PEAK GROUND ACCELERATIONS

SAN FERNANDO EARTHQUAKE OF FEBRUARY 9, 1971

CIRCLE DIAMETER PROPORTIONAL TO MAGNITUDE OF LARGER HORIZONTAL COMPONENT OF GROUND ACCELERATION

○ 0.10g

○ 0.20g

○ 0.30g

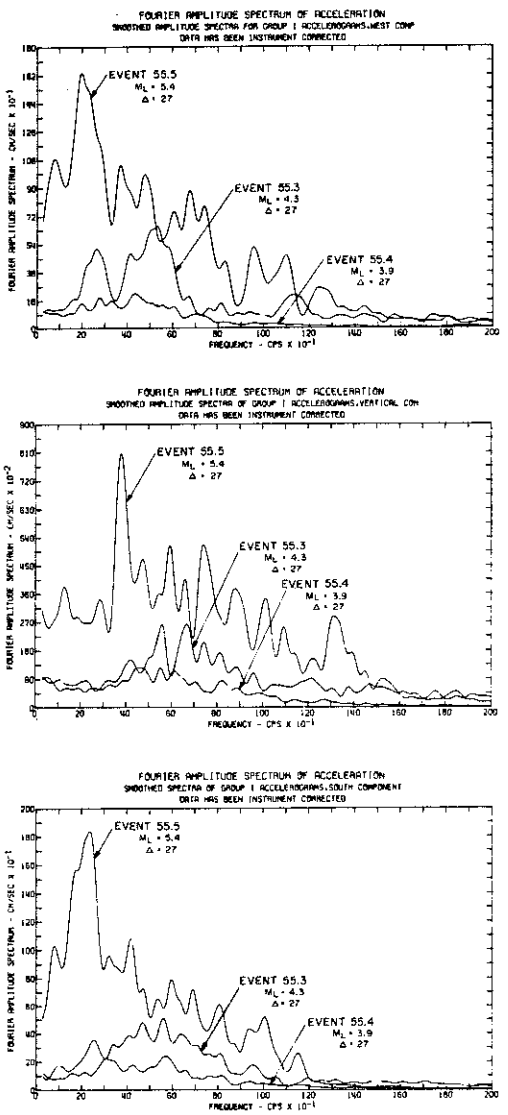

FIGURE 2

CALCULATED FROM ACCELEROGRAMS FROM THE EL CENTRO, CALIFORNIA, STRONG MOTION STATION EVENTS OF DECEMBER 16, 1955

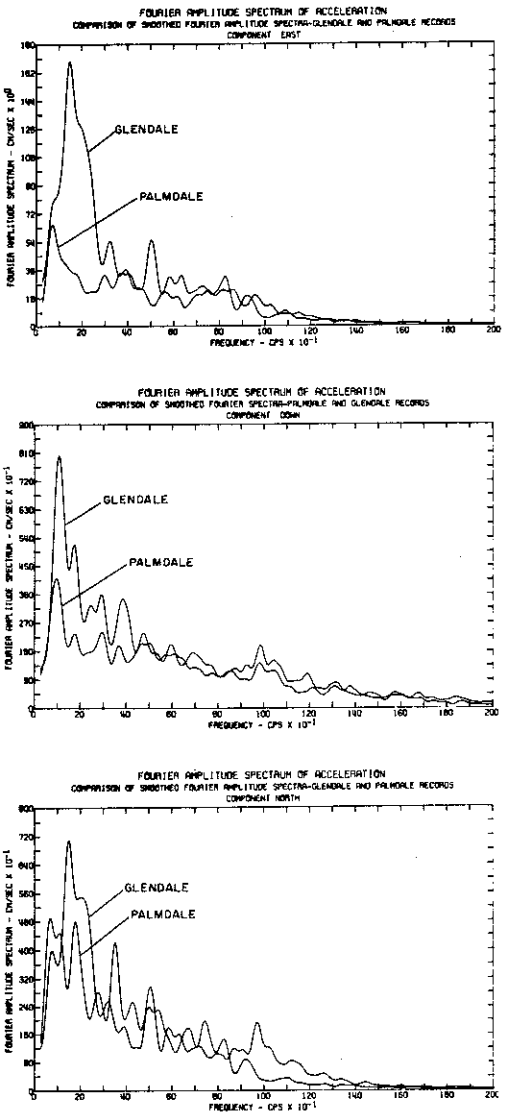

FIGURE 4

CALCULATED FROM ACCELEROGRAMS OF THE SAN FERNANDO EARTHQUAKE OF FEBRUARY 9, 1971

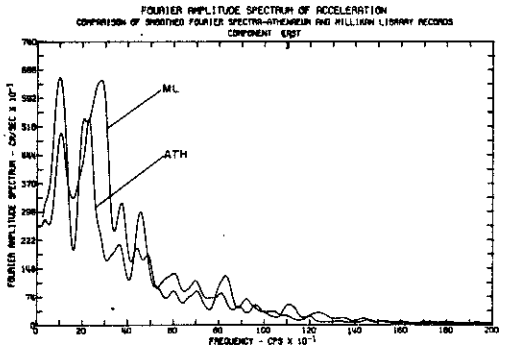

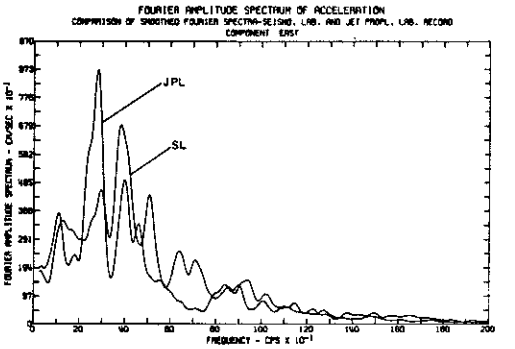

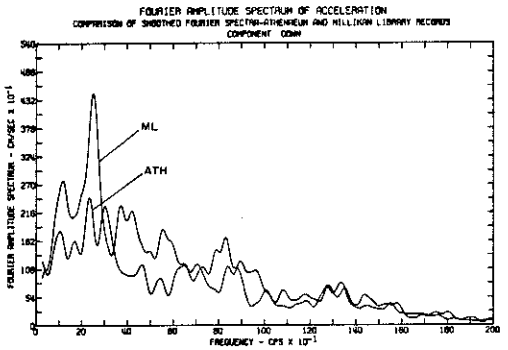

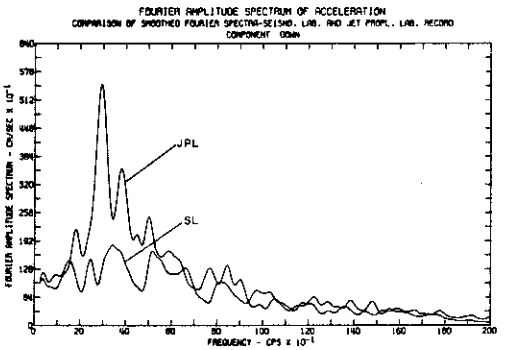

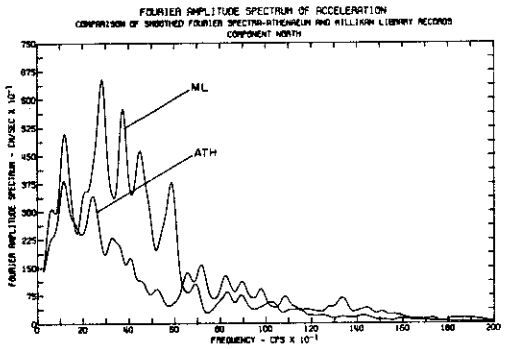

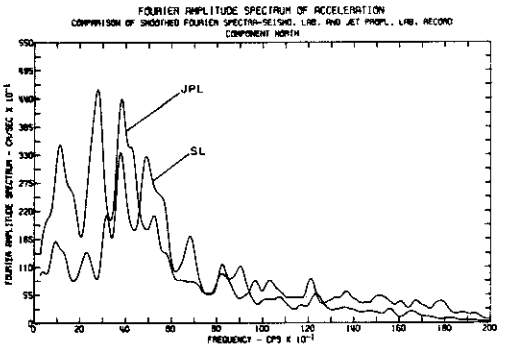

FIGURE 5
CALCULATED FROM ACCELEROGRAMS OF
THE SAN FERNANDO EARTHQUAKE OF
FEBRUARY 9, 1971

FIGURE 6
CALCULATED FROM ACCELEROGRAMS OF
THE SAN FERNANDO EARTHQUAKE OF
FEBRUARY 9, 1971

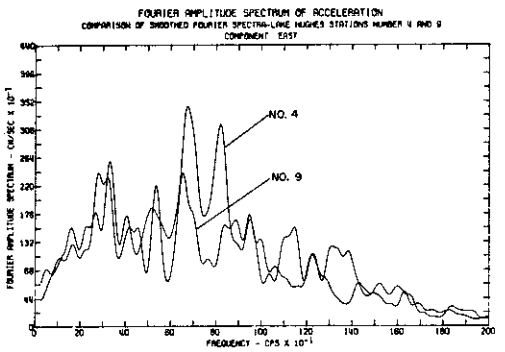

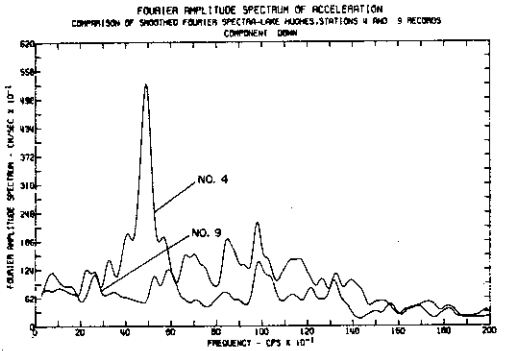

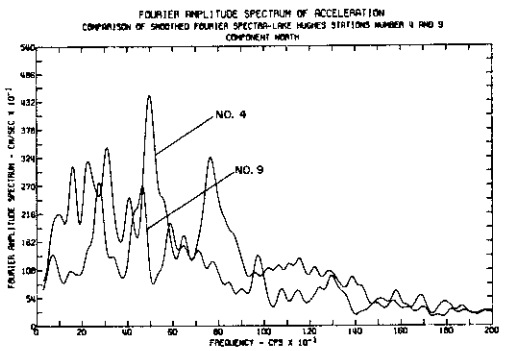

FIGURE 7
CALCULATED FROM ACCELEROGRAMS OF
THE SAN FERNANDO EARTHQUAKE OF
FEBRUARY 9, 1971

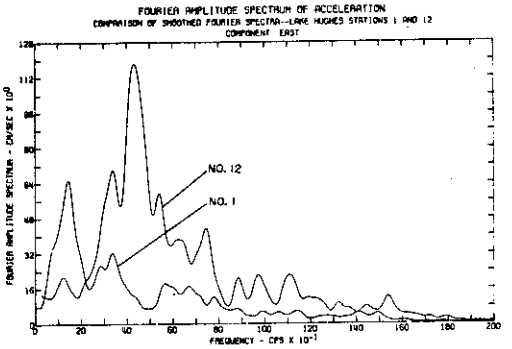

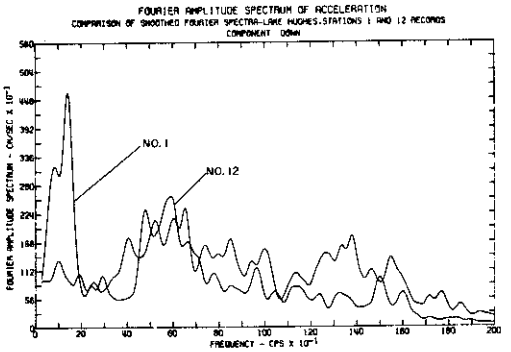

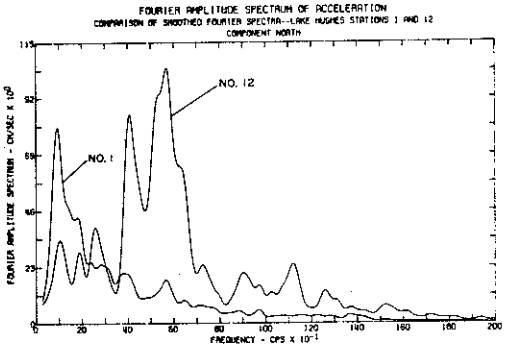

FIGURE 8
CALCULATED FROM ACCELEROGRAMS OF
THE SAN FERNANDO EARTHQUAKE OF
FEBRUARY 9, 1971

STANDARD DATA PROCESSING OF STRONG MOTION ACCELEROGRAMS

by

A. G. Brady[I] and D. E. Hudson[II]

SYNOPSIS

A collection of some 500 strong motion accelerograms now exists for United States earthquakes, about one-half of which were obtained during the 1971 San Fernando earthquake. These records have all been digitized by a uniform technique, and the digitized data are available in the form of printouts, punched card decks, and digital magnetic tapes. Corrected digitized data involving high frequency transducer corrections and long-period baseline adjustments are also available, as are calculated velocity and displacement curves, response spectrum curves and Fourier spectra. Information on how to obtain the available results is given.

INTRODUCTION

The basic instrument for strong motion seismology is the strong motion accelerograph which records three components of ground acceleration versus time. As presently designed, these instruments record accelerations up to 1 g with a resolution of the order of 0.001 g over a frequency range of 0.06 Hz to 25 Hz. The devices are triggered by the earthquake itself, using a vertical electrodynamic starter having a flat acceleration response over 1 to 10 Hz which can be set to various triggering levels of the order of 0.005 g. Accelerographs of this kind were first installed in California in 1933, and the Long Beach earthquake of that year provided the first strong motion accelerograms. Under the direction of the Seismological Field Survey of the National Oceanic and Atmospheric Administration, the U. S. Network steadily developed and at the present time consists of approximately 1000 instruments. This development was paralleled by a similar network in Japan, which now also has approximately 1000 recording accelerographs. Smaller numbers have been introduced into other parts of the world, the present distribution being roughly Italy 120, Yugoslavia 100, New Zealand 80, Mexico 40, Canada 30, with an additional 20 countries having one or several accelerographs.

DATA PROCESSING

The purposes to which the information in the accelerograms are to be put establish the basic data handling procedures. These procedures include: (a) approximate scaling of peak acceleration, duration of strong ground motion, and predominant periods; (b) integration to determine

---

[I]Senior Research Fellow, Earthquake Engineering Research Laboratory, California Institute of Technology

[II]Professor of Mechanical Engineering and Applied Mechanics; Earthquake Engineering Research Laboratory, California Institute of Technology

ground velocities and displacements; (c) frequency analysis by means of Fourier spectra, response spectra, autocorrelation curves, power spectral density, etc.; (d) use as input functions for structural response calculations. For (a), only a hand scaling of the record is required, with no special correction techniques. For (b), (c) and (d), an accurate digitization of the analog traces to preserve information over the maximum frequency range is required. In view of the accuracy with which digital computers can reproduce results, it is highly advantageous if all investigators can begin their studies with the same digitized data. Differences in final results can then be confidently attributed to different computational techniques or to different mathematical models. This has been the motivation for the program of standard digitization and data processing of strong motion accelerograms which was started some five years ago at the Earthquake Engineering Research Laboratory of the California Institute of Technology under the sponsorship of the National Science Foundation.

The first stage in this program was the development of standardized digitization processes which would produce digitized data on a routine basis at a known level of accuracy. This involved for a particular semi-automatic digitizing system (a) training and cross-checking of machine operators to establish levels of personal error in setting a cross-hair on the accelerogram trace; (b) ascertaining various sources of error in the digitization equipment itself, and the development of suitable corrections; and (c) the evolution of standardized formats for the presentation of the digitized data in the form of digital printouts, punched card decks, and digital magnetic tapes. The aim of this first stage is to present the basic information in the accelerogram trace in as direct a form as possible with a minimum of interpretation or correction (1, 2, 6).

The second stage of the program introduces certain correction techniques with the object of recovering information at a known level of accuracy over the widest possible frequency band permitted by the overall instrumentation system. This involves: (a) high frequency digital filtering to reduce digitization noise (3, 5), (b) transducer corrections to account for drop-off of output at high frequencies (3, 5), and (c) long-period baseline corrections to permit accurate integrations for velocity and displacement (4). These corrections produce a set of adjusted accelerograms which will preserve the maximum possible information set by transducer characteristics, trace quality, and digitization limitations. At the long period end, acceleration levels fall below background digitization noise.

A third stage in the processing involves development of computer programs which will calculate velocities and displacements and various frequency spectra and plot the results in a standard form ready for reproduction and publication (7, 8, 9).

Comprehensive experimental and analytical studies have established that all elements of the strong-motion accelerograph and data processing system have achieved a reasonable compatibility as far as accuracy level and frequency response are concerned, with no single link in the

chain playing a significant limiting role. The quality of the analog trace, the personal errors of hand-setting a cross-hair on the trace, the basic frequency limits of the instrument transducer, and the computational techniques developed for a reasonable computing cost all seem to reach various limiting conditions at about the current level of development. Major improvements in accuracy, dynamic range, or frequency response will require simultaneous major developments in several elements of the system. The data processing itself should not be a limiting feature of the instrumentation system. With modern digital image processing based on high resolution cathode-ray scanning, completely automatic digitization of analog traces can be carried out at a resolution higher than existing semi-automatic systems involving hand-setting of a cross-hair on a trace. Improvements must come first in basic transducer design for high frequency response and freedom from higher mode distortions and second in the basic recording medium itself, be it film or magnetic tape.

STANDARDIZED DATA

The present (1973) status of the standard data processing program is as follows: (1) The digitization of the backlog of 500 U. S. accelerograms has been completed on a uniform basis of accuracy. "Uncorrected" accelerograms in this standard digitized form are available as punched card decks or as computer-compatible digital magnetic tape. About one-half of the records are also available as published reports which include complete printouts of the digitized data plus computer plotted accelerograms [6]. The remainder of the reports are being issued regularly and the whole series should be complete in approximately one year. (2) The "corrected" accelerogram data are available in the form of punched card decks or digital magnetic tapes for approximately one-half of the records. Digital printouts are included in a series of reports of which about one-third have already been issued [7]. These reports include as well computer plots of the velocity and displacement curves. (3) A third volume series contains calculated response spectrum curves in standard format for all ground accelerograms, along with printout of coordinates [8]. About one-quarter of the records have been issued in this form, and the remainder will appear over the next two years. (4) A fourth volume series contains plotted Fourier spectra in two standard formats for all accelerograms, including building response records [9]. For multiple accelerograph installations in buildings, transfer function plots are included. The first part A of each of the above four volumes contains detailed background information on the techniques and procedures used. Examples of the standard plotted curves may be seen in reference (1).

The above reports, cards, and tapes can be obtained from the following sources: (1) National Information Service for Earthquake Engineering, Earthquake Engineering Research Laboratory, California Institute of Technology, Pasadena, California 91109 - Reports, card decks, and magnetic tapes at nominal costs for postage and handling. (2) National Geophysical Data Center, National Oceanic and Atmospheric Center, D6, Environmental Data Service, NOAA, 6001 Executive Boulevard, Rockville, Maryland 20852 - Copies of full-scale accelerograms, standard digitized data. (3) National Technical Information Service,

U. S. Department of Commerce, Springfield, Virginia 22151 - Copies o digitized data reports containing digital printouts and spectrum plots. (4) Seismological Field Survey, National Oceanic and Atmospheric Administration, 390 Main Street, Room 7067, San Francisco, Californi 94105 - Copies of full-scale accelerograms, punched card decks, and magnetic tapes.

BIBLIOGRAPHY

(1) Trifunac, M.D., Udwadia, F.E., and A.G. Brady, "Recent Developments in Data Processing and Accuracy Evaluations of Strong-Motion Acceleration Measurements," 5WCEE, Rome, 1973.

(2) Trifunac, M.D., and D.E. Hudson, "Laboratory Evaluations and Instrument Corrections of Strong Motion Accelerographs," Report EERL 70-04, Earthquake Engineering Research Laboratory, California Institute of Technology, Pasadena, 1970.

(3) Trifunac, M.D., Udwadia, F.E., and A.G. Brady, "Analysis of Errors in Digitized Strong-Motion Accelerograms," Bull. Seism. Soc. Amer., vol. 63, no. 1, February, 1973.

(4) Trifunac, M.D., "Zero Baseline Corrections of Strong-Motion Accelerograms," Bull. Seism. Soc. Amer., vol. 61, no. 5, pp. 1201-1211, 1971.

(5) Trifunac, M.D., "A Note on Correction of Strong-Motion Accelerograms for Instrument Response," Bull. Seism. Soc. Amer vol. 62, no. 1, pp. 401-409, 1972.

(6) Hudson, D.E., and A.G. Brady, "Strong Motion Earthquake Accelerograms - Digitized and Plotted Data, Vol. I - Uncorrected Accelerograms, Part A," Report EERL 70-20, Earthquake Engineering Research Laboratory, California Institute of Technolog Pasadena, 1969 (and subsequent Parts B, D, etc.).

(7) Hudson, D.E., Brady, A.G., Trifunac, M.D., and A. Vijayaraghavan, "Strong Motion Earthquake Accelerograms, Vol. II - Corrected Data and Integrated Ground Velocity and Displacement Curves, Part A," Report 71-50, Earthquake Engineering Research Laboratory, California Institute of Technology, Pasadena, 1971 (and subsequent Parts B, C, etc.).

(8) Hudson, D.E., Trifunac, M.D., and A.G. Brady, "Analyses of Strong Motion Earthquake Accelerograms, Vol. III - Response Spectra, Part A," Report EERL 72-80, Earthquake Engineering Research Laboratory, California Institute of Technology, 1972 (and subsequent Parts B, C, etc.).

(9) Hudson, D.E., Trifunac, M.D., Udwadia, F.E., Vijayaraghavan, and A.G. Brady, "Analyses of Strong Motion Accelerograms, Vol. IV - Fourier Amplitude Spectra, Part A," Report EERL 72-1(Earthquake Engineering Research Laboratory, California Institute of Technology, Pasadena, 1972. (and subsequent Parts B, C, etc.)

RECENT DEVELOPMENTS IN DATA PROCESSING AND ACCURACY EVALUATIONS OF STRONG MOTION ACCELERATION MEASUREMENTS

by

M. D. Trifunac[I], F. E. Udwadia[II] and A. G. Brady[III]

SYNOPSIS

Strong-motion accelerograph systems have been examined in detail from the standpoint of the recovery of the maximum amount of information from the record. This has involved a detailed evaluation of errors, including such factors as transducer properties, high and low frequency digitization errors, various distortions in photographic processing, and accuracy considerations of computing procedures. It is shown that existing standard accelerograph systems consisting of optical-recording analog accelerographs, photographic processing, semi-automatic hand digitization of analog records, and computer digital filtering and correction techniques form a reasonably compatible system from the standpoint of accuracy limits of the various components. Standard correction techniques are described, and overall frequency limits and accuracy estimates are presented.

INTRODUCTION

Basic information on the detailed time history of close-in destructive earthquake ground motions comes from strong motion accelerographs that record three mutually perpendicular components of ground acceleration(1). Instruments of this kind were first deployed in early 1933, and the Long Beach, California, earthquake of 1933 provided the first strong motion accelerograms. Since that time, numerous invaluable strong motion accelerograms have been recorded, mainly in the western United States. With the data most recently acquired during the San Fernando, California, earthquake of Februray 9, 1971, there are presently over 500 recorded accelerograms of excellent quality.

In the late 1960's, an extensive program of strong motion data processing was initiated at the Earthquake Engineering Research Laboratory of the California Institute of Technology. The principal objective for initiating this program was to provide all investigators with the basic data in a form as accurate as possible. The first volume, IA, which appeared in 1969(2) contained "uncorrected" accelerograms, and it was soon followed by the first parts of the volumes IIA, IIIA and IVA which

I Assistant Professor, Applied Science, EERL, Calif. Inst. Tech., Pasadena, California.

II Research Fellow, Applied Science, EERL, Calif. Inst. Tech.

III Senior Research Fellow, Applied Mechanics, EERL, Calif. Inst. Tech.

presented corrected accelerograms and integrated velocity and displacement curves[3], response spectra[4] and Fourier amplitude spectra[5]. Numerous subsequent parts (B, C, D, etc.) of all volumes are now being issued.

Perhaps the most important recent development in the experimental strong-motion seismology has been the improvement of the methods of data processing of strong-motion accelerograms emerging from the work on the above mentioned project. By using the modern techniques of trace digitization and the digital computer processing, it has become possible to significantly increase the accuracy and the amount of information that can be extracted from the recorded ground motions.

In this paper we summarize our present knowledge of the errors and corrective procedures which are associated with accelerogram data processing and attempt to outline briefly the state of the art in computation of velocity and displacement curves. This summary is based mainly on instruments recording on paper or film and on the semi-automatic digitization process. Therefore, many aspects of the outlined accuracy evaluations and error corrections may change with the development of new technology for recording and data processing. Nevertheless, the experience summarized here will remain essential for future processing of paper and film records.

Modern strong-motion instruments with optical recording are capable of measuring ground accelerations up to about 1g with a resolution of the order of 0.001g. This corresponds to a dynamic range of about 60 db. Although, theoretically, the usable frequency range for these instruments is from D.C. to about 25 cps, the low amplitudes of measured acceleration at long periods can be used only for frequencies higher than about 0.06 cps since the digitization noise becomes significant at longer periods. Since the recorded amplitude of long-period waves is a function of earthquake magnitude and the hypocentral distance it is clear that this cut-off frequency may vary from one record to the other. However, for the routine accelerogram processing it is impractical to change its value from one accelerogram to another and the optimum cut-off frequency must be selected. This frequency is about 0.06 cps for a typical accelerogram and the overall processing accuracy at the Earthquake Engineering Research Laboratory. Other equipment and different processing procedures will, of course, lead to other cut-off frequencies. The high frequency limit for data retrieval which is currently at 25 cps results from the signal modifications imposed by the natural frequency of the transducer and the semi-automatic digitization procedures. With modern image processing methods and increased speed of record motion in the instrument (now between 1 and 2 cm/sec. this frequency will increase in the future.

Accelerographs recording on analog magnetic tape are commercially available and have 30-35 db nominal dynamic range, but presently they do not offer an improvement over high quality photographic instruments.

ERRORS IN DIGITIZED ACCELEROGRAMS

The modification of harmonic input amplitudes and phases by the strong-motion accelerographs are caused by the relatively low natural frequency of transducer element (Figure 1), usually between 10 and 30 cps for most of the mechanical-optical strong-motion accelerographs.

The relative motion X(t) of the transducer mass is described by the differential equation of motion $\ddot{X}(t) + 2\omega_o \zeta_o \dot{X}(t) + \omega_o^2 X(t) = -a(t)$ (Figure 9), where ζ_o is the fraction of critical damping, ω_o is the natural frequency ($\omega_o = 2\pi f_o$), a(t) is the absolute base acceleration, and t is the time coordinate. For acceleration transducers, the largest possible ω_o is chosen so that the term $\omega_o^2 X(t)$ dominates on the left hand side of the differential equation. For input frequencies ω that are several times smaller than ω_o, $\ddot{X}(t)$ and $2\omega_o \zeta_o \dot{X}(t)$ are small and $\omega_o^2 X(t)$ is therefore nearly same as -a(t) (Figures 1 and 9). For higher input frequencies, both amplitudes and phases are significantly modified and the correction terms involving $\ddot{X}(t)$ and $2\omega_o \zeta_o \dot{X}(t)$ may not be neglected.

To simplify instrument response interpretation, the strong-motion acceleration transducers are usually designed to represent a single-degree-of-freedom viscously damped oscillator (Figure 2). Unfortunately, it is not always possible to design an ideal single-degree-of-freedom system. For example, the transducer mass supported by two leaf springs (Figure 2) is meant to vibrate in its fundamental transverse mode only. However, in addition to the higher modes in the transverse direction, the transducer configuration allows torsional vibrations as well. These torsional vibrations may be excited, for example, by a slight eccentricity of the electromagnetic damping force[9].

There may be various other instrumental errors present in the recorded accelerogram, such as the transverse play of the recording paper, nonuniform velocity of record-driving mechanism, inaccurate timing, misalignment of the three transducers, cross-axis sensitivity of transducers, waveform clipping, etc. However, these will not be discussed here for a more detailed account on these errors may be found in our previous papers[6].

Errors due to the warping of film negatives and translucent Mylar copies are caused by chemical processing and later by aging. Other photographic processing errors may be caused by the lens imperfections, or by the stretching of the film negatives while duplicating long rolls continuously. These errors are almost entirely eliminated by subtracting the digitized fixed trace from the accelerogram and by the proper scaling[6].

The digitizing errors come from two principal sources: (1) an imperfect mechanical traverse mechanism of the digitizer cross hair system, and (2) the random errors generated by the operators. Whereas the errors from the first group can be eliminated in most cases by simultaneous digitization of the acceleration and fixed traces, the random digitization errors remain in the digitized data as "noise".

Through the detailed analysis of the above mentioned errors, it has been possible to show that the minimum resolution of a digitizer should be better than about 1/300 cm - the variance of an almost norma distributed human reading error, and, that the discretization process i the digitizer does not seriously add to the human error[6]. Perhaps another intuitively clear result indicates that a greater number of digitized data points decreases the amplitude of the digitization noise spectrum but extends the same spectrum to higher frequencies[6]. Finally, it has been possible to show that the unequally spaced digitized points in time which are connected with straight line segments define a new continuous function which has all Fourier spectrum amplitudes the same as those of the original function up to the average Nyquist frequen of digitization. In other words, discrete digitized points interconnectec with straight lines play the role of a low pass filter with the cut-off frequency equal to the average Nyquist frequency of digitization.

OVERALL EFFECTS OF ERRORS IN DIGITIZED ACCELEROGRAMS

While the detailed studies of different errors have led to the det mination of their properties and helped develop procedures for elimination of many of them at their source[6], the ultimate objective of such a error analysis has been to find their combined overall effect and to determine the frequency band in which the digitized data accurately represent ground acceleration. One can specify this frequency band by defining the cut-off frequencies f_L and f_H, where L stands for low and H for high frequencies. Ideally, the frequency f_L should be greater than all frequencies associated with long-period recording and digitizin errors whose spectral amplitudes and phases cannot be corrected, and the frequency f_H should be smaller than all frequencies representing high-frequency recording and digitizing errors. These frequencies change from one instrument to another, and depend on instrument recording speed and sensitivity[6]. For the standard acceleration correction, f_L and f_H are chosen to represent the average for all records.

The density of digitized points varies from one operator to another, and has been illustrated in Fig. 3 by plotting the average number of digitized points per one cycle versus period. The least-square-fitted straight lines show a tendency towards the increase in the number of points for longer periods. Certain distinct features of these curves distinguish this kind of hand-digitized data from equally spaced hand or machine digitization[6]. For example, a dashed line is plotted corresponding to the $\Delta t=0.1$ sec. This line intersects the level of 2 points per cycle at the period of 0.2 seconds in agreement with the Nyquist frequency criterion (5 cps). On the other hand, the lines calculated for the four typical acceleration digitizations with unequally spaced data never go below the level of 2 points per cycle.

Fig. 4 gives a histogram for the lowest average period present in the early 48 hand digitized paper records[2]. From this histogram, we observe that the lowest average period picked over one record is greater than 0.04 seconds and corresponds to the highest frequency being less than 25 cps. Since this histogram has been obtained from the data averaged over one second and from the operator's own

judgment of the number of points to be digitized according to the local frequency content, the highest frequency actually resolved in a short segment of record is substantially above the average. Numerous other records recently hand-digitized contain on the average about 40 or more points per second, and they are well represented by the steepest curve in Fig. 3. For these records, the average Nyquist frequency is well above 20 to 25 cps. The fundamental frequencies of most instruments fall between 10 and 30 cps. Recorded signals with frequencies higher than 30 cps have a low signal-to-noise ratio and are distorted by the higher modes of vibration of the instrument transducers (Figs. 1 and 2). Therefore, it appears that most hand-digitized paper accelerograms contain information on the frequencies up to about 25 cps.

From the analysis of random digitization noise, it has been found that the expected average errors in the ground displacement are relatively small up to periods of about 16 seconds[6] and then rapidly build up thereafter for longer periods. Thus, it was decided to filter out these long-period errors starting at about a 16 sec period. Whether this period should be chosen as the limit period beyond which the errors are to be considered as serious is a delicate question that depends on the expected use of the accelerogram, and in particular, on the required accuracy of the computed ground motion. If one could expect long-period ground displacements of several meters, then errors of several centimeters would certainly be acceptable and it would be possible to extend the validity of twice-integrated accelerograms up to, perhaps, 30 or 50 sec periods.

To examine the validity of $f_L = 1/16$ cps as determined from the analysis of random digitization errors alone[6], four experiments have been performed. A typical accelerograph was mounted on a horizontal table constrained to move along a horizontal line. The table was moved by hand following approximately a single cycle of a sinusoid, with the fundamental period increasing in successive tests from about 10 sec to about 35 sec. The absolute table motion has been monitored by a laboratory displacement meter which records on a Brush pen recorder.

The displacements from the four experiments were calculated from accelerations recorded on the 70 mm film. The negatives were enlarged to prints 24 inches long, and were digitized in the same way as the standard uncorrected accelerograms. A sloping zero acceleration baseline was inserted in each of the four digitized accelerograms by minimizing the root mean square of the acceleration, and the accelerations were double integrated in the usual way to obtain displacement. The measured and calculated displacements were plotted on the same graphs (with ordinates displaced by 5 in.) to allow comparison (Figs. 5, 6, 7 and 8).

The agreement between the recorded and double-integrated accelerograms and the measured displacement curves for periods of about 10 sec (Fig. 5) and 12 sec (Fig. 6) is excellent. The agreement for the period close to 20 sec (Fig. 7) is still very good, but it indicates small long-period drifts of several inches in amplitude which are very similar to the fluctuations caused by the random digitization errors[6].

In experiment No. 4 (Fig. 8) with a predominant period of about 35 sec, the agreement between computed and measured table displacements is poor. These tests indicate that good agreement between computed and recorded displacement may be obtained for waves with periods shorter than 10 to 12 seconds and 10-20 inch amplitudes, with digitization error becoming noticeable at about a 20 sec period.

CORRECTED ACCELEROGRAMS

The standard processing of corrected accelerograms first involves instrument correction[8] and then baseline correction[3, 7]. From uncorrected accelerograms digitized at unequally spaced interval equally spaced data with 50 points per second are generated after low-pass filtering the original data. This process eliminates the high-frequency instrumental digitization errors and aliasing. The filtering is performed by using an Ormsby filter with a cut-off frequency $f_C = 25$ cps and a roll-off termination frequency $f_T = 27$ cps.

Instrument correction is performed by using a differential equation of motion for the single-degree-of-freedom system (Fig. 9). The instrumental constants ω_o and ζ_o required for this correction are determined from the calibration tests of each accelerograph component(

Accelerograms corrected for instrument response are next baseline corrected by high-pass filtering with an Ormsby filter (Fig. 1(This process filters out periods longer than about 16 sec and eliminates the long-period errors introduced by recording, digitization, and recor processing. The final result is a corrected accelerogram that accurate represents the absolute acceleration of instrument base in the frequenc band between 0.06 cps and 25 cps.

Recent experiments have shown that small errors, which are associated with the extension of the accelerogram by a zero outside the interval 0 to T, a procedure required for digital filtering, and those resulting from the estimation of v_o and a_o (step 2 in Fig. 10), may lead to small but undesirable long-period components of the computed groun displacement. These errors are a consequence of applying the lease square fitting method, which, from the point of view of the physical nature of the accelerogram, is only a mathematical fiction. To elimin these effects, a new refinement has been added to the standard baseline correction procedures[7] which consists of extending the accelerogram as an even function outside the interval 0 to T[3].

When a straight line $v_o + a_o t$ is fitted to the velocity v(t) (step 2 in Fig. 10), small errors Δv_o and Δa_o are introduced in the estimates of v_o and a_o. Upon integration Δv_o and Δa_o lead to $\Delta v_o t + 1/2 \Delta a_o t^2 +$ const., an error in the computed displacements that possesses periods longer than 16 sec. Therefore, the second refinement added to the standard baseline correction procedures[7] consists of high-pass filtering the velocity and displacement curves (steps 8, 10 and 12 in Fig. 10).

For routine processings of strong-motion accelerograms, the above mentioned procedures are believed to adequately restore the

basic data for typical research work. For special applications when greater accuracy is required, further improvements in the above described methods may be called for. In such cases uncorrected accelerograms can be used as a starting point in the analysis.

Figs. 11 to 14 summarize the standard format of data presentation in Vols. II, III and IV[10]. Fig. 11 consists of the corrected accelerogram and computed velocity and displacement curves[3]. Fig. 12 presents the tripartite logarithmic plot of pseudo relative velocity spectrum; the corresponding true velocity spectrum (SV) and the Fourier amplitude spectrum (FS) are shown in Fig. 13[4]. Fig. 14 shows the Fourier amplitude specturm with the 95% confidence level[5].

REFERENCES

(1) Hudson, D.E., Ground Motion Meausrements, Chapt. 6, Earthquake Engineering, ed. by Wiegel, Prentics Hall, New Jersey (1970).

(2) Hudson, D.E., A.G. Brady and M.D. Trifunac, Strong-motion earthquake accelerograms, digitized and plotted data, Vol. IA, Earthquake Eng. Res. Lab., EERL 69-20, Calif. Inst. Tech., Pasadena (1969).

(3) Hudson, D.E., M.D. Trifunac, A.G. Brady and A.Vijayaraghavan, Strong-motion earthquake accelerograms, Vol. IIA, Corrected accelerograms and integrated velocity and displacement curves, Earthquake Eng. Res. Lab., EERL 71-50, Calif. Inst. Tech., Pasadena (1971).

(4) Hudson, D.E., M.D. Trifunac and A.G. Brady, Strong-motion earthquake accelerograms, Vol. IIIA, Response Spectra, Earthquake Eng. Res. Lab., EERL 72-80, Calif. Inst. Tech., Pas.(1972).

(5) Hudson, D.E., M.D. Trifunac, F.E. Udwadia, A. Vijayaraghavan and A. G. Brady, Strong-motion earthquake accelerograms, Vol. IVA, Fourier Spectra, Earthquake Eng. Res. Lab., EERL 72-100, Calif. Inst. Tech., Pasadena (1972).

(6) Trifunac, M.D., F.E. Udwadia and A.G. Brady, Analysis of errors in digitized strong-motion accelerograms, Bull. Seism. Soc. Amer., 63, (in press) (1973).

(7) Trifunac, M.D., Zero baseline correction of strong-motion accelerograms, Bull. Seism. Soc. Amer., 61, 1201-1211 (1971).

(8) Trifunac, M.D., Note on correction of strong-motion accelerograms for instrument response, Bull. Seism. Soc.Am., 62, 401-409(1972).

(9) Trifunac, M.D. and D.E. Hudson, Laboratory evaluation and instrument corrections of strong-motion accelerographs, Earthquake Engineering Research Laboratory, EERL 70-04, California Institute of Technology, Pasadena (1970).

(10) Brady, A.G., and D. E. Hudson, Standard Data Processing of Strong Motion Accelerograms, 5WCEE.

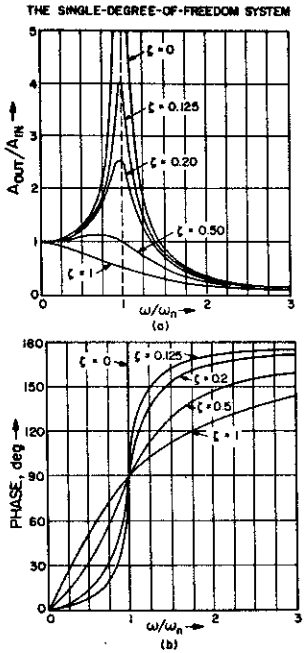

Figure 1

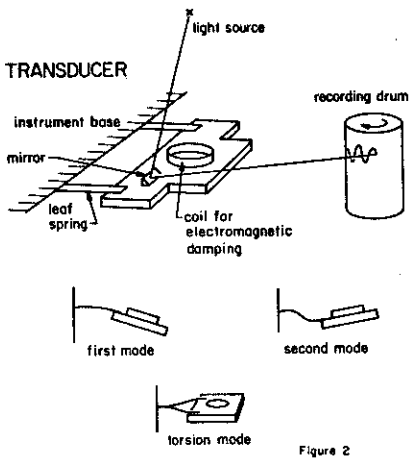

Figure 2

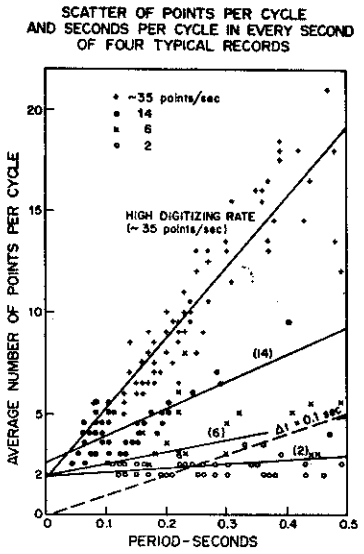

Figure 3

Figure 4

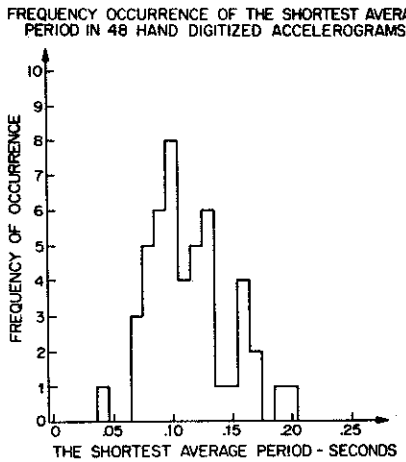

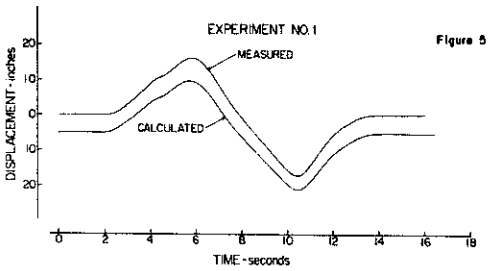

Figure 5

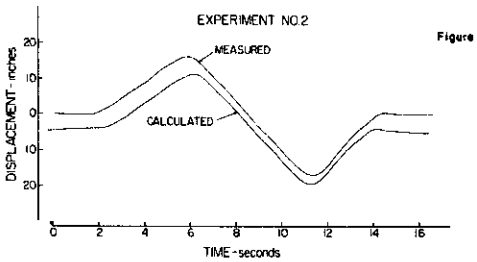

Figure 6

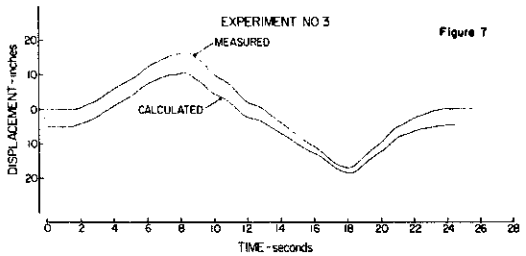

Figure 7

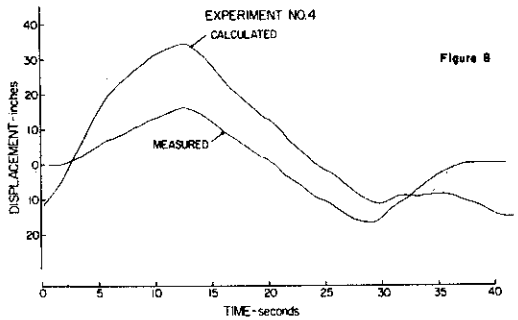

Figure 8

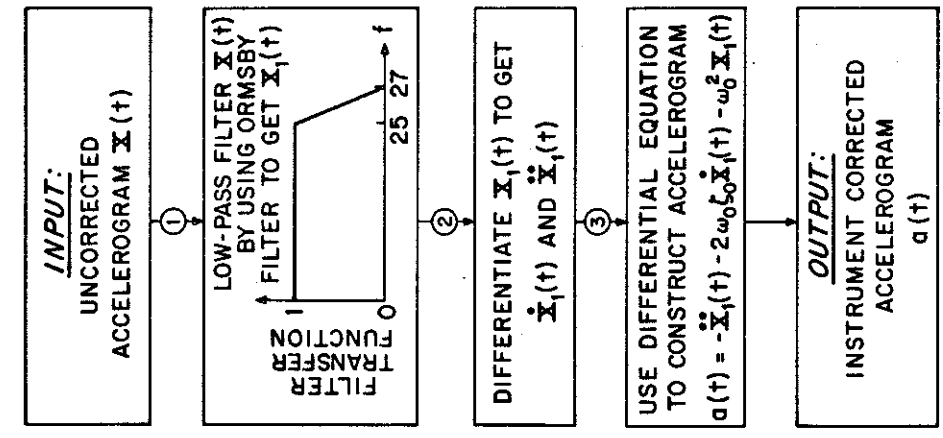

Figure 9

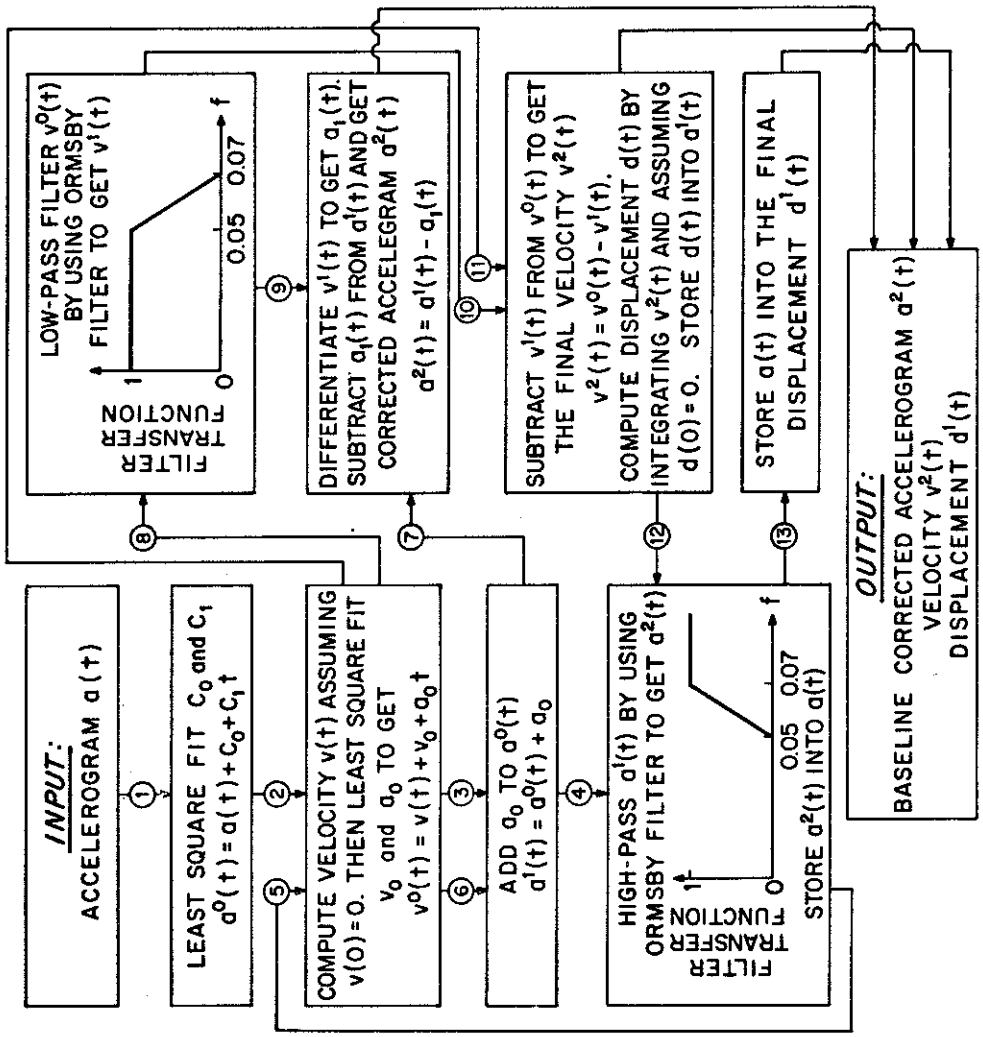

Figure 10

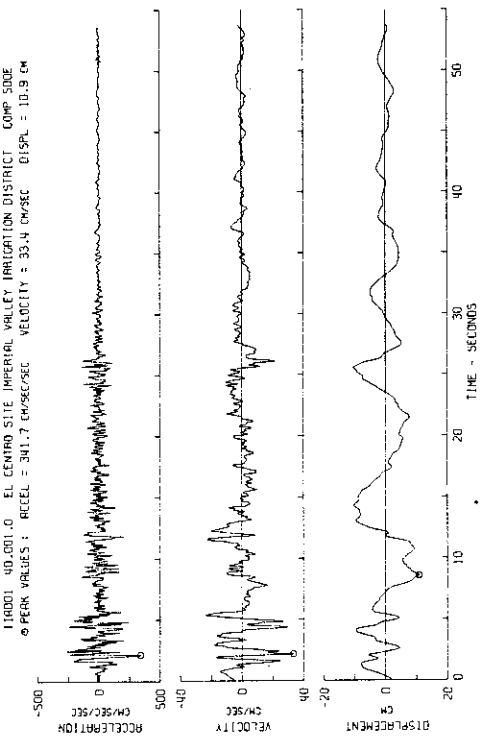

Figure 11

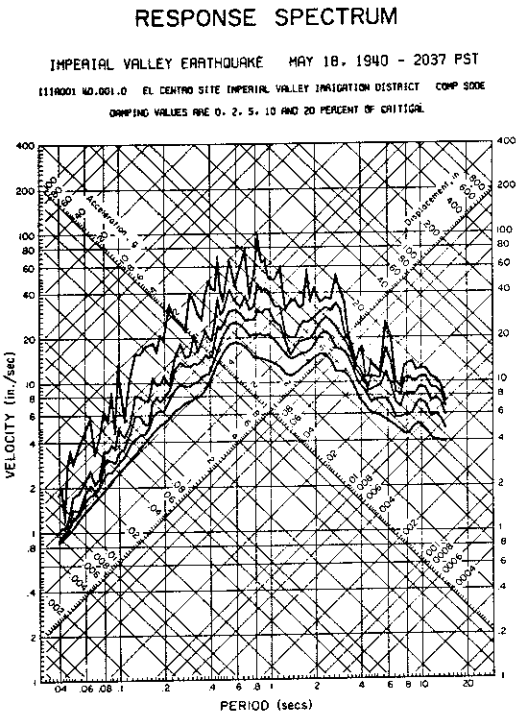

Figure 12

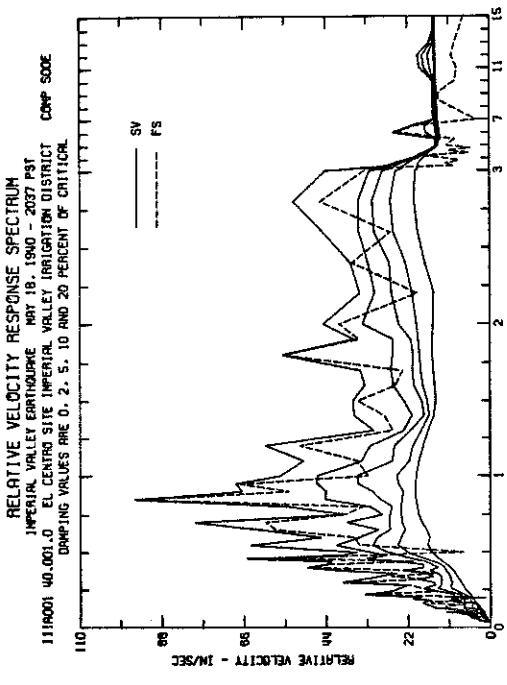

Figure 13

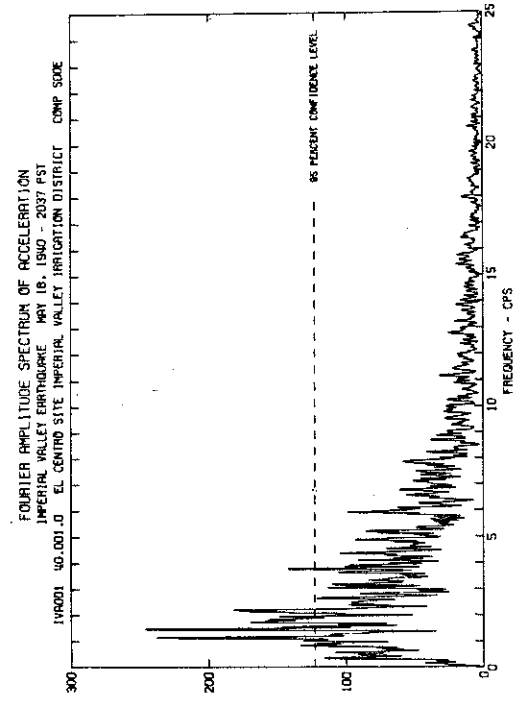

Figure 14

A MODEL FOR THE DYNAMIC ANALYSIS OF DETERIORATING STRUCTURES

by

W. D. Iwan[I]

SYNOPSIS

An analytical model for the dynamic load-deflection behavior of deteriorating structures is presented. The model is of the distributed element or assemblage type and is based on certain phenomenological properties of the structure. The response of simple deteriorating structures to earthquake excitation is examined using the analytical model. The role of different system parameters in determining the nature of the response is discussed and the response compared to that of simple yielding and linear viscous damped structures.

INTRODUCTION

There have been numerous studies of the earthquake response of linear and simple yielding structures and many of the results of these studies have now been incorporated into design manuals and codes. There has been far less attention devoted to the study of the dynamic behavior of deteriorating systems. Deterioration here refers to those changes in a structure which result in loss of stiffness and reduced energy absorbing capacity with cyclic loading. In many cases, deterioration is a consequence of the actual loss of material in structural components as in the case of crushing and spalling of reinforced concrete members[1]. However, deterioration has also been observed in structures subjected to only moderate loading[2]. Clearly, an understanding of the dynamic behavior of this class of systems is important to an understanding of the ultimate failure or collapse of many types of structures.

One reason why there has not been a more systematic and thorough analysis of the response of deteriorating structures is the difficulty in establishing realistic yet analyzable models for this type of structural behavior. The models which have thus far been proposed tend to fall into two categories. In the first category are highly idealized models which lead to considerable simplification of the mathematics of the dynamic response problem but which only very roughly approximate the behavior of real structures[3, 4]. In the second category are very elaborate empirical models which very precisely describe a particular system and a particular loading history[5, 6] but cannot be easily generalized to other systems or loading histories and hence are difficult to apply to the general dynamic response problem.

The model which is the subject of the present paper is a physically motivated model which is based on a phenomenological description of the behavior of deteriorating structures during cyclic loading. At the same time, the model is sufficiently well defined mathematically to make its use in dynamic analysis straightforward. The parameters of the model could be related directly to data from tests of real structures as has been done for simpler models of the same general type[7]. However, this

[I] Professor of Applied Mechanics, California Institute of Technology, Pasadena, California.

particular aspect of the modeling problem is not considered in the present paper. We shall here make a detailed analysis of the response of only a fairly narrow subclass of models having a minimum number of characterizing parameters. Even though this subclass is somewhat restricted, it is felt that it is sufficiently general to justify drawing several important conclusions about the response of general deteriorati systems.

THE MODEL

The model considered is of the distributed element or assembla type[7]. In its most general form, it consists of an infinite collection o different elements each of which is constructed so as to describe a part ular type of observed structural behavior. In the case of deteriorating structures, it is postulated that three general types of behavior can be identified. These are: perfectly elastic behavior, elastic-plastic or simple coulomb slip behavior and irreversible or directional slip behav The existence of the first category is easily accepted as there are many components in a structure which remain essentially elastic even for ver large displacements. The second category may be viewed in two ways. On a macro-scale, this category of behavior would include those eleme of a structure which could be idealized by the elastic-plastic characteri tic such as slip plates, certain bolted and riveted joints, etc. On a micro-scale, the general nondeteriorating yield behavior of many metal lic structural members can be adequately represented by a collection o ideal elasto-plastic elements[7].

The last category is intended to represent those structural elements which are irreversibly modified by loading; that is, the deteriorating elements of a structure. This modification may be associated with actual loss of material as in the case of crushing and/or spalling o concrete or it may be a consequence of some internal material changes. With an eye toward modeling reinforced concrete structures, it is assumed that the most fundamental form of the third category of behavior consists of simple yielding behavior for loading in one direction combin with simple slip behavior for loading in the opposite direction. In the case of a material like concrete, the simple yielding behavior would correspond to compressive loading up to the point of crushing and the reverse loading slip behavior would correspond to cracking under tensil loads.

A physical idealization for each of the three broad types of structural behavior is indicated in Fig. 1. Also shown is the nature of the generalized force-deflection response of each basic element for one cycle of loading from a virgin state. The behavior of the E and Y-type elements is well known and need not be discussed further. However, th behavior of the C-type element merits some additional consideration.

If the C-type element is loaded in a positive (compressive) direction, from a virgin (no internal loads) state, the component with slip level f_{c1} locks up and the system behaves exactly like an elasto-plastic element with a yield level f_{c2}. However, on the first reversal o loading the component f_{c1} will slip before f_{c2} releases and the system will behave as an elasto-plastic element with a generalized yield level f

Upon reloading in a positive direction, the system will continue to respond as an element with yield level f_{c1} until the space opened up in the corresponding slip element has closed, at which point, the system again behaves as an elasto-plastic element with yield level f_{c2}. The behavior of the idealized C-type element may be related to that of certain engineering materials by associating the lower level slip behavior of the model with cracking of the material and the higher level slip behavior with crushing or spalling of the material.

The distributed element or assemblage generalization of the model would appear as indicated in Fig. 2. Since the C-type elements are sensitive to the direction of loading, they will normally occur in pairs with opposite orientation for structures with symmetric loading characteristics. The extension to structures with unsymmetric loading characteristics is straightforward. The E- and Y-type elements are not directionally sensitive and are shown in symmetric pairs only as a convenience in representation.

Figure 3 shows a typical generalized force-deflection relation obtained with a model consisting of one E-type element, three Y-type elements and three pairs of C-type elements. The similarity between the loading behavior indicated in the figure and that obtained from cyclic testing of large scale structures and structural components is apparent[8].

The model may be generalized by allowing two or more elements to have an initial preload in such a way that the assemblage is still in equilibrium. This extension of the basic model will not be discussed here.

FORMULATION OF THE DYNAMIC RESPONSE PROBLEM

For purposes of dynamic analysis, it is convenient to identify certain gross characteristics of the generalized force-deflection behavior. Let the virgin loading response of the system be as indicated in Fig. 4a. Let x_y be the generalized displacement at which all of the Y- and C-type elements have just slipped and f_y be the corresponding generalized force. Let k_o denote the generalized linear stiffness of the system as calculated assuming that all $f_{c1}^{(i)} = 0$; that is, assuming no tensile strength in the C-type elements. In this way, k_o corresponds to the linear stiffness that would normally be specified for structures in which the cracking components have very low tensile strength. Note, however, that by this definition the actual small amplitude stiffness of the system will generally be somewhat greater than k_o when $f_{c1}^{(i)} \neq 0$.

Consider a single-degree-of-freedom or single mode system with generalized mass m, fraction of viscous damping ζ and generalized restoring force $f[x(t)]$ specified by the model of the present paper. Let x be the generalized relative displacement of the mass with respect to a base which is excited with an acceleration a(t). Then, the differential equation of motion for the system may be written in the form

$$\ddot{x} + 2\zeta\omega_o\dot{x} + \omega_o^2 f[x(t)]/k_o = a(t). \qquad (1)$$

Define the displacement ratio z and the system parameters β and a_y as

$$z = x/x_y \quad ; \quad \beta = f_y/(k_o x_y) \quad ; \quad a_y = f_y/m. \tag{2}$$

Then, the equation of motion becomes

$$\ddot{z} + 2\zeta\omega_o\dot{z} + \omega_o^2\bar{f}[z(t)] = \beta\omega_o a(t)/a_y. \tag{3}$$

The virgin loading behavior of the dimensionless restoring force $\bar{f}[z(t)]$ $f[x_y z(t)]/(k_o x_y)$ is shown in Fig. 4b.

The magnitude of the excitation in equation (3) may be specified some characteristic acceleration a^* which might be taken as the peak acceleration, the r.m.s. acceleration, or some other measure of the strength of the excitation. The right-hand side of the equation of motio would then be expressed as

$$\beta\omega^2 a(t)/a_y = \beta\omega^2\rho[a(t)/a^*] \text{ where } \rho = a^*/a_y. \tag{4}$$

In this form $[a(t)/a^*]$ is a dimensionless normalized excitation and the parameter ρ specifies the strength of the excitation relative to that valu of steady input acceleration which would just cause complete yielding of the system.

SYSTEM PARAMETERS

In order to gain some insight into the way in which the general form of the present model effects system response without becoming overly involved in the details of parameter specification, it is instructi to consider the subclass of systems which can be modeled adequately by means of only one E-type element, one Y-type element and one pair of C-type elements. This subclass may be thought of as the fundamental building block of the general distributed element model and is shown enclosed by dashed lines in Fig. 2.

If attention is restricted to this subclass of the general model, the important system parameters become

$$\gamma = \frac{f_s/k_s}{f_{c2}/k_c} = \frac{\text{gen. displ. at which significant yielding occurs}}{\text{gen. displ. at which significant crushing or spalling occurs}}$$

$$\mu = \frac{k_s}{k_c} = \frac{\text{effective modulus of simple yielding component}}{\text{effective modulus of deteriorating component}}$$

$$= \frac{\text{load carried by simple yielding component}}{\text{load carried by deteriorating component}}$$

$$\alpha = \frac{k_e}{k_o} = \frac{\text{limiting large amplitude stiffness of yielding component}}{\text{"linear" stiffness of system}} \geq 0$$

$$\delta = \frac{f_{c1}}{f_{c2}} = \frac{\text{cracking strength of deteriorating component}}{\text{crushing strength of deteriorating component}}.$$

All of these parameters have a direct physical interpretation and are in some way related to the parameters used in structural design. The parameter γ, for example, denotes the degree of ductility of the structure. If $\gamma < 1$, the system is said to be of ductile design with yielding of steel components occurring before significant crushing of concrete components. In this case, $x_y = f_{c2}/k_c$.

The system parameters γ and μ could be deduced directly from an analysis of a given beam or column section according to the rules of normal design practice[9]. This gives a range of values for γ between approximately 0.2 and 0.5 and for μ between 5 and 15. However, from tests of full scale structural components it would appear that if the model is used to describe the gross behavior of a structure including joints, the parameter γ should be allowed to vary from 0.2 to 1.0 while the meaningful range of μ is 0.2 to 5.

One additional parameter may be introduced to account for the fact that the generalized force associated with crushing normally decreases with increasing displacement. This behavior is shown by a dashed line on the restoring force diagram for the C-type element in Fig. 1. Define the parameter ν as

$$\nu = \frac{\text{limiting large amplitude stiffness of deteriorating component}}{\text{small amplitude stiffness of deteriorating component}}$$

where $\nu \leq 0$.

For the present investigation, the system parameters α, δ, ν and ζ are fixed with values $\alpha = 0.05$, $\delta = 0.10$, $\nu = -0.05$ and $\zeta = 0.02$. The parameters γ and μ are allowed to take on the values $\gamma = 0.2$, 0.6, 1.0 and $\mu = 0.2$, 1.0 and 5.0. The nature of the restoring force diagram for different combinations of the parameters γ and μ is shown in Fig. 5. The diagrams shown are for a loading history consisting of a cyclic displacement with monotonically increasing amplitude. Note that the range of parameters considered encompasses a wide variety of structural behavior. Generally speaking, for γ and μ large the restoring force diagram resembles that of a bilinear hysteretic system while for small γ and μ the restoring force diagram has a severely necked down central portion after only a few loading cycles. The role of the stiffness ratio parameter μ in determining the character of the restoring force diagram is not at all surprising. The greater the ratio of the effective stiffness of steel to that of concrete in a structure, the more one would expect that structure to behave like a steel structure and vice versa.

In the numerical examples to follow the "linearized" period of the structure is taken to be $T = 2\pi/\omega_o = 1$ sec. The general response trends observed do not appear to be particularly sensitive to period within the range $T = 0.8$ to 3.0 sec.

EXCITATION

In order to minimize the possiblity of making false conclusions concerning the nature of the response due to pecularities in the input

ductile structure in which the simple yielding or reinforcing component carries a sizeable fraction of the total dynamic load. The greatest response ratio is obtained when $\gamma=1$ and μ is small which would be the case for a structure with gross properties similar to those of concrete alone. The response ratio in this case is at least two and one-half time the value obtained when μ is small and γ is large.

The results of Fig. 7 indicate that the maximum response ratio referenced to x_y is a very strong function of the system parameters γ and μ. It is therefore concluded that the detailed nature of the restorin force characteristic must be taken into account in order to predict the response of a structure relative to its actual yield displacement x_y. Th fact would appear to make it very difficult to make any kind of meaningf analysis of dynamic structural response during an earthquake. Fortunately, there is more to be said.

A most significant observation is made by comparing the maximum response of the class of deteriorating systems to that of a bilinear hysteretic system having the same linearized stiffness k_o and yield strength f_y. It is found that the bilinear hysteretic system and the deteriorating system have nearly the same maximum response independ of the parameters of the deteriorating system. Stated another way, the bilinear hysteretic restoring force characteristic which has the same linearized stiffness as the deteriorating characteristic and which just circumscribes that characteristic gives essentially the same maximum response. For the 160 cases of different system parameters, excitatio ratios and earthquakes considered here, the ratio of the maximum response of the deteriorating system to that of the circumscribing bilinea system was 1.06 with a standard deviation of 0.14. The above result should prove helpful in the dynamic analysis of structures. However, i must be pointed out that this result does not imply equivalence of the bilinear hysteretic characteristic and an arbitrary deteriorating characteristic in all applications. For periods appreciably less than on sec, the response of the deteriorating system has been found to be signi ficantly greater than that of the bilinear system. Moreover, the ultima collapse behavior of a deteriorating system may be quite different from that of the circumscribing bilinear system.

ACKNOWLEDGMENT

The author wishes to express his appreciation to Mr. Nathan Ga for his valuable assistance in many phases of this investigation and to th National Science Foundation for their support of the project under grant #GK-25892.

BIBLIOGRAPHY

1. Jennings, P. C., Ed., "Engineering Features of the San Fernando Earthquake", EERL Report 71-02, California Institute of Technolog Pasadena, pp. 142-179.

acceleration, consider an ensemble of four earthquakes normalized so as to represent excitations of the same relative strength. The normalization is accomplished by obtaining a characteristic velocity spectrum amplitude S_v^* defined as the approximate average of the 0-20% damped response spectrum of each earthquake in the range of 1 to 3 seconds period as determined from a tripartite log representation. The characteristic acceleration a^* of the earthquake is then taken as the peak pseudo acceleration corresponding to S_v^* at a one second period. That is $a^* = 2\pi S_v^*$.

For most earthquakes a^* will be comparable in magnitude to the peak acceleration a_{max}. The latter acceleration is commonly used as a measure of the strength of an earthquake. However, the characteristic acceleration a^* has been found to give more consistent and realistic results for structures in the general period range of 0.75 to 3 seconds.

Table I gives a summary of the earthquakes employed along with their characteristic and peak accelerations.

DISCUSSION OF NUMERICAL RESULTS

The results of numerical integration of the equation of motion for different values of system and excitation parameters are shown in Figs. 6 and 7 and Table II. Figure 6 shows typical displacement time histories for a linear system with 5% viscous damping, a bilinear hysteretic system and a deteriorating system with $\mu = \gamma = 0.2$. The excitation is the El Centro earthquake in each case and $\rho = 8$ for both the bilinear hysteretic and deteriorating systems. The differences in the general character of the response for the three systems is readily apparent. The linear system response appears to be a symmetrically modulated one second period oscillation which reaches a maximum early in the time history and decays fairly rapidly thereafter. By contrast, both the bilinear hysteretic and deteriorating systems have a markedly asymmetric response and the predominant period of oscillation of the deteriorating system is substantially greater than one second. The deteriorating system also exhibits a noticeable low frequency response peak late in the time history which is not present in the other two displacement records. Both the bilinear hysteretic and deteriorating systems show a permanent set.

Figure 7 gives the maximum response ratio x_{max}/x_y averaged over the ensemble of four earthquakes as a function of the system parameters μ and γ and the excitation parameter $\rho = a^*/a_y$. Table II gives the actual numerical values of the average of the maximum response ratio along with the standard deviation of this ratio over the ensemble.

From Fig. 7 it is clear that x_{max}/x_y is an increasing function of the ductility parameter γ and a decreasing function of the stiffness parameter μ. When μ is small, the stiffness of the simple yielding component is small and the response ratio is essentially independent of γ. However, when μ is large so that the stiffness of the simple yielding component is appreciably greater than that of the deteriorating component, the response ratio is a very strong function of γ. The smallest response ratio is obtained when μ is large and γ is small; that is, for a very

2. Ibid., pp. 101-103.
3. Clough, R. W. and S. B. Johnston, "Effects of Stiffness Degradation on Earthquake Ductility Requirements",

4. Penzien, J. and S. C. Liu, "Nondeterministic Analysis of Nonlinear Structures Subjected to Earthquake Excitations", Proc. Fourth World Conf. Earthquake Eng., Santiago, Chile, 1969, Vol. 1, A-1, pp. 114-1
5. Park, R., "Theorization of Structural Behavior with a View to Defining Resistance and Ultimate Deformability", Symposium on Resistance and Ultimate Deformability of Structures Acted on by Well Defined Repeated Loads, Intnl. Assn. for Bridge & Str. Eng., Lisbon, 1973.
6. Takeda, T., M. A. Sozen and N. N. Nielsen, "Reinforced Concrete Response to Simulated Earthquakes", Jour. of Str. Div., ASCE, Vol. 96, Dec. 1970, pp. 2557-25.
7. Iwan, W. D., "The Distributed Element Concept of Hysteretic Modeling and its Application to Transient Response Problems", Proc. Fourth World Conf. Earthquake Eng., Santiago, Chile, 1969, Vol. 2, A-4, pp. 45-57.
8. Corley, W. G. and N. W. Hanson, "Design of Beam-Column Joints for Seismic Resistant Reinforced Concrete Frames", Proc. Fourth World Conf. Earthquake Eng., Santiago, Chile, 1969, Vol. 2, B-3, pp. 69-82.
9. Blume, J. A., N. M. Newmark and L. H. Corning, "Design of Multi-story Reinforced Concrete Buildings for Earthquake Motion", Portland Cement Assn., Chicago, 1971, pp. 92-113.

TABLE I

Earthquake	Ave. Vel. Spect. S_v^* (m/sec)	Char. Accel a^*(g's)	Peak Accel a_{max}(g's)	Re Stren
El Centro, 1940, N-S	0.66	0.42	0.35	1.0
Taft, 1952, S69E	0.30	0.20	0.18	0.4
Pacoima Dam, 1971, S16E	1.83	1.17	1.17	2.7
Holiday Inn, 1971, N-S	0.69	0.44	0.25	1.0

TABLE II

mean / std. dev.	$\mu = 0.2$			$\mu = 1.0$			$\mu = 5.0$		
	$\gamma = 0.2$	$\gamma = 0.6$	$\gamma = 1.0$	$\gamma = 0.2$	$\gamma = 0.6$	$\gamma = 1.0$	$\gamma = 0.2$	$\gamma = 0.6$	$\gamma = 1.0$
$\rho = 2$	1.68 0.48	1.75 0.45	1.93 0.42	1.24 0.32	1.51 0.39	1.98 0.40	0.67 0.12	1.31 0.25	1.96 0.41
$\rho = 4$	4.15 0.30	4.13 0.35	4.26 0.44	2.51 0.32	2.99 0.24	3.88 0.34	1.35 0.29	2.46 0.24	3.54 0.14
$\rho = 8$	9.91 2.15	10.24 2.16	10.74 2.43	6.58 1.02	8.13 1.60	10.18 1.68	3.49 0.39	6.44 0.53	9.56 0.81
$\rho = 12$	17.40 4.46	17.64 3.50	18.32 3.55	11.20 1.76	13.19 2.64	15.60 3.68	5.82 0.86	9.77 2.03	14.10 2.84

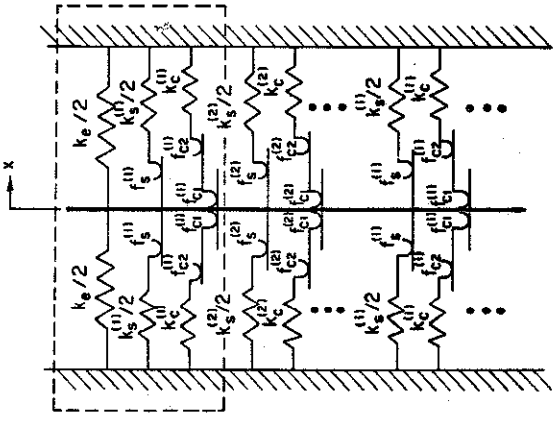

Fig. 2

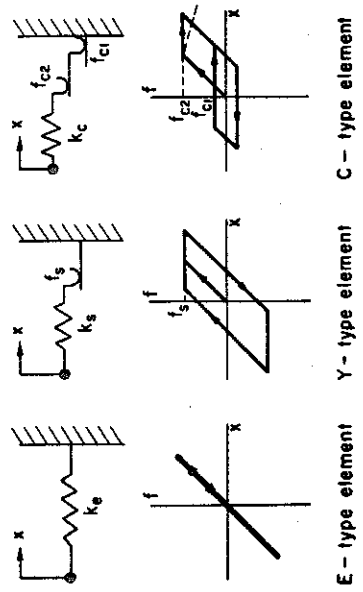

Fig. 1

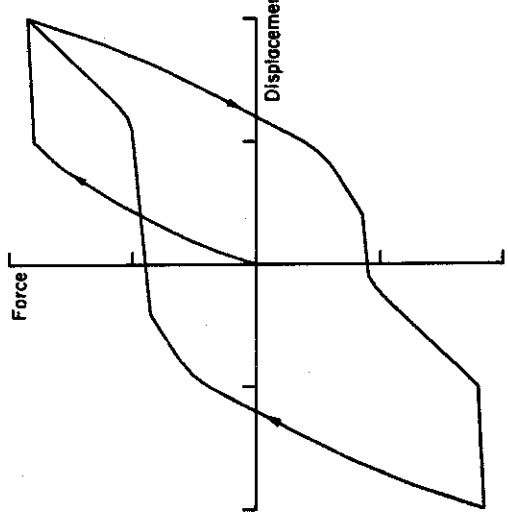

Fig. 3

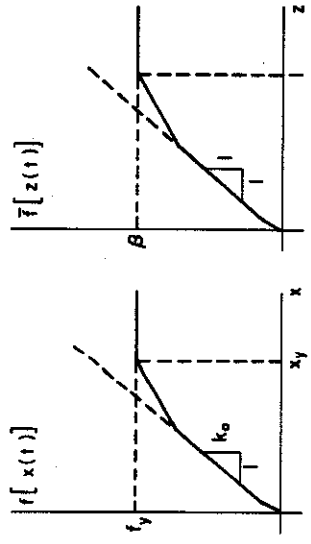

Fig. 4

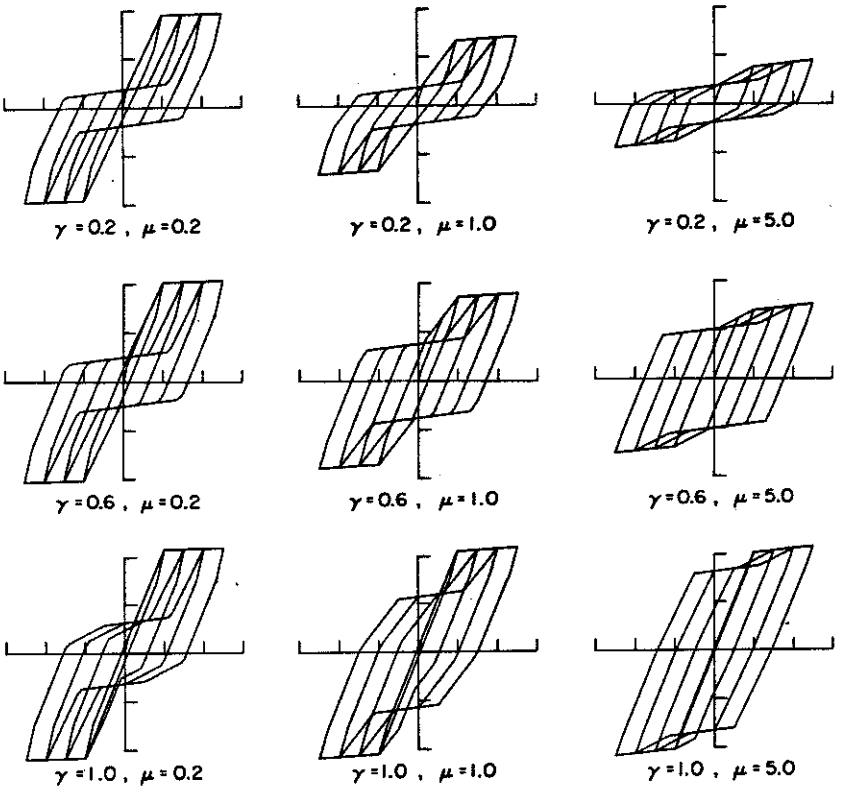

Fig. 5

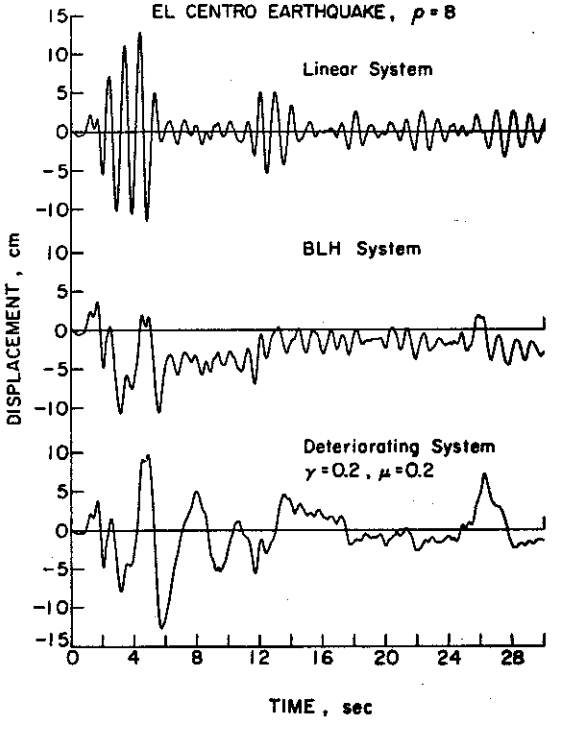

Fig. 6

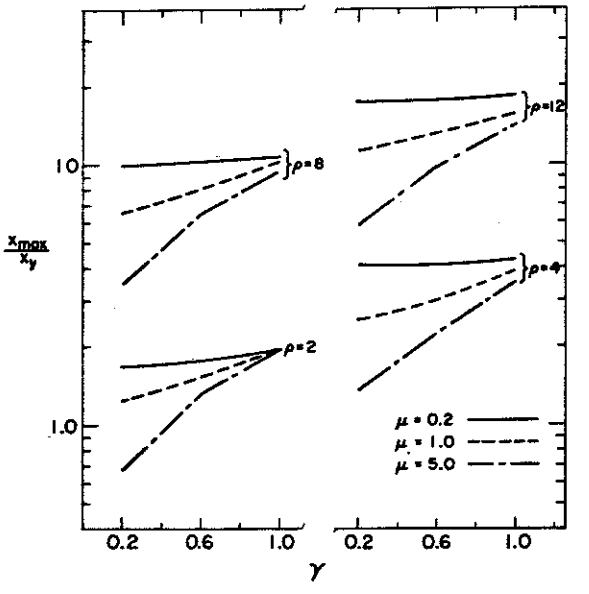

Fig. 7

EARTHQUAKE-INDUCED EARTH PRESSURES ON RETAINING WALLS

by R. F. Scott[I]

SYNOPSIS

A model for the dynamic behaviour of a soil-retaining wall system is presented. From the model, expressions are derived for the pressures, forces, and moments which may act on the wall during a design earthquake. In the analysis, modifications enable the variation of soil properties with depth and the flexibility of the wall to be taken into account.

INTRODUCTION

The calculation of the pressures developed on retaining structures by earthquake vibration is generally based on a static Coulomb wedge analysis with the addition of a horizontal acceleration, as suggested by Mononobe (4) and Okabe (5). Such an analysis leads to a pressure distribution on the wall increasing linearly from top to bottom. An evaluation of the Mononobe-Okabe calculation method has been given by Seed and Whitman (6). They conclude from small-scale experiments of the investigators that the calculated force on the wall is approximately correct. However they point out that to give the measured base moment, the calculated force must be applied at a height of about 0.6 of the wall height from the base, rather than 0.33. There are a number of disadvantages with this theory. It does not represent the dynamic conditions which occur, particularly with respect to large walls, during an earthquake. The relation of a static seismic coefficient to a given design earthquake is tenuous. No accounting for the flexibility of the wall is possible in the analysis. In this paper, an alternative design method will be described. It conforms more closely to the approaches currently in use in structural analysis.

DYNAMIC ANALYSIS

In Fig.1 is shown a two-dimensional cross section through a typical wall and backfill with horizontal surface. It is supposed that the design earthquake input is known at the level AB of the problem profile and that the region of soil ABCD constitutes the backfill or natural soil and backfill adjacent to the wall. In the analysis to be discussed here the soil is treated as a one-dimensional shear beam attached to the wall or walls by springs representing the soil-wall interaction. In the shear-beam method of calculating the dynamic pressure on the retaining wall, either a lumped parameter (Fig.2), or a continuous shear beam (Fig.3) may be employed.

I Professor of Civil Engineering, California Institute of Technology, Pasadena, California, 91109, U.S.A.

CONTINUOUS SHEAR BEAM

The geometry, variables, and properties are shown in Fig.3. In this arrangement the shear beam is connected to the wall BC and the left-hand boundary AD by a continuous Winkler spring foundation of spring constant k. For this model, a resisting pressure is developed at each level, x, of the shear beam proportional to the instantaneous lateral displacement u at that level. In general, the soil properties of density, ρ, Young's modulus, E, and shear modulus, G will vary with depth so that the density and shearing stiffness of the beam, as well as the spring constant k, will also vary with depth. For generality, also, the wall should be considered flexible, but this case will be deferred until later in the paper. The wall is considered to be rigid at first. Various cases of property variation with depth will be considered in order. Damping is left for later inclusion with the selected spectra of ground motion.

(a) Properties constant with depth

In this case the equation of motion is

$$\frac{\partial^2 u}{\partial t^2} = \frac{G}{\rho}\frac{\partial^2 u}{\partial x^2} - \frac{2ku}{\rho b} \tag{1}$$

Solving in the usual way by separation of the time and space variables shows the deflected shape of the beam to be a cosine function, harmonic in time, t, with frequency ω,

$$u = D \cos \lambda x \sin \omega t, \tag{2}$$

where D is a constant for each mode and the various modes of vibration are given by the requirement that

$$D \cos \lambda h = 0 \tag{3}$$

where h is the wall height.

Thus, for the successive mode shapes, λ has the values

$$\lambda_1 = \pi/2h;\ \lambda_2 = 3\pi/2h;\ \cdots\cdots\cdots\ \lambda_n = (2n-1)\pi/2h \tag{4}$$

Substitution of Eq.(2) in Eq.(1) gives the frequencies of the modes

$$\omega_n = \left[\frac{(2n-1)^2\pi^2 G}{4\rho h^2} + \frac{2k}{b\rho}\right]^{1/2} \tag{5}$$

The first term on the right-hand side of Eq.(5) is the frequency of the unrestrained one-dimensional shear beam; the effect of the restraining springs is indicated in the second term.

The participation factors α_n are given by the equation

$$\alpha_n = \frac{\int_o^h \rho(x) X_n(x)\,dx}{\int_o^h \rho(x) X_n^2(x)\,dx} \tag{6}$$

where $X_n(x)$ is the deflected shape of the shear beam in the nth mode. Here, with constant density,

$$\alpha_n = \frac{\int_o^h \cos\lambda_n x\,dx}{\int_o^h \cos^2\lambda_n x\,dx} = \frac{4\sin\lambda_n h}{2\lambda_n h + \sin 2\lambda_n h} \tag{7}$$

The maximum deflection, u_{mn}, associated with a particular mode, at the elevation x, due to a specified design earthquake is given by the equation

$$u_{mn} = \frac{S_{vn}\alpha_n \cos(\lambda_n x)}{\omega_n} \tag{8}$$

where S_{vn} is the relative velocity response at the frequency ω_n in the spectrum used for design purposes, with suitable damping.

The "most probable" deflection at elevation x, u_{mp}, is found from a root-mean-square summation

$$u_{mp} = \left\{ \sum_1^\infty \left[\frac{S_{vn}\alpha_n \cos(\lambda_n x)}{\omega_n} \right]^2 \right\}^{1/2} \tag{9}$$

The most probable pressure at this elevation p_{mp} is given by the expression

$$p_{mp} = k u_{mp} \tag{10}$$

From the most probable pressure distribution values of a most probable total force and moment can be calculated.

Analysis, by this method, of problems with typical dimensions and soil properties shows that the first mode is principally responsible for the pressure distribution on the wall during the design earthquake; the higher modes contribute substantially smaller pressures. Under these conditions, the equations for the most probable displacement and pressure distribution can be considerably simplified, since only the first mode need be taken into account.

$$\omega_1 = \left(\frac{\pi^2 G}{4h^2\rho} + \frac{2k}{b\rho} \right)^{1/2} \tag{11}$$

$$\lambda_1 = \pi/2h \tag{12}$$

$$\alpha_1 = \frac{4}{\pi} \tag{13}$$

and the first mode shape is

$$u_1 = D \cos \frac{\pi x}{2h} \tag{14}$$

Consequently the maximum deflection u_{m_1} (equal in the absence of other modes, to the most probable deflection) is given from Eqs.(8), (11), (12) and (13) to be

$$u_{m_1} = \frac{4S_{v1}}{\pi\omega_1}\cos\left(\frac{\pi x}{2h}\right) \tag{15}$$

From Eqs.(10) and (15) the maximum pressure distribution p_{m_1} on the wall is also a cosine function

$$p_{m_1} = \frac{4kS_{v1}}{\pi\omega_1}\cos\left(\frac{\pi x}{2h}\right) = p_o\cos\left(\frac{\pi x}{2h}\right) \tag{16}$$

in which p_o, the maximum pressure at ground surface, is given by the equation

$$p_o = \frac{4kS_{v1}}{\pi\omega_1} \tag{17}$$

The total maximum force on the wall P_{m_1} per lineal foot is given by the area under the cosine pressure distribution curve

$$P_{m_1} = \frac{2}{\pi}p_o h \tag{18}$$

The point of action of this force is located $2h/\pi$ above the base of the wall, as compared with h/3 in the Mononobe-Okabe method. The location of the maximum force compares with the empirically-modified Mononobe-Okabe value of 0.6h as suggested by Seed and Whitman (6).

The maximum moment at the base M_{m_1} per lineal foot is

$$M_{m_1} = \frac{2P_{m_1}h}{\pi} = \frac{4}{\pi^2}p_o h^2 \tag{19}$$

It would be of interest at this stage to obtain a calibration as to the accuracy with which the shear beam-Winkler model yields the natural frequency of at least the first mode A two-dimensional solution has been obtained by Wood (7) to the problem of Fig.1 when no vertical displacements are permitted. This artificial restraint will cause the resulting frequencies to be too high in comparison with a solution in which both displacements occur. A comparison between Wood's solution for the first mode and Eq.(11) indicates that the two frequencies will be close if b = L and

$$k = \frac{4E(1-\nu)}{L(1+\nu)(1-2\nu)} = \frac{8G(1-\nu)}{L(1-2\nu)} \tag{20}$$

This permits the identification of k in a physical model The value of k in Fig.3 can be considered to represent the stiffness of a completely confined soil column of length L/4.

Substituting Eq.(20) in Eq.(11) gives the fundamental frequency of the system

$$\omega_1 = \frac{\pi v_s}{2h}\left[1 + \frac{64}{\pi^2}\frac{(1-\nu)}{(1-2\nu)}\left(\frac{h}{L}\right)^2\right]^{1/2} \qquad (21)$$

where $v_s = (G/\rho)^{\frac{1}{2}}$ is the velocity of shear waves in the soil. When Eq.(20) is employed in Eq.(17) the maximum pressure on the wall, p_o, is found to be

$$p_o = \frac{32 G S_{v1}(1-\nu)}{\pi \omega_1 L(1-2\nu)} \qquad (22)$$

For a typical value of Poisson's ratio ν, the ratio $(1 - \nu)/(1 - 2\nu)$ has the value 2. For initial design calculations, Eqs.(21), (22), (18) and (19) give the necessary maximum pressure, force and moment when the soil properties, wall proportions, and design earthquake are inserted. The effect of variations in some of the values can easily be ascertained.

(b) Properties increasing with depth.

In many soils, the elastic constants increase with depth, although the density can be considered to remain almost constant. To represent such cases, a solution is required to the problem of Fig.3 with G and k both functions of depth.

Solutions have been obtained for the cases where G is considered to be a general power function of depth, with ρ and k kept constant, and for the situation where density is constant, but k and G increase linearly with depth from zero or arbitrary values at the surface. These solutions are lengthy and will be presented elsewhere. In general they give rise to maximum first mode moments acting on the wall as a result of the maximum force being applied at a height of 0.6 to 0.7 of the wall height above the base.

However, one particular case of a variation of shearing modulus with depth has a special significance, as shown by Bielak (1), and will be analysed further. For this example, it is convenient to locate the zero x-cordinate at the base of the wall rather than at the top, and take x positive upwards. It will be assumed now that G(x) is parabolic with the equation

$$G = a(h^2 - x^2) \qquad (23)$$

where a is a constant. Here G is zero at ground surface and increases with depth.

The equation of motion is found to be

$$\frac{\partial^2 u}{\partial t^2} = \frac{a(h^2-x^2)}{\rho}\frac{\partial^2 u}{\partial x^2} - \frac{2ax}{\rho}\frac{\partial u}{\partial x} - \frac{2ku}{\rho b} \qquad (24)$$

On separating the variables, the motion is again found to be sinusoidal with time, and the equation governing the deflected shape of the shear beam, X(x) is

$$(h^2-x^2)\frac{\partial^2 X}{\partial x^2} - 2x\frac{\partial X}{\partial x} + \left(\frac{\rho\omega^2}{a} - \frac{2k}{ab}\right)X \qquad (25)$$

It is convenient to substitute the new variable s = x/h in Eq.(25) so that it becomes

$$(1-s^2)\frac{\partial^2 X}{\partial s^2} - 2s\frac{\partial X}{\partial s} + \left(\frac{\rho\omega^2}{a} - \frac{2k}{ab}\right)X \qquad (26)$$

This is the Legendre equation, whose solution is expressed in Legendre functions $P_p(s)$ of order p, where p is given by the equation

$$p(p+1) = \left(\frac{\rho\omega_n^2}{a} - \frac{2k}{ab}\right) \qquad (27)$$

The deflected shape of the beam is therefore given by the solution of Eq.(26), taking into account the boundary conditions

$$X = DP_p(s) \qquad (28)$$

The only Legendre functions which are finite at s = 1 (the top of the wall) are those in which p is an integer; these are the Legendre polynomials. However, X must be zero at s = 0, so that $P_p(0)$ must be zero, since D is non-zero. The Legendre polynomials which have zero value at s = 0 are those for which p is an odd integer. Consequently, the modes of vibration of the shear beam are found from Eq.(27) by substituting successively p = 1, 3, 5, etc.

The first mode has a particular interest in this special case. The Legendre polynomial $P_1(s)$ is a straight line, with equation

$$P_1(s) = s \qquad (29)$$

so that the shear beam remains straight as it oscillates in the first mode. All of the equations reduce to particularly simple forms in this circumstance. The first participation factor is 1.5, and the first natural frequency is

$$\omega_1 = \left[\frac{2a}{\rho} + \frac{2k}{b\rho}\right]^{1/2} \qquad (30)$$

The maximum pressure distribution on the wall is triangular, with the maximum at the top, and is given by the equation

$$p_{m_1} = p_o s \qquad (31)$$

where

$$p_o = \frac{1.5kS_{v1}}{\omega_1} \qquad (32)$$

The maximum force acting on the wall P_{m_1} is obtained from the area under the pressure diagram, as given by Eq.(31).

$$P_{m_1} = \tfrac{1}{2} p_o h \qquad (33)$$

Since the pressure distribution is triangular, the maximum force acts at a height of 2/3h from the base of the wall, so that the maximum moment M_{m_1} is found to be

$$M_{m_1} = \frac{1}{3} p_o h^2 \qquad (34)$$

Bielak (1) has demonstrated a further interesting and important property of this special case. Because of the linear nature of the first mode shape, and the orthogonality of the modes, no mode other than the first develops any base moment. Consequently, for a specified earthquake, the moment at the base of a rigid wall is given by Eq.(34) only; there are no additional moments due to the higher modes. The higher modes do, however, cause additional pressures and forces on the wall. The simple polynomial nature of the Legendre functions in this problem makes the contributions of the higher modes easy to calculate.

Linear first mode shapes also occur as special cases when variations of both G and k with depth are employed in the analysis. These will be discussed elsewhere.

(c) Boundary effects

For the constant property shear beam, the variation of the first mode frequency as the boundary AD in Fig.3 (or the other wall) becomes more distant from BC can be seen from Eq.(21). For values of L/h less than unity, it may be concluded intuitively that the model presented in this paper is not applicable; the two-dimensional nature of the real motion is important. The shear beam method probably represents the actual motion of the soil in a first mode realistically in the region L/h > 1.0. However, for L/h > 2 a second mode of vibration still describable by a shear beam can be recognised. In this mode, the vertical plane, half-way between AD and BC in Fig.3 becomes a node, and the soil in the contained space would be represented by two shear beams vibrating symmetrically. However this mode would not be excited by the rigid boundary conditions assumed here. The next mode to be excited under these restraints would be the antisymmetrical one with two nodal planes at the third points along the length L. When AD moves still further from BC the effect of the restraint conditions at AD become unimportant, and the pressures on the wall at BC become those of a wall restraining a backfill of unlimited extent. For this case, it is suggested that the calculational method described above still be employed, but with a value of L/h = 10. Thus the second term in the brackets of Eq.(21) will generally become negligible, but the value of k to be used in the pressure calculations, still based on L/4, will be 2.5h in these conditions.

(d) Effect of flexibility of wall

In reality a wall deflects both by bending and by rotation and translation on its base. The incorporation of bending deflections in the present analysis is complicated,

and a simpler treatment was adopted. A rigid wall hinged at its base was assumed. Only base rotations are represented with rotational stiffness being accounted for by a torsional spring. Simplified calculations indicating the effect of wal flexibility are possible with this model if it is employed with the soil model associated with the Legendre equation, Eq.(26) which gives a linear first mode of vibration. For simplicity, the mass of the wall is neglected. In practice a mass of soil would accompany the wall in its vibrations, which could be significantly affected in consequence. In particular, phase differences between wall and soil vibrations would be possible. The simplified analysis is briefly described.

With a torque spring of value T at the base of the wal the equation of the angular deflection of the wall, θ, under moment M is

$$M = T\theta \tag{35}$$

Because the wall is rigid, the lateral displacement is linear with height. For a linear first mode, the dynamic lateral displacements of the soil shear beam are also linear with height, so that the pressure on the wall at any instant is given by k times the difference of the soil and wall displace ments. The pressure thus also increases linearly with height as in the case of the rigid wall. The effect of the base rotation of the wall can thus be seen to be a reduction in the effective soil stiffness k. By consideration of the moment acting on the base of the wall it can be shown that the wall rotation gives rise to a new soil stiffness k' where

$$k' = \frac{1}{1 + \frac{kh^3}{3T}}\, k \tag{36}$$

Thus, for the first mode, Eqs.(30) and (32) still hold, but in them k must be replaced by k' from Eq.(36). Consequently, the pressures, forces and moments can be calculated as before but taking into account the wall rotation. By substituting appropriate values of various soil properties and reinforced concrete wall dimensions, it appears that in practice the fac tor modifying k in Eq.(36) will be around 0.5.

DISCUSSION

A solution to the problem of Fig.1 with linearly elastic soil, rigid wall, and a sine wave input was obtained by Matsu and Ohara (3) under certain displacement restrictions. The forces and moments in the solutions presented here for a rigi wall are of the same magnitude as those shown by Matsuo and Ohara, and are significantly higher than those calculated by the Mononobe-Okabe method.[III] For the same problem and displacement restrictions, but with a hinged wall as in section (d) above, but including the wall mass, Ishii et al (2) gave a solution which they evaluated to show the phase domains.

Study of the appearance of real retaining walls followi earthquakes as well as the model experiments gives rise to

III My interpretation of the results of Matsuo and Ohara (their Fig.17) is different from that of Seed and Whitman (their Figs.25 through 27).

the following hypothesis as to the sequence of events. Dynamic pressures and moments (higher than Mononobe-Okabe) act to cause wall movements during an earthquake. Irreversible soil displacements occur as the wall deflects away from the retained soil so that residual pressures develop and the wall deflections drift. Eventually partial or complete wall failure occurs with such a large deflection that a wedge of soil slides down behind the wall. On post-earthquake inspection the soil wedge is apparent and looks like confirmation of a Mononobe-Okabe failure mechanism. However, as indicated, the wedge formation is a post-failure condition. Partial failures of flood control channel walls in the 1971 San Fernando, California earthquake, and of the Showa bridge wing walls in the 1964 Niigata earthquake illustrate intermediate stages in the above sequence. Model experiments probably do not adequately represent full-scale wall behaviour during earthquakes.

ACKNOWLEDGMENT

This work was carried out with the assistance of U.S.A. National Science Foundation Grant No.GI-29937. Discussions with J.H.Wood, graduate student at the California Institute of Technology were of great assistance.

REFERENCES

(1) BIELAK, J., Proc.Amer.Soc.Civ.Eng., 95, Jour.Eng.Mech.Div., EM5, Oct.1969.
(2) ISHII, Y., ARAI, M., and H.TSUCHIDA, Proc.2nd World Conf. Earthqu.Eng., 1, 211-230, 1960.
(3) MATSUO, M., and S.OHARA, Proc.2nd World Conf.Earthqu. Eng. 1, 165-173, 1960.
(4) MONONOBE, N., Proc.World Engineering Congress, 9, 275, 1929.
(5) OKABE, S., Jour.Japanese Soc.Civ.Eng., 12, No.1, 1926.
(6) SEED, H.B. and R.V.WHITMAN, Conference on Lateral Stresses and Earth-Retaining Structures, Amer.Soc. Civ.Eng., 103-147, 1970.
(7) WOOD, J.H., Personal communication, 1971.

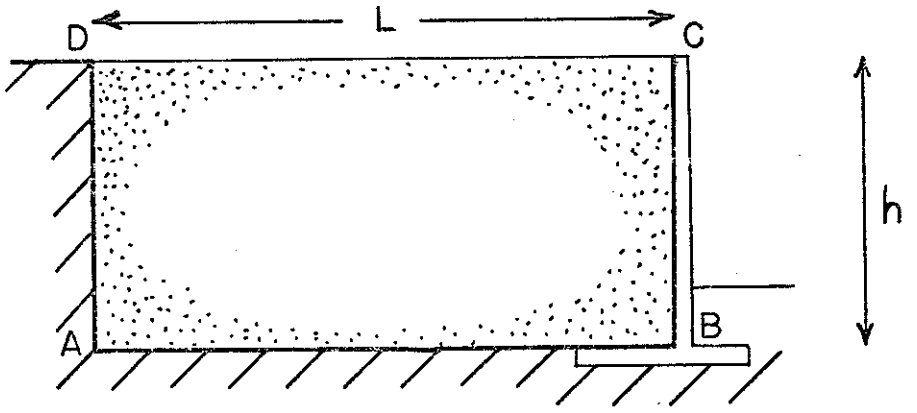

FIG.1 REGION OF PROBLEM

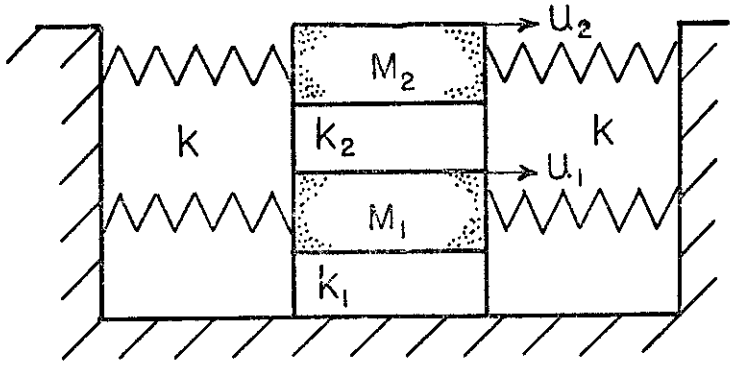

FIG.2 LUMPED PARAMETERS

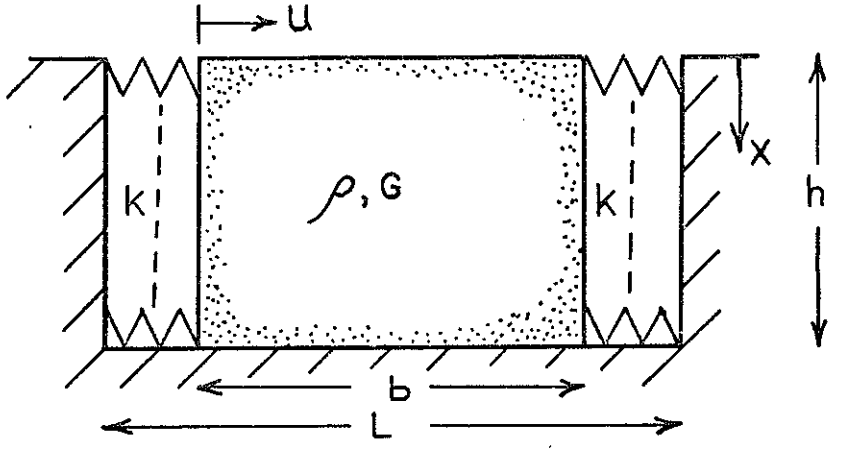

FIG.3 CONTINUOUS SHEAR BEAM

AMBIENT VIBRATION TESTS OF FULL-SCALE STRUCTURES

by

F. E. Udwadia[I] and M. D. Trifunac[II]

SYNOPSIS

Ambient vibration testing of full-scale structures excited by wind and microtremor ground motions is discussed in terms of (1) comparison with higher level vibration generator tests; (2) comparison with earthquake-excited motions; (3) changes in ambient vibration response between pre- and post-earthquake conditions; and (4) analysis of three-dimensional building models. Information is given on modern methods of ambient test measurements based on magnetic tape recording and electronic analog-digital conversion.

INTRODUCTION

Parameters of fundamental engineering importance in the dynamic analysis of structures are the natural frequencies of vibration and the damping in the various modes[1,2,3]. Since these parameters determine the behavior of structures during strong ground shaking until yielding becomes significant, it is important to develop experimental procedures for measuring them in full scale structures.

Engineering structures are usually large and require large forces for their excitation. One is therefore led to utilize dynamic loadings which may arise naturally. Larger loads created by strong winds or earthquakes can also be used to study the response at higher excitation levels. Most of the wind and background noise loadings, however, represent low level excitations[4-7] when compared with structural design loads. Though the use of these low level excitations has not been completely ignored in the past[8] it has gained considerable attention in the past few years with the advent of superior instrumentation[5-12]. The advantages of these tests over forced vibration measurements[13,14] are that they are quick, easy to perform and can be conducted by a small group of people. Also, with improved methods of analysis, excellent data on three-dimensional oscillations[15] can be obtained.

Since the frequencies during large earthquakes show marked differences from those ascertained by pre-earthquake low amplitude vibration tests, pre- and post-ambient testing of structures gives valuable data on the overall reduction in structural stiffness caused by large deformations. This paper, therefore, attempts to present the state of the art in ambient vibration testing of structures through an outline of studies made on four typical modern buildings.

DESCRIPTION OF MEASURING EQUIPMENT

Seismometers with velocity type transducers are usually used in ambient vibration tests. The natural period of these instruments is close to one second and the damping is adjusted to 0.7 of the critical

[I] Research Fellow, Applied Science, EERL, Calif. Inst. Technology, Pasadena, California.

[II] Assistant Professor, Applied Science, EERL, Calif. Inst. Technology.

value. Amplification of all frequencies higher than about 1 cps is nearly a constant with a 6 db per octave fall off for lower frequencies. This lov frequency fall off can be used to advantage in the study of tall structures with fundamental periods close to two seconds or longer, for the low frequency modes do not dominate the records, thus facilitating the study of some of the higher modes of vibration.

The transducer output is amplified through a signal conditioner having a maximum amplification of 350,000. When used with a velocity transducer, output voltages proportional to velocity, displacement or acceleration can be obtained depending on the frequency ranges of interest.

The amplified signal is recorded on a low noise FM-tape recorder with high tape speeds (15 ips) to reduce wow and flutter. The analog data are then converted to digital form on an analog-digital converter. During each measurement a direct visual display on ink recorders is made. This permits the digital data blocks to be edited before the spectral analysis proceeds, and assists in monitoring the measurements during the field tests.

Various sources of error may arise at different points in the measurement chain. The generator constant of the transducer may vary by about 1-2% depending on the level of excitation and the frequency content of the signal. The amplification process may introduce noise voltages and FM modulation-demodulation errors in the tape recording equipment may occur. Noise in the analog to digital conversion of data can be more effectively reduced through improved resolution of the converter rather than through increased sampling rates[16].

FIELD PROCEDURES, DATA ANALYSIS AND INTERPRETATION

Most ambient or shaker excited building vibration tests assume that the structure can be approximated by a damped, linear, discrete or continuous system whose properties vary with reference to a line. In some cases[4] measurements indicate that floor structures are sufficiently stiff so that the above assumption of a one-dimensional line model is acceptable. In the experimental studies, it is then assumed that building vibrations can be expressed as a superposition of modes associated with discrete frequencies. This approach requires a simultaneous measurement of motion at a minimum of two different floor lev

Typically, two simultaneous velocity recordings are made in each run. One of the transducers (the reference instrument) is left in place while the other is shifted up and down or sideways along a line suitable for the defining of a mode that is to be measured. The recorded data are converted to digital form and low pass filtered[6,9] to remove any aliasing effects in the computed spectrum. The sampling frequency which governs the Nyquist frequency of the time series is chosen so as to be capable of retrieving information up to the desired frequency limit. Generally an instrument correction[16] is also applied to compensate for the frequency characteristics of the data acquisition chain. The data are next Fourier analysed and the ratio of the Fourier spectra amplitude at any floor to that at the reference floor is determined. Thi

ratio is proportional to the mode shape amplitude at the floor for a given frequency of vibration.

Since the effectiveness of this testing procedure depends on the accuracy of the recorded motions at the reference level, it is necessary to ensure a high signal to noise ratio at that key station. To do this, the reference point is usually chosen so that it does not lie near any of the nodes of the mode shapes of vibration that are being studied.

When choosing the frequencies[9] at which the ratios are to be taken it may not be desirable to pick exactly the peak values of the spectra. It may happen that two translational modes, or a translational and a torsional mode, may have very close frequencies and the problem of separating the modes may become troublesome. In such cases, a point away from the peak might be selected in such a way that it is as far as possible from the other frequency in question. On the other hand it must be remembered that picking a mode amplitude at a frequency differing by more than a few percent from the natural frequency in question may lead to serious perturbations of the actual mode amplitudes[18]. Therefore when two modes happen to have very close frequencies a special method of analysis may be required. The identification of natural frequencies is considerably simplified by a simultaneous study of cross spectral amplitude as well as cross spectral phase plots[6,15].

Torsional modes of vibration can be recovered by placing two instruments on the same floor in diagonal corners and appropriately summing their outputs so as to recover predominantly the torsional motions[9].

BRIEF DESCRIPTION OF THE FOUR STRUCTURES STUDIED

Building A[5] consists of a twenty-two story ductile moment resisting steel frame (180 ft x 70 ft in plan), separated by a seismic joint from a two-story U-shaped structure which surrounds it.

Building B[9] is a thirty-nine story moment resisting steel frame with a story height of 13 ft 1 in. The tower is structurally separated from the parking structure by a joint allowing two inches of horizontal movement.

Building C[4] is a nine story reinforced concrete building 75 ft x 69 ft in plan having a central core wall and two shear walls in the N-S direction.

Building D[1] is a symmetrical nine story steel frame with plan dimensions 220 ft x 40 ft. Typical floor height is 16 ft. The large length to width ratio of this structure indicates interesting dynamic features.

COMPARISON OF AMBIENT AND HIGHER LEVEL VIBRATION TESTS

As the amplitudes involved in ambient vibration tests are of the order of 10 microns, a natural question is whether these low amplitude motions involve the major structural elements in essentially the same way as larger motions.

Figure 1 indicates such a comparison between ambient and forced vibration test results for Building A. The open circles refer to the ambient test while the full circles refer to the forced vibration test. Th nature of the load distributions on the structure in the two types of test are quite different. Shaker tests essentially involve a point source of sinusoidal excitation whereas ambient loads are distributed over the structure. The frequencies and the mode shapes calculated[5,17] show that except for the fifth N-S (4.03 cps) and torsional mode (4.61 cps) frequencies measured from ambient tests are either the same as or higher than those determined from the forced vibration tests. On an average, ambient tests show frequencies about 4% higher than those obtained by the shaker experiment. A comparison of the various mode shapes indicates systematic differences mainly occurring at the upper floor levels. The divergence is largest at the top of the building and generally leads t higher modal amplitudes from shaker than from ambient tests. This phenomenon, which is more pronounced for higher modes[18], is attributable to modal interference, and is a consequence of the concentrated source of excitation being at a frequency only slightly different from the resonant frequency. Average percentage differences in the mode shape amplitudes relative to the peak ambient vibration amplitudes are about 2 for the fundamental mode and increase to about 20% for the fifth mode.

Mode shapes and fundamental frequencies of vibration obtained frc ambient and higher level excitation tests of Building C are shown in Fig. Typical acceleration amplitudes during the ambient test were 10^{-8} g whi those for the forced vibration test were 10^{-2} g, a difference of six orde of magnitude. Unlike Building A, the present comparison of forced and ambient tests does not indicate any systematic changes in frequency for changes in amplitude of about six orders of magnitude. The mode shape of vibration for the first modes in both directions are in excellent agree ment. Small systematic changes probably caused by modal interference are detectable in the second E-W mode.

PRE- AND POST-EARTHQUAKE AMBIENT VIBRATION RESPONSE

The frequencies and mode shapes of vibration of Building B prior to and after the San Fernando, California, Earthquake of February 9, 1971 are given in Fig. 2. Reduction in the natural frequencies in the N-S and E-W directions as well as in torsion are observable. The average percent reduction in the N-S frequencies is about 19%, in the E-W about 15%, and in torsion about 17%. This percentage reduction in frequency is almost a constant for all the modes of any one kind (i. e., either N-S, E-W or torsion). The ratios of the higher frequencies to th fundamental frequency in the N-S direction from both pre- and post-earthquake ambient testing follow closely the sequence 1,3,5,7,9... indicating that the overall N-S structural response in these tests remained predominantly of the uniform shear beam type[9]. A constant percentage reduction in all the frequencies can then be attributed to a roughly constant reduction in rigidity all along the height of the structur Pre- and post-earthquake response are also shown for Building C (Figs. 3 and 4). As seen from Fig. 4, Building C has undergone a series of ambient vibration tests. The percentage reductions in the first and second E-W mode are 13.8% and 9.3% respectively while in the stiffer N-S direction a frequency change of only 4.75% is indicated. The

fundamental E-W period since the San Fernando main shock seems to show a gradual decrease. Ambient vibration tests in February after the main shock indicated a fundamental E-W period of 0.8 secs (Fig. 3) whereas a smaller aftershock in March indicated a fundamental period of about 0.75 secs. Later in the same month ambient tests indicated a period of 0.77 secs. Recent man-excited ambient tests indicate a period of 0.73 secs. The mode shapes determined from post- and pre-San Fernando ambient tests (Fig. 3) indicate little change in the first N-S and both E-W modes.

COMPARISON OF AMBIENT VIBRATION TESTS WITH EARTHQUAKE RESPONSE

Figure 4 indicates the NS and EW transfer functions of Building C computed from the basement and roof records obtained during the San Fernando earthquake[19]. Both components of ground motion were studied yielding fundamental periods in the N-S and E-W directions. The figure indicates marked shifts in the frequencies from those measured in the ambient or forced vibration tests. The broad peaks at about 1.7 cps in the N-S direction and at 1.0 cps in the E-W direction (Fig. 4) seem to represent the integrated effect of gradual shifts in the fundamental frequencies of the structure for different levels of excitation. To study this effect further, transfer functions were computed for 8 sec "window lengths" of both N-S and E-W records, starting from the beginning and displacing the window each time by 2 secs. The fundamental periods in the E-W direction are shown plotted in Fig. 7 versus the time corresponding to the center of each window. The first 8 secs of the E-W component of motion (Fig. 7) show a fundamental frequency of 1.32 cps which quickly reduces to 1 cps and remains thereat up to about 16 secs at which time the response shows a much lower amplitude. The transfer function at this time indicates a "double peak", the higher frequency peak being more predominant. As the window shifts out of this rather low response zone the fundamental frequency drops back to 1 cps and remains there till the rather quiescent segment of response between about 44 secs to 54 secs sets in. The frequency jumps back then to 1.33 cps. Later excitations cause the frequency to drop back to 1.0 cps and gradually increase to about 1.23 cps for the window centered at 80 secs. A similar behavior of the N-S component of motion is shown for the first two modes in Fig. 6. Figure 5 shows the transfer functions obtained from an analysis of the complete records at basement and roof in Building D. Changes in the fundamental frequency at these large levels of excitation together with measurements of the pre- and post-earthquake responses of the structure are clearly indicated.

TWO-DIMENSIONAL TESTING OF STRUCTURES

In the testing of most structures it is generally assumed that their behavior will be similar to continuous or discrete mass line models, the floor slabs acting as rigid members. However for structures having a high length to width ratio, such as Building D, at least a two-dimensional testing procedure, if not a three-dimensional procedure, may be required. Forced vibration testing aimed at obtaining three-dimensional modes will generally be far more time consuming than ambient tests and will require repetitious response determinations for different shaker positions.

Higher dimensional vibrations involve the added complexity that corresponding to any one mode in the vertical direction, the building could theoretically vibrate at an infinite number of modes in the horizontal direction. This is clearly indicated in Fig. 8. For example at frequencies 2.90 cps, 3.6 cps and 4.9 cps the mode shape as seen in any vertical N-S plane would be a "second mode" of vibration. Differences in the nature of vibration of the floor slabs however arises, the floor slabs vibrating as free-free beams at 3.6 cps and 4.9 cps.

CONCLUSIONS

Ambient vibration testing is an easy, quick and efficient way of studying the linear response of structures. Results from ambient and forced vibration tests show good argument. Though pre- and post-ambient testing of structures gives valuable data on the overall reductio in structural stiffness caused by damaging earthquakes, structural frequencies during large earthquakes show marked differences from those ascertained by pre-earthquake low amplitude vibration tests. Ambient vibration testing has been shown to be an invaluable tool for the study of two or three dimensional vibrations of extended structures.

REFERENCES

(1) Nielsen, N., "Dynamic Response of Multistory Building", Earthquake Eng.Res.Lab., EERL, Calif.Inst.Tech., Pas. (1964).

(2) Caughey, T.K., "Classical Normal Modes in Damped Linear Systems", J.Appl.Mech. 27, 269-271 (1960).

(3) Jennings, P.C., and J. Bielak, "Dynamics of Soil-Structure Inte action", Earthquake Eng.Res.Lab., EERL 72-01, California Institute of Technology, Pasadena, California (1972).

(4) Kuroiwa, J., "Vibration Test of a Multistory Building", Earthqua Eng.Res.Lab., EERL, Calif.Inst.Tech., Pasadena, (1967).

(5) Trifunac, M.D., "Wind and Microtremor Induced Vibrations of a 22 Story Steel Frame Building", Earthquake Eng.Res.Lab., EERL 70-1, Calif.Inst.Tech., Pasadena (1967).

(6) Udwadia, F.E. and M.D. Trifunac, "Vertical Vibrations of Struc tures" (Abstract) presented at the meeting of the Seism. Soc. of America, Riverside, (1971).

(7) Hudson, D.E., Keightley, W.O. and N. Nielsen, "A New Method for Measurement of Natural Periods of Buildings", Bull. Seisn Soc. America, 54, 233-241, (1964).

(8) U.S. Coast and Geodetic Survey, "Earthquake Investigations in California, 1934-1935", Special Publication No. 201, U.S. Dept. of Commerce, Washington, D.C. (1936).

(9) Trifunac, M.D., "Ambient Vibration Test of a 39 Story Steel Frar Building", Earthquake Eng.Res.Lab., EERL 70-2, California Institute of Technology, Pasadena (1970).

(10) Ward, H.S. and R. Crawford, "Wind Induced Vibrations of Building Modes", Bull. Seism. Soc. Amer. 56, 793-813 (1966).

(11) Blanford, R.B., McLamore, R.V. and J.A. Aunon, "Structural Analysis of Millikan Library from Ambient Vibrations", Earth Sciences, Teledyne Co., Rept. No. 616-0268-2107 (1968)

(12) McLamore, R.V., "Ambient Vibration Survey of Chesapeake Bay Bridge", Teledyne Geotronics Rept. No. 0370-2152 (1970).

(13) Englekirk, R.E. and R.B. Matthiesen, "Forced Vibration of an 8 Story Reinforced Concrete Building", Bull.Seism.Soc.Am. 57, 421-436 (1967).

(14) Takeuchi, M., "Vibrational Characteristics of Buildings, Part I. Vibrational Characteristics of Actual Buildings Determined by Actual Tests", Proc. 2nd World Conf. Earthquake Eng., Tokyo (1960).

(15) Udwadia, F.E. and M.D. Trifunac, "Two-Dimensional Ambient Vibration Tests of Structures", (Abstract) presented at the meeting of the Seismological Soc. of Amer., Hawaii (1972).

(16) Udwadia, F.E., "Investigations of Earthquake and Microtremor Processes", Earthquake Eng.Res.Lab., EERL 72-02 (1972).

(17) Jennings, P.C., Matthiesen, R.B. and J.B. Hoerner, "Forced Vibration of a 22 Story Frame Building", Earthquake Eng.Res. Lab., Calif.Inst.Tech., Pasadena and Earthquake Eng. and Struct. Lab., University of California, Los Angeles.

(18) Trifunac, M.D., "Comparison Between Ambient and Forced Vibration Experiments", Earthquake Eng. and Struct. Dynamics, Vol. 1, 133-150 (1972).

(19) Hudson, D.E., Trifunac, M.D., Udwadia, F.E., Vijayaraghavan A. and A. G. Brady, "Analysis of Strong Motion Accelerograms, Vol. IV--Fourier Amplitude Spectra, Part A", Earthquake Eng. Res.Lab., EERL 72-100, Calif.Inst.Tech, Pasadena (1972).

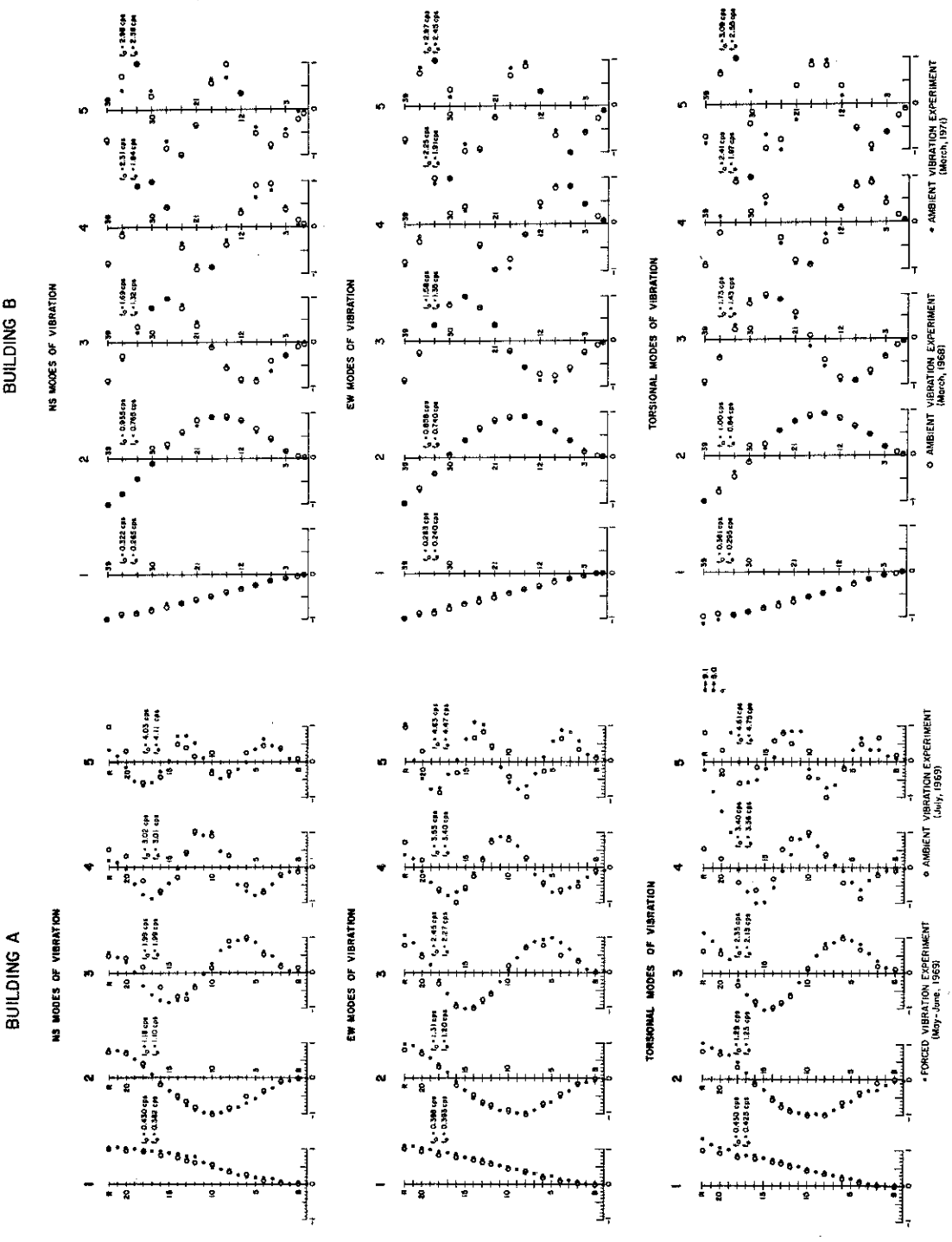

Figure 1

Figure 2

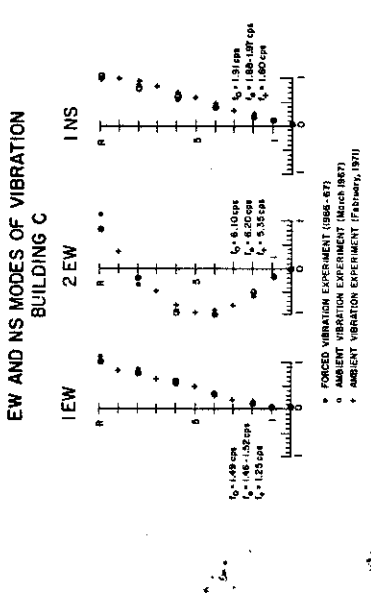

Figure 3

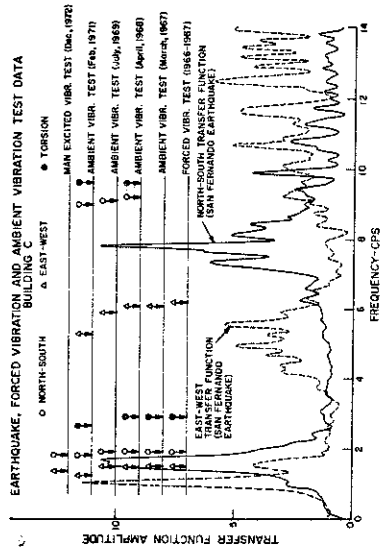

Figure 4

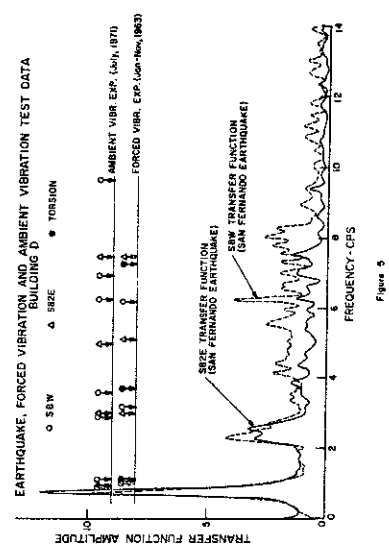

Figure 5

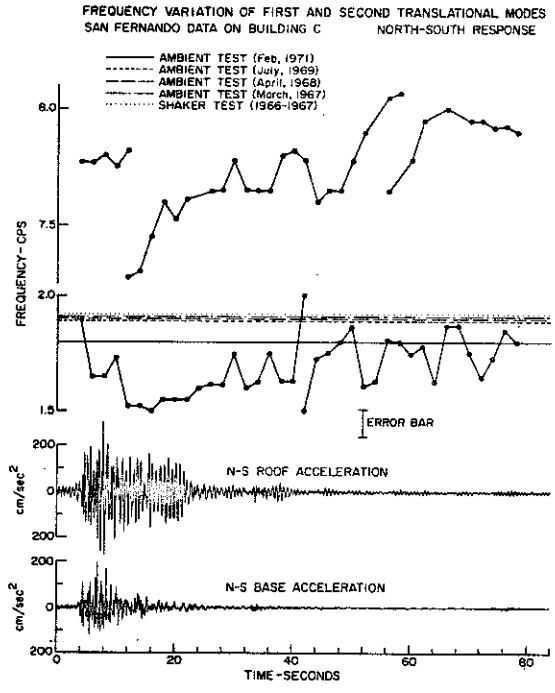

Figure 6

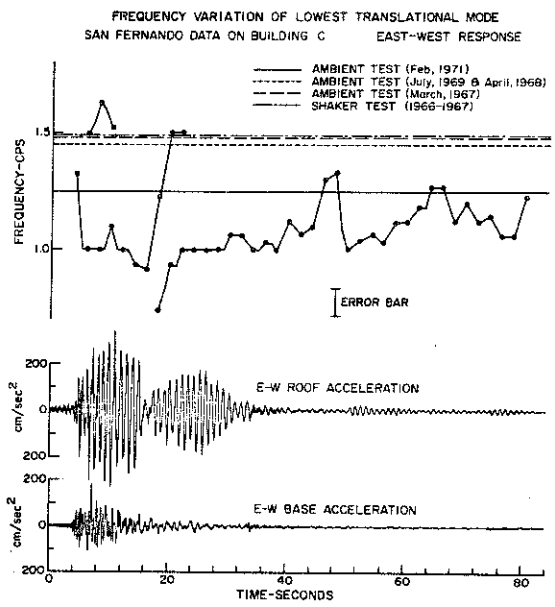

Figure 7

TWO DIMENSIONAL N-S MODES OF VIBRATION
BUILDING D

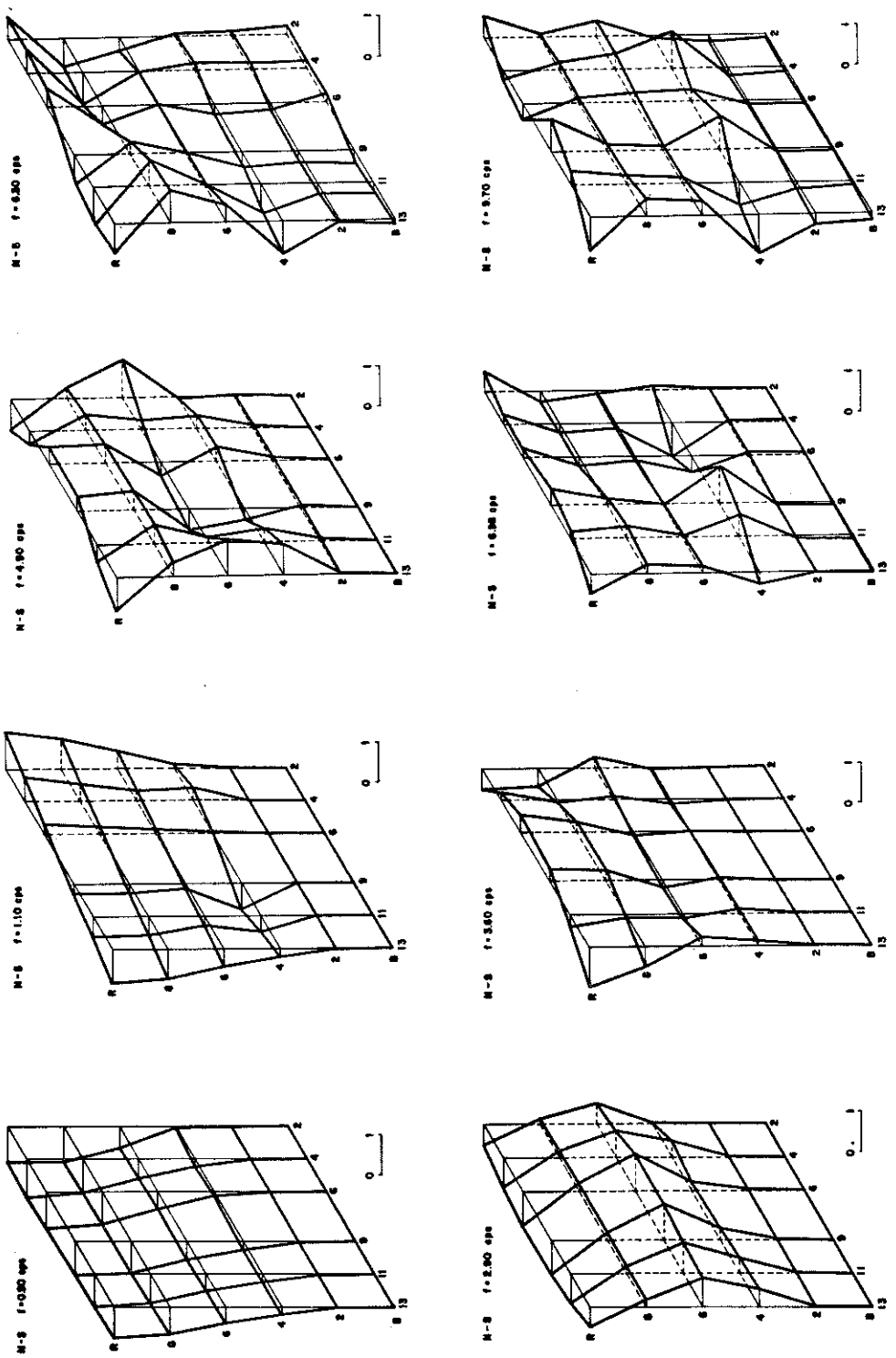

Figure 8

CHARACTERIZATION OF RESPONSE SPECTRA BY PARAMETERS GOVERNING THE GROSS NATURE OF EARTHQUAKE SOURCE MECHANISMS

by

Mihailo D. Trifunac[I]

SYNOPSIS

Prediction of response spectra for earthquake engineering purposes is considered from the point of view of the dislocation theory of earthquakes. It is shown that the traditional scaling of response spectra by the predicted peak acceleration should be limited to the high-frequency end of the spectrum, and that the peak acceleration in the near field is not strongly correlated with earthquake magnitude. The amplitude of the long-period end of the response spectrum at source to station distances greater than about 10 source dimensions should be correlated with seismic moment, while for distances less than about one source dimension this amplitude should be proportional to the permanent ground displacement. To reconcile the existing extensive data on seismicity of active regions based on the magnitude scale, it is shown that magnitude correlates approximately with seismic moment.

SIMPLE DISLOCATION MODEL

Although many parameters are required to describe fault motion in time and space, strong-motion studies of the source mechanism are, at the present time, mainly concerned with those parameters that have the most prominent influence on the nature of recorded ground motion. These are: (1) effective stress σ (Figure 1) and (2) the seismic moment M_o. The seismic moment $M_o \equiv \mu \bar{u} A$ combines information on rigidity in the source region μ, average dislocation $\bar{u}$ and the area of faulting A in one parameter. The significance of seismic moment[1] emerges from the fact that it specifies the amplitude of the long-period level ($\omega \to 0$) of the Fourier amplitude spectrum $\Omega_{FF}(\omega)$ of the far-field S-wave displacement through $\Omega_{FF}(\omega) \to M_o(4\pi\rho R\beta^3)^{-1}$. Here ρ is the material density, R is the source to station distance and $\beta = (\mu/\rho)^{1/2}$ is the shear wave velocity. However, near a fault the significance of the overall fault size and therefore its moment M_o are lost and the static displacement u after the earthquake becomes the only dominant factor for the long-period components of the near-field Fourier amplitude spectrum $\Omega_{NF}(\omega)$ which for $\omega \to 0$ tends to $\Omega_{NF}(\omega) \to u/\omega$.

As shown in Figure 1, an earthquake dislocation in an infinite space might be modeled by a plane surface area A whose size is measured by the radius r of an equivalent circular disc[2]. For simplicity it can be assumed[1, 2] that the stress pulse σ (Figure 1) produced by a sudden drop of surface tractions on A during an earthquake is applied instantaneously over the whole fault surface. The approximate nature of the resulting S-wave displacement is then as shown in Figure 1 and the resulting Fourier amplitude spectra of ground displacement[1, 2] become

---

[I]Assistant Professor, Applied Science, Earthquake Engineering Research Laboratory, California Institute of Technology.

$$\Omega_{NF}(\omega) = \frac{\sigma\beta}{\mu}\,\omega^{-1}(\omega^2+\tau^{-2})^{-1/2}$$ (for near-field S-wave motion at P, Fig. 1) (1

and

$$\Omega_{FF}(\omega) = \frac{r}{R}\,\frac{\sigma\beta}{\mu}\,\frac{1}{\omega^2+\alpha^2}$$ (for far-field S-wave motion at Q, Fig. 1) (2

The time constant τ can be shown to be related to the size of an earthqua
r and shear wave velocity β through $\tau = \eta r/\beta$ where η is a dimensionless
parameter depending on the fault geometry, elastic constants and the poi
of observation. Values of η range from 0 to η_{max}, which is given in Tal
for several simple fault geometries. Parameter α, also called the "corn
frequency" is given by $\alpha = 2.34\beta/r$[1, 2, 3].

The effective stress $\sigma = \sigma_o - \sigma_f$ (Figure 1) is therefore the principal parameter specifying the spectral displacement amplitudes at high frequencies. As $\omega\to\infty$, $\Omega_{NF}(\omega)\to(\sigma\beta)/(\mu\omega^2)$ for $\omega>>1/\tau$ and $\Omega_{FF}(\omega)\to(r\sigma\beta)/(R\mu\omega$ for $\omega>>\alpha$. Although these results imply that the acceleration spectra of S waves would have constant amplitudes for high frequencies, attenuation a scattering reduce the observed amplitudes significantly. The precise nat of attentuation of high-frequency seismic waves is not well understood, p because of the sparsity of recorded accelerograms. It may be assumed the purpose of this qualitative discussion, however, that the attenuation body waves is adequately described by $2\exp[-(\omega R)/(2Q\beta)]$ where the Q fa may range from about 50 to 500[2, 3], and 2 models the amplification due the half-space boundary. The normalized spectra (1) and (2) corrected fo attenuation are plotted versus period $T = 2\pi/\omega$ in Figure 2 for an arbitrary choice of $\alpha = 1/\tau = \pi/5$.

CHARACTERIZATION OF EARTHQUAKE RESPONSE SPECTRA

A method often used in scaling of the design spectrum amplitudes based on an assumed empirical relationship between peak acceleration a earthquake magnitude. Figure 3 shows data on peak acceleration, plotte versus distance from the fault, and indicates no strong correlation betwe peak acceleration and earthquake magnitude. In fact, this figure shows an earthquake with smaller magnitude can have higher peak acceleration the same distance. This is consistent with the simplified theory in this p which suggests that peak acceleration should be correlated with the effec stress σ, since the peak acceleration usually samples the high-frequency spectral amplitude for $\omega>\alpha$ or $\omega>1/\tau$.

One must know μ, $\bar{u}$, and A to scale the long-period end of the spectrum by the moment M_o for intermediate and large distances ($R>>r$) Although these quantities might be estimated from geological and seismo gical investigations in the area under consideration, frequently the only statistics available are in terms of earthquake magnitude. There are se magnitude scales currently in use, but in this paper we will employ Rich local magnitude M_L for shocks less than 6 and the surface wave magnitu M_s for shocks greater than 6. The magnitude gives an estimate of the amplitude of the long-period end of the spectrum if the frequency band of the recording instrument is centered between 0 and α. Therefore, since $\Omega_{FF}(0) = M_o(4\pi\rho R\beta^3)^{-1}$ a relationship should exist between the magnitude an earthquake and the seismic moment M_o. Figure 4 presents such a relationship based on data from central and southern California[2, 3, 4]. though there is an appreciable scatter a definite trend exists that is give approximately by $\log_{10}M_o = 1.45M + 16.0$, where M stands for $M_L \le 6$ or M_s

For a transient, band-limited, ground acceleration the amplitude of the high-frequency end of the SD spectrum (relative displacement spectrum) tends to $(T/2\pi)^2$ times the peak ground acceleration, where T is the undamped natural period of an oscillator, while the long-period end of the SD spectrum tends to the maximum ground displacement. Depending on the degree of conservatism desired, one may take the average or the maximum of the observed accelerations at a given distance from a fault (Figure 3) to find the high-frequency amplitude of the pseudo relative velocity spectrum $PSV \equiv (2\pi/T)SD$. The long-period amplitude of the same spectrum would be $2\pi u/T$ for a station essentially at the fault. For a distant station using the approximate pulse shape shown in Figure 1 and approximating the dislocation surface A with a disc of radius r, it can be shown that for $R \gg r$, $u_{max} = [0.069/(\mu r R)] \times 10^{1.45+16}$. Thus at large distances, where only the dynamic field contributes to the ground displacement this result can be used to approximate the maximum amplitude associated with S-wave motion.

The above characterization of earthquake spectra, of course, gives only the general spectral trends for body waves in an elastic homogeneous infinite space. Although this characterization may be used as the first order approximation of Fourier and response spectra of strong ground motion, it must be remembered that local geologic formations may change the spectral amplitudes appreciably through reflection, refraction, scattering, and focusing effects, and through wave-guide phenomenon leading to surface waves. Since destructive earthquake ground motion is largely involved with the near-field phenomenon the above model applies directly to a large group of practical problems.

REFERENCES

(1) J. N. Brune, Tectonic Stress and the Spectra of Seismic Shear Waves, J. Geophys. Res. 75, 4997-5009 (1970).

(2) M. D. Trifunac, Stress Estimates for the San Fernando, California, Earthquake of February 9, 1971: Main Event and Thirteen Aftershocks, Bull. Seism. Soc. Am., 62, 721-750 (1972).

(3) M. D. Trifunac, Tectonic Stress and Source Mechanism of the Imperial Valley, California, Earthquake of 1940, Bull. Seism. Soc. Am., 62, 1283-1302 (1972).

(4) M. Wyss and J. N. Brune, Seismic Moment, Stress, and Source Dimensions for Earthquakes in the California - Nevada Region, J. Geophys. Res. 73, 4631-4694 (1968).

TABLE I

Type of faulting and fault geometry	η_{max}	r represents
Dip-slip displacement along an infinitely long narrow strip in a uniform shear field	$\frac{3}{4}$	fault width
Infinitely long vertical surface fault with strike slip displacement	2	fault width
Circular fault plane in an infinite medium	$\frac{12}{7\pi}$	radius of circular dislocation
Elliptical fault plane $x^2/a^2 + y^2/b^2 \leq 1$; ν depends on the ratio a/b, direction of faulting and elastic constants, $1 < \nu < 2$.	$\frac{2}{\nu}$	r = b

(figure 1)

BRUNE'S DISLOCATION MODEL FOR S WAVES

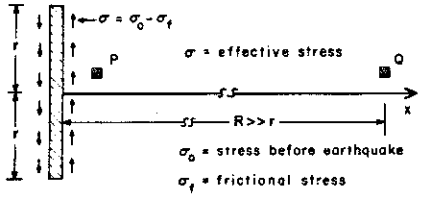

AT POINT P (NEAR-FIELD; X≈0):

$u = \frac{\sigma}{\mu}\beta\tau\,(1-e^{-t/\tau})$

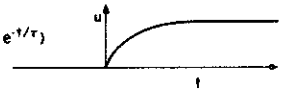

AT POINT Q (FAR-FIELD; R>>r):

$u = \frac{r}{R}\frac{\sigma\beta}{\mu}\,t'e^{-\alpha t'}$

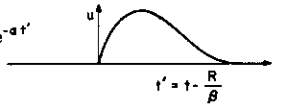

(figure 2)

NORMALIZED FOURIER AMPLITUDE SPECTRA OF GROUND ACCELERATION

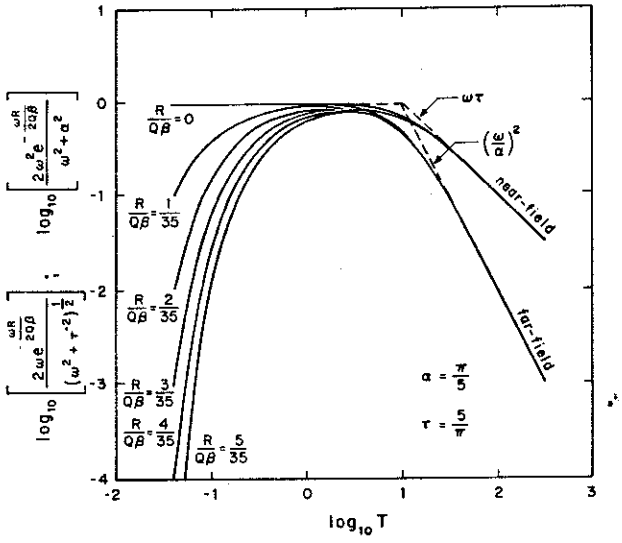

(figure 3)

ATTENUATION OF MAXIMUM ACCELERATION

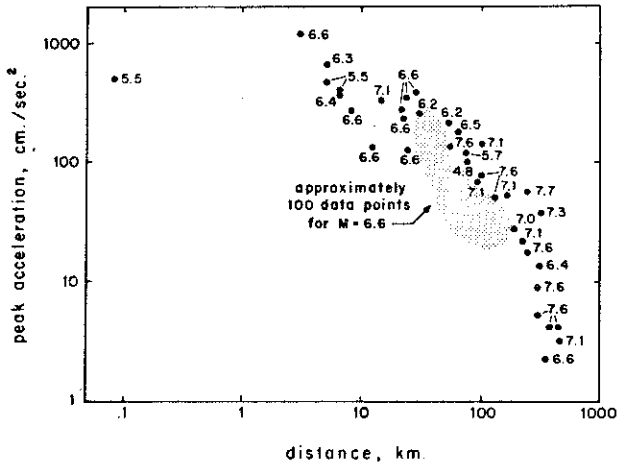

(figure 4)

LOGARITHM OF SEISMIC MOMENT AS A FUNCTION OF MAGNITUDE

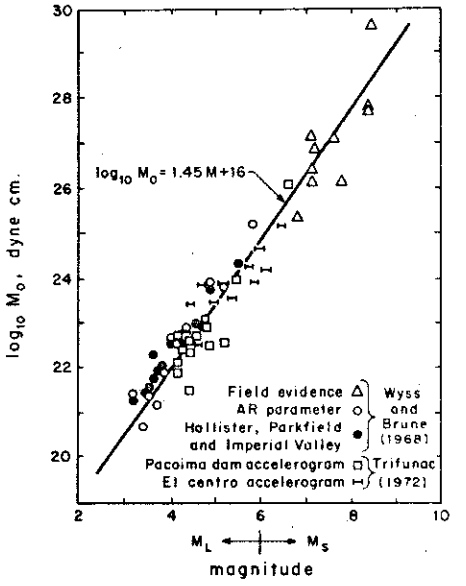

COMPUTATION OF INDIVIDUAL FOURIER SPECTRUM ORDINATES

by

P. C. Jennings[I]

SYNOPSIS

A method is presented to calculate selected ordinates of Fourier amplitude and phase spectra. The approach is based on the relation between the Fourier spectra of an accelerogram and the final displacement and velocity of an undamped oscillator subjected to the same accelerogram. Because only the final values of response are required, superposition is used to form equivalent excitations with durations of only one-quarter of the period of the corresponding undamped oscillator.

INTRODUCTION

Fourier spectrum techniques have become common in earthquake engineering in recent years because of the efficiency of the Fast Fourier Transform (FFT) and the general use of Fourier methods in other technical fields. Typically, the FFT operates on 2^N equally spaced points in the time domain to produce 2^{N-1} Fourier amplitude spectrum ordinates, equally spaced in the frequency domain from 0 to $1/2\Delta T$ cps, Δt being the interval of digitization. To complement the capabilities of the FFT, there is occasionally a need to calculate a few spectrum points in narrow frequency bands or to analyze, over selected frequency bands, records of longer duration than can be accommodated conveniently by standard FFT programs. The present calculation method, based on the relation between Fourier spectra and the response of an undamped linear oscillator, permits accurate and rapid calculation of selected Fourier spectrum ordinates.

FOURIER SPECTRA AND EARTHQUAKE RESPONSE

Ordinates of Fourier amplitude spectra are closely related to the response of an undamped single degree of freedom oscillator (1, 2, 3, 4). The analysis can also be extended to relate the ordinates of phase spectra to the undamped response (5). If $|F(\omega)|$ and $\psi(\omega)$ are the Fourier amplitude and phase spectrum ordinates as a function of ω for an accelerogram $\ddot{z}(t)$ of duration T, and if $x(t)$ and $\dot{x}(t)$ are the displacement and velocity of an undamped oscillator with natural frequency ω subjected to the same accelerogram, then it can be shown (5) that

$$|F(\omega)| = [\dot{x}^2(T) + \omega^2 x^2(T)]^{\frac{1}{2}} \; ; \quad \tan\psi = \frac{\omega x(T) \cos \omega T - \dot{x}(T) \sin \omega T}{\dot{x}(T) \cos \omega T + \omega x(T) \sin \omega T} \qquad (1)$$

These results can be related to an associated free vibration problem as shown in Fig. 1. First as indicated in 1a and 1b, a segment of zero excitation and response is added at the beginning to make the total duration an integer multiple of the natural period, $T_o = 2\pi/\omega$. Then, as shown

[I]Professor of Applied Mechanics, California Institute of Technology, Pasadena, California.

in 1c, an undamped oscillator released with $x(T)$ and $\dot{x}(T)$ will have these same values at the end of the excitation. If the free vibration is treated as a response and Eq. (1) applied, it will be seen that the associated free vibration has the same Fourier ordinates as the accelerogram. The conditions at the original origin, $t = 0$, can be analyzed to show that $|F(\omega)|^2$ is twice the total energy per unit mass of the associated free vibration, and $\tan^2\psi$ is the quotient of the initial potential and kinetic energies of the associated free vibration.

CALCULATION OF RESPONSE AND FOURIER ORDINATES

The calculation is performed by computing the velocity and displacement, at the end of the earthquake, of an undamped oscillator subjected to $\ddot{z}(t)$. Equations (1) are then used to find the Fourier spectrum ordinates. To set up the calculations, the length of record can be taken as a multiple of the natural period (by assuming an initial segment of zeroes) without loss of generality. The computation method is based on superposition; Fig. 2 shows that two impulses at corresponding times with respect to the period can be superposed as far as the response at $t = T$ is concerned. This feature allows the excitation to be cut into segments of duration T_o and superposed to form an equivalent excitation, $\ddot{z}_o(t)$, with duration of only one natural period.

The response of the undamped oscillator to $\ddot{z}_o(t)$ is basically four integrations of the accelerogram with one-quarter of a sine wave. By appropriate definition of quarter-cycle time scales and associated accelerograms, the calculation of $x(T)$ can be reduced to the calculation of the final velocity of an undamped oscillator to an equivalent quarter-cycle accelerogram. Similarly, $\dot{x}(T)$ is the final displacement of an undamped oscillator subjected to a different quarter-cycle accelerogram These relations can be written as

$$x(T) = -\frac{1}{\omega}\dot{x}^*(T_o/4, \ddot{z}_S) \quad \dot{x}(T) = \omega x^*(T_o/4, \ddot{z}_S) \qquad (2$$

in which $\ddot{z}_S(t)$ and $\ddot{z}_S(t)$ are reduced, quarter-cycle accelerograms and x^* and $\dot{x}^*$ are the final displacement and velocity, respectively, o an undamped oscillator subjected to the reduced accelerograms in the usual manner. Hence, the calculation of $x(T)$ and $\dot{x}(T)$ is reduced to two calculations of the final response of an undamped oscillator to accelerograms of duration $T_o/4$. Any method can be used to calculate th response.

A subroutine has been developed to perform the calculations outline above (5), using the technique developed by Nigam and Jennings (6). Examples are shown in Fig. 3 ($T_o = 1$ sec) and Fig. 4 ($T_o = 0.1$ sec). In eac case the original accelerogram is artificial earthquake C-1 (7) for whic $\Delta t = 0.025$. The equivalent one-period excitations (3b and 4b) are show along with the reduced quarter-cycle accelerograms $\ddot{z}_S$ and $\ddot{z}_S$ for use Eq. (2) (3c, 3d, 4c, 4b).

DISCUSSION AND CONCLUSIONS

It has been found that the method can calculate about 16 Fourier spectrum ordinates for a 1024-pt record in the same time the FFT calculates all 512, indicating the relative computing time involved. Th absolute time is 22 ms/pt on the IBM 370/155. Of course, the present

method can be used to calculate ordinates at any selected period and for records of any length, and is not intended to duplicate the computation of the entire spectrum as given by the FFT. The two methods are related, however, (5), and this relation can be used to guide the use of the FFT in earthquake engineering.

In mathematical terms, the essential feature of the method is the periodicity of the kernel in the Fourier transform, which allows superposition of the function to be transformed. This fact is well known in the field of numerical analysis, but these mathematical studies have not yet found their way into earthquake engineering.

One possible application appears to be in the analysis of data from ambient vibration tests, where the method might be used to investigate resonance peaks in detail, after the general nature of the Fourier spectra had been established by use of the FFT on a relatively short record. This application illustrates the two primary advantages of the computing method: the capability of selecting a small number of arbitrary frequencies for analysis, and the ability to handle long records with little difficulty.

ACKNOWLEDGMENTS

The author is grateful to Mr. Kwak Lo Kam for development of computer programs and other contributions to this study. The work was supported in part by a grant from the National Science Foundation.

REFERENCES

1. Kawasumi, H., "Notes on the Theory of Vibration Analyzer," Bulletin Earthquake Res. Inst., Tokyo Univ., Vol. XXXIV, Pt. 1, 1956.

2. Rubin, S., "Concepts in Shock Data Analysis," Chapter 23 of Shock and Vibration Handbook, McGraw-Hill Book Co., New York, 1961.

3. Hudson, D. E., "Some Problems in the Application of Spectrum Techniques to Strong-Motion Earthquake Analysis," BSSA, 52, 417-430, 1962.

4. Jenschke, V. A., "Relation Between Response and Fourier Spectra of Shock Functions," Int. J. Solids Structures, 6, 1259-1265, 1970.

5. Jennings, P. C., "Rapid Calculation of Selected Fourier Spectrum Ordinates," Earthquake Engrg. Res. Lab. Report 72-05, Calif. Inst. of Tech., Pasadena, Calif., 1972.

6. Nigam, N. C. and P. C. Jennings, "Calculation of Response Spectra from Strong-Motion Earthquake Records," BSSA, 59, 909-922, 1969.

7. Jennings, P. C., G. W. Housner and N. C. Tsai, "Simulated Earthquake Motions for Design Purposes," Proc. 4WCEE, I, Santiago, Chile, 1969.

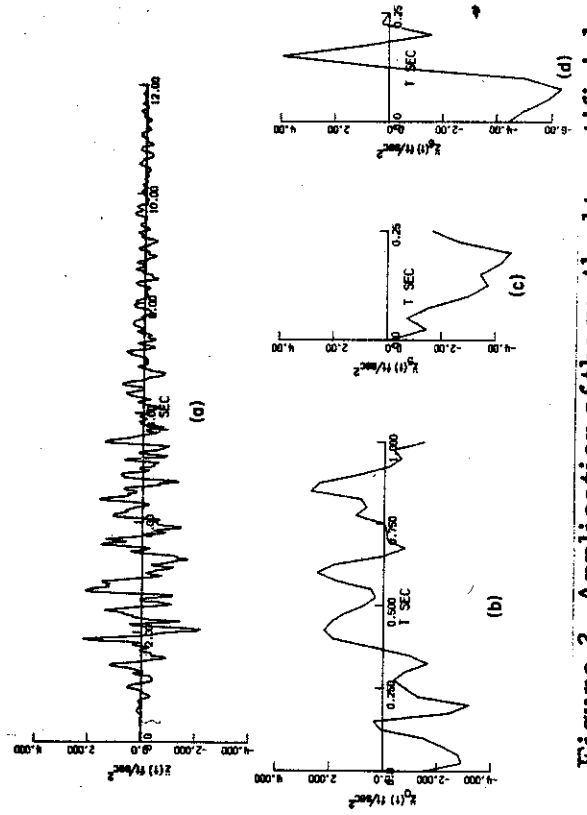

Figure 3. Application of the method to artificial earthquake C-1 for T_o = 1 sec.

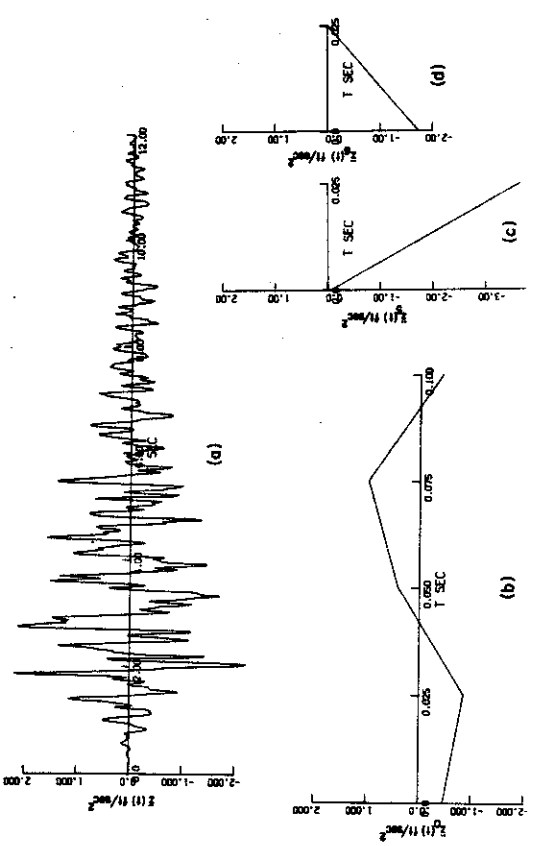

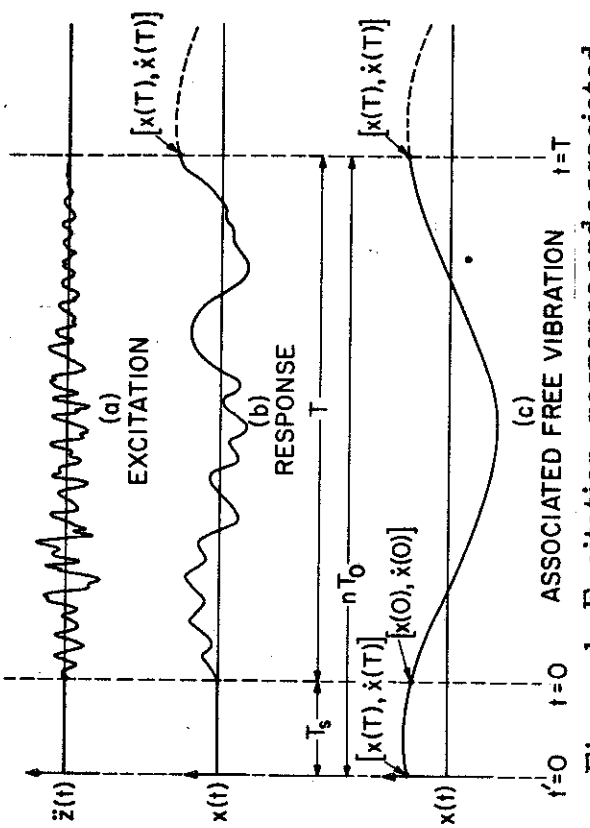

Figure 1. Excitation, response and associated free vibration.

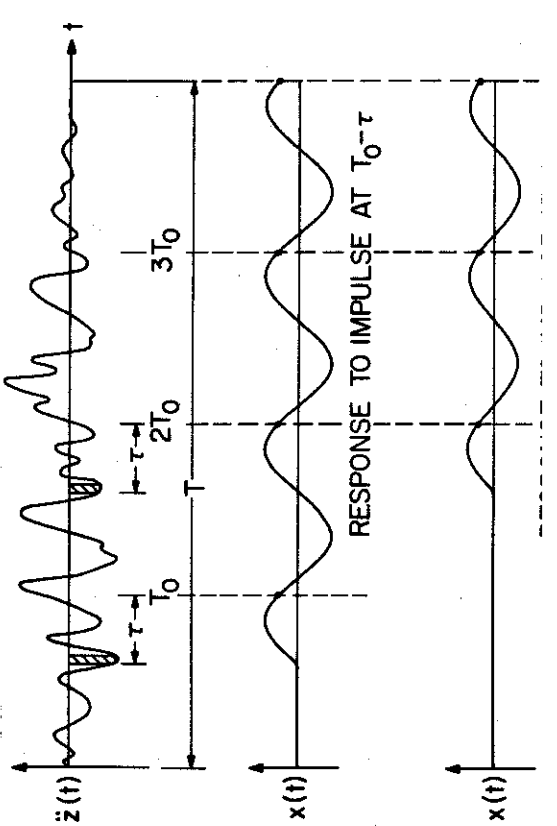

THE ROLE OF EARTHQUAKE GROUND MOTIONS IN EARTHQUAKE ENGINEERING

by

George W. Housner[I]

SYNOPSIS

Knowledge of earthquake ground motions that can be expected is of fundamental importance for earthquake engineering. There is a need for better capability of assessing when and where earthquakes may occur. The nature of the amplitude, duration, and frequency content of the ground motion, and the spatial distribution of these quantities about the fault needs to be known better. Greater efforts should be expended in recording and studying ground motions produced by earthquakes of different magnitudes in a variety of geologic settings. The influences of type of faulting and nature of source mechanism on ground shaking need elucidation.

INTRODUCTION

Earthquake engineering requires a thorough knowledge of the nature of ground shaking sufficiently intense to be destructive, and thus differs from seismology which is concerned mainly with ground shaking at large distances from the source where the intensity is not of practical significance. In earthquake engineering, ground shaking is studied from the scientific and the practical points of view. The scientific point of view has as its objective to learn how seismic waves are generated, how they are influenced as they travel through the ground, and what are the characteristics of the ground shaking that are significant for the construction of buildings, bridges, etc. This point of view seeks to determine information about ground shaking without asking what its immediate practical value may be. On the other hand, the practical point of view is to study ground motions with the objective of making applications. In earthquake engineering the practical point of view should, of course, take precedence; however, it is usually difficult or impossible to determine on order precisely that information needed to solve an immediate practical problem. As a result, it is expedient to carry on research from the scientific point of view with the expectation that as knowledge is accumulated it will in time provide information that can be put to practical use. It is, therefore, essential that earthquake engineering cultivate both the scientific and the practical points of view when studying earthquake ground motions.

Knowledge of destructive ground shaking has been greatly expanded during the past decade, but there is yet much to learn. The ground-shaking problem is very complex and our knowledge of the occurrence of earthquakes is imperfect. Three of the fundamental problems of earthquake ground motions, from the practical point of view, are: how to

---

[I] Professor of Civil Engineering and Applied Mechanics, California Institute of Technology, Pasadena, California.

estimate where and when earthquakes of various magnitudes may occur, how to assess the nature of the source mechanism that the earthquake may have when it occurs, how to make a practical analysis of the propagation of the seismic waves through the earth's crust to the general vicinity of the site of a proposed structure. The solutions to these problems are needed to make more reliable estimates of ground shaking to be expected. At present, it appears that the best estimate of ground shaking to be expected is by extrapolating from ground motions recorde under similar circumstances.

SEISMIC HISTORY AND GEOLOGIC EVIDENCE

Source Mechanism. Recent advances in knowledge have shown that the characteristics of strong ground shaking in the general vicinity of th causative fault can be strongly influenced by the nature of the source mechanism. When an earthquake occurs, its effect can depend on the ki of faulting that generates the seismic waves. The following four types of faulting merit consideration in the study of destructive ground shakin

a. Low-angle, compressive, underthrust faulting. According to the theory of sea-floor spreading (Continental Drift) certain crustal plat underlying the oceans are moving into adjacent continental crustal plate and underthrusting beneath them, as along the western coast of South America, along the Aleutian Islands, and the northern coast of Alaska, and along the eastern coast of Japan. In these locations, the compressive forces generated by the movement of the sea-floor crustal plate against the continental plate leads to shearing-stress failures along a lo angle, compressive underthrust fault, such as illustrated in Figure 1. The great 1964 Alaska earthquake, and the large 1960 Chile earthquake considered to be examples of such underthrust faulting.

b. Compressive, overthrust faulting. In this type of faulting, con pressive forces cause shear failure on an inclined fault with the upper portion of rock moving upward along the fault plane, as shown in Figure The 1971 San Fernando, California earthquake was generated by faultin of this type.

c. Extensional faulting. Slip on an inclined fault can also occur when there are extensional strains in the earth's crust. In this kind of earthquake, the upper portion of the rock overlying the fault displaces downward along the fault during the earthquake, as shown in Figure 3. Examples of earthquakes generated by this type of faulting are the 1954 Fairview Peak-Dixie Valley events in Nevada, U.S.A.

d. Strike-slip faulting. The famous 1906 San Francisco, Californi earthquake was an example of ground shaking generated by strike-slip faulting on the San Andreas fault. As shown in Figure 4, relative horizontal displacement of the two sides of the fault takes place across an essentially vertical fault plane.

Pure examples of the foregoing types of faulting do not occur often. In most cases the displacement on the fault is not solely upward or

downward along the fault, in the case of compressive or extensional faulting, nor is the relative displacement across the fault usually absolutely horizontal in the case of strike-slip faulting. In most cases, the displacement on the fault has components both parallel and normal to the surface fault trace. Furthermore, the fault slip does not necessarily take place along a plane, but may take place along an irregular surface, and there also may be branch faulting.

Because of geometrical differences the shaking of the surface of the ground may be significantly different in the vicinity of the causative fault for the different kinds of faulting. The nature of the seismic waves generated by the fault slipping will depend mainly on the following items:

a. Stress drop during the faulting process. During the fault movement the rock stress across the fault will change from the initial value, σ_1, to a lower stress, σ_2, and the size of the stress drop $(\sigma_1 - \sigma_2)$ will have an influence on the amplitude of the seismic waves that are generated.

b. Total fault displacement. An earthquake of small magnitude will be associated with relatively small displacement across the fault, whereas an earthquake of large magnitude will be associated with a relatively large permanent displacement across the fault. A large displacement indicates a longer duration of fault movement, and a greater amplitude in the long-period waves that are generated.

c. Size of slipped area. An earthquake of large magnitude will be generated by fault slip over a fault plane of relatively large area. For example, the 1964 Alaska earthquake (Magnitude 8.4) slipped over a length of fault of about 450 miles and over a width of fault estimated to have been some tens of miles. This can be compared with a much smaller area of fault slip of the Magnitude 6.5 San Fernando, California earthquake of 1971. In this earthquake, slip took place on a fault estimated to be approximately 12 miles in length and about 12 miles in width. The great difference in slipped-fault area between these two earthquakes corresponded to significant differences in the nature of the ground shaking.

d. Roughness of the slipping process. During an earthquake, slip originates at a certain point on the fault plane (hypocenter) and the slip progresses from this point. During this event the rock on the two sides of the fault are displacing relative to each other for a length of time that may be different at different points on the fault. The propagation of the fault slip and the slipping process at various points on the fault plane may progress with greater or lesser smoothness, that is, the energy released by the slip at a point may be quite irregular in time. It is clear that the nature of the ground shaking will be different if it is generated by a relatively uniform propagation of the slipped area and by smooth slipping at all points on the fault plane, than if it is generated by relatively rough slipping and relatively erratic propagation of the slip boundary.

Some earthquakes which appear to be large magnitude events when view from a large distance may show up in near-field measurements as being actually a close sequence of smaller earthquakes generated by a non-uniform propagation of slipping.

e. Fault shape. It should be noted that for small magnitude earthquakes, say, below Magnitude 6. the slipped area of the fault is presumusually to have dimensions approximately the same in all directions. Sometimes, however, a small earthquake, such as the Magnitude 5.6 Parkfi California earthquake of 1966, has a relatively narrow, elongated fault area. This Magnitude 5.6 earthquake is estimated to have been generat by slip over a fault area that was approximately 20 miles in length and perhaps one or two miles in depth (strike-slip). Large magnitude earthquakes can be expected to be generated on fault areas that are elongated that is, the length of faulting is much greater than the width. It is clear that the dimensions of the slipped area will have a very strong influence on the nature of the ground shaking as regards frequency characteristic duration, and surface area covered by strong shaking.

f. Proximity of fault plane. Another aspect of the faulting which c have a strong influence on the ground shaking in the central region of ar earthquake is the proximity of the slipped area of fault to the surface of ground. If the upper portion of the slipped fault is at considerable dept beneath the ground surface, the shaking will not be the same as it would if the slipped fault plane actually reached the surface of the ground. In latter case, a point on the surface of the ground could be much closer t area of fault that is generating strong seismic waves. Recently, surpris high peak accelerations have been recorded in the near-field of relative small earthquakes; for example, a peak acceleration of approximately 7(was recorded during the Magnitude 4.5 Bear Valley, California earthqua in 1972. The duration of the ground shaking was very short and the pea acceleration pulse was very narrow, so that the ground shaking had litt structural effect. Similar results were obtained during the 1972 Ancon Italy earthquakes. It is important to note that in the very near field the amplitude of the accelerations depends more on the proximity of the faulting process than on the magnitude of the shock.

At present, although we understand the general features of the faul mechanism and the seismic waves, our knowledge of the details is inadquate for predicting the features of the ground shaking, and more research is needed.

TRAVEL-PATH GEOLOGY

As the seismic waves radiate from the fault, they undergo certain changes. Some of these result from geometrical spreading as the seism energy travels away from the fault. This effect is particularly pronoun in the near field and for small magnitude earthquakes. In addition, as waves travel outward, they undergo some attenuation because energy is lost as they travel through the rocks. This energy loss seems to be no so important in the near field as the geometrical attenuation. Also,

more important is the effect of the dispersion of the waves that results from changes in modulus of rigidity or of density of the rock. Dispersion seems to be a dominant factor, so that at a distance the ground motion exhibits the influence of travel-path geology. This effect is illustrated in Figures 6 and 7 which show the change in the character of the ground motion produced by a Magnitude 5.6 earthquake as the waves travel a distance of 5 miles. It can be seen in Figure 6 that the near-field ground motion very close to the fault reflects strongly the time-history motion of the fault displacement, but at a distance of 5.3 miles the character of the fault displacement has little effect on the accelerations, velocities, or displacements. At this distance, the nature of the ground motion presumably reflects mainly the very heterogeneous nature of the travel-path geology.

It appears that in deposits of alluvium, a wide variety of wave types may be traveling during an earthquake, and these may have a wide variety of travel-path directions. Unfortunately, very little is known about the details of wave propagation in the softer surface deposits at the surface of the earth. An essential distinction can be made between the soft soil deposits, which vibrate with one predominant mode, such as in Mexico City in 1962, in which case the spectrum curves show a pronounced peak corresponding to the natural period of vibration of this highly excited mode. In other situations, the spectrum curves of ground motion recorded on alluvial deposits do not show pronounced resonant peaks; presumably, in these cases the motion is not dominated by the response of a single mode of vibration, but many modes of vibration each contribute a small portion.

Sometimes the surface ground motion shows anamolous behavior which presumably reflects certain features of the geology at depth, as, for example, happened in the Borrego Springs, California earthquake of 1968.

It has been observed, also, that ground motions recorded at two nearby points on the same local geology may show appreciable difference in intensity of ground shaking. This, presumably, reflects the fact that many waves traveling in the medium, with different orientation of travel paths, may superpose in different ways at adjacent points. The highly complex nature of travel-path geology would seem to require a statistical viewpoint to be taken of ground motions. The variation of geology is seldom likely to be known with sufficient accuracy to make a reliable deterministic analysis of a particular site during a specified future earthquake. The effect of the geological variations can probably best be treated in a practical way by introducing the notions of statistical variations in the ground motion.

There is a great need for additional research on the influence of travel-path geology on ground shaking in the near-field region. At present, we have a very inadequate knowledge of how the waves travel in the near-field region.

NATURE OF SURFACE GROUND SHAKING

Strong-motion accelerographs record essentially a time-history of the ground acceleration, though in some cases the natural frequency of

the accelerograph is too low and the record must be corrected for instr ment properties. The velocity and displacement of the ground can be derived from the accelerogram, which thus contains most of the inform tion needed for engineering purposes. The response spectrum and the Fourier emplitude spectrum are useful ways of presenting some of the information contained in the accelerogram. The response spectrum ha the advantage that it is indicative of the vibrations of structures, and, therefore, it can be concluded that only those features of ground shakin that have a significant influence on the response spectrum are of practi significance for elastic vibrations of structures.

Ground shaking recorded during earthquakes usually has the prope of a random transient process that attenuates with distance from the fa and, because of dispersion, the duration of ground shaking increases w increasing distance from the fault. The intensity of shaking attenuates with distance from the fault more rapidly in the high frequencies than i the low frequencies. Because of this, tall buildings having long period of vibration will be subjected to strong shaking at greater distances fro the fault than will low buildings with short periods of vibration. For en neering purposes, the motion in the near field close to the fault is of greatest practical interest because this is where the most severe dama is sustained.

The amplitude of the highest acceleration pulse is not by itself sign cant for structural applications, but the greatest area of acceleration pulse that may occur is very significant. More study should be devoted to pulse areas; especially upper bounds and statistical distribution.

IDEAL ACCELEROGRAMS

At distances sufficiently far from the causative fault so that the details of fault displacement are not significantly reflected in the recorded ground shaking, the most evident feature of the ground motion i that of a random process having a rather abrupt beginning, followed by portion having more or less uniform intensity of shaking, and this is followed by a rather gradual attenuation of the ground motion. It is, therefore, possible to generate random functions having the foregoing features which can be used to represent earthquake ground motions. Th is usually done by starting with a segment of white noise, $W(t)$, which filtered to $f(t)$ whose ensemble average Fourier spectrum has a prescribed shape that is deduced from actual records. To give the proces a beginning, middle, and end, the filtered function is multiplied by an amplitude function $f(t) \cdot A(t) = a(t)$, and the resultant simulated accelerogram, $a(t)$ is viewed as a random sample from an ensemble having a prescribed average Fourier spectrum or average response spectrum. This method of generating earthquake ground motions enables the engineer to construct idealized ground shaking to represent earthquakes of any specified magnitude at specified distances. In addition, he can generate several ground motions for a specified design earthquake and make response calculations which thus take into account statistical variations.

It must be remembered, however, that actual earthquake ground motions may differ somewhat from ideal ground motions. They may reflect details of the faulting mechanism, or may reflect influences of the geology through which the seismic waves travel. It is necessary, therefore, to continue to obtain records of destructive earthquakes under a great variety of conditions so that the engineer will know the different characteristics of ground motion that it is possible to experience.

CONCLUSIONS

It is very important from an engineering point of view to build up knowledge of the nature of ground shaking combined, of course, with a knowledge of frequency of occurrence of earthquakes. This requires the recording of ground motions during many earthquakes of various magnitudes in a variety of geologic settings. Also, recordings should be made at a number of different points surrounding the causative fault over a range of distances. This is not intended to imply that there is insufficient knowledge of ground motions to do successful earthquake engineering. Our knowledge is adequate for most engineering problems, but it is not adequate to answer all questions, and it is precisely these unanswered questions that may be of special importance to public safety and economy.

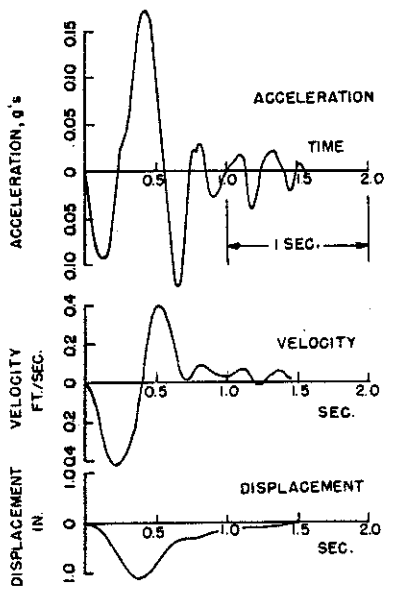

Fig. 11 Near-field N-S ground motion recorded during Port Hueneme, California earthquake of March 18, 1957. (M = 4.7)

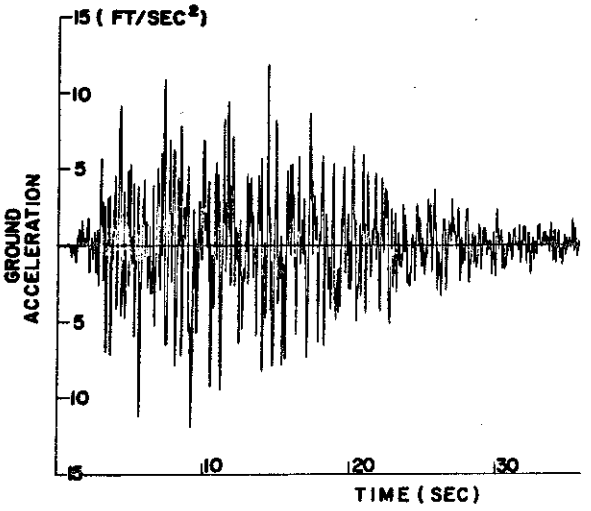

Fig. 12 Simulated accelerogram generated on a digital computer by filtering and shaping a white-noise random function.

Fig. 1 - Underthrust faulting under compressive forces. Example, faulting in Alaska earthquake, 27 March 1964.

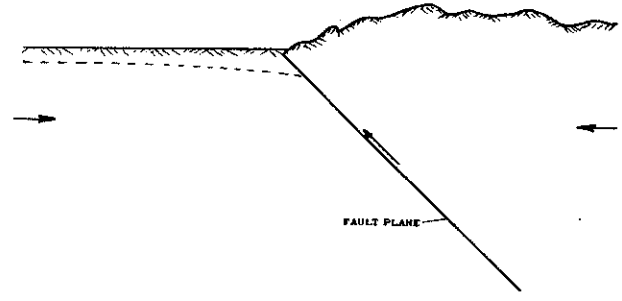

Fig. 2 - Thrust faulting under compressive forces. Example, San Fernando earthquake, 9 February 1971.

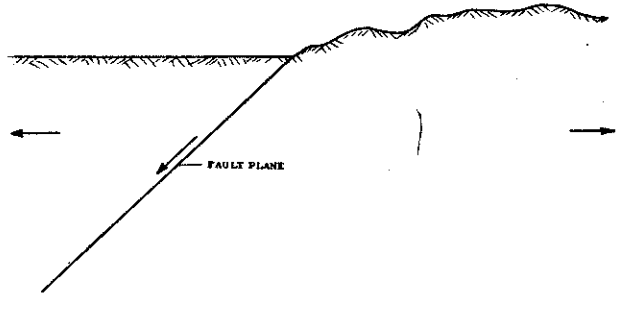

Fig. 3 - Faulting under extensional strains. Example, Dixie Valley - Fairview Peak, Nevada earthquake, 16 December 1954.

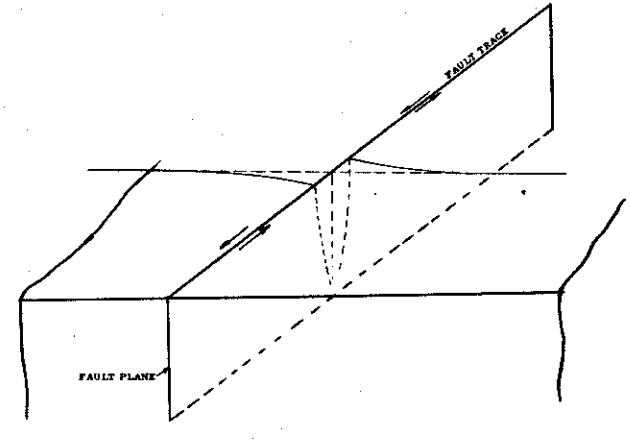

Fig. 4 - Strike-slip displacement on a vertical fault plane. Example, San Andreas fault in California,

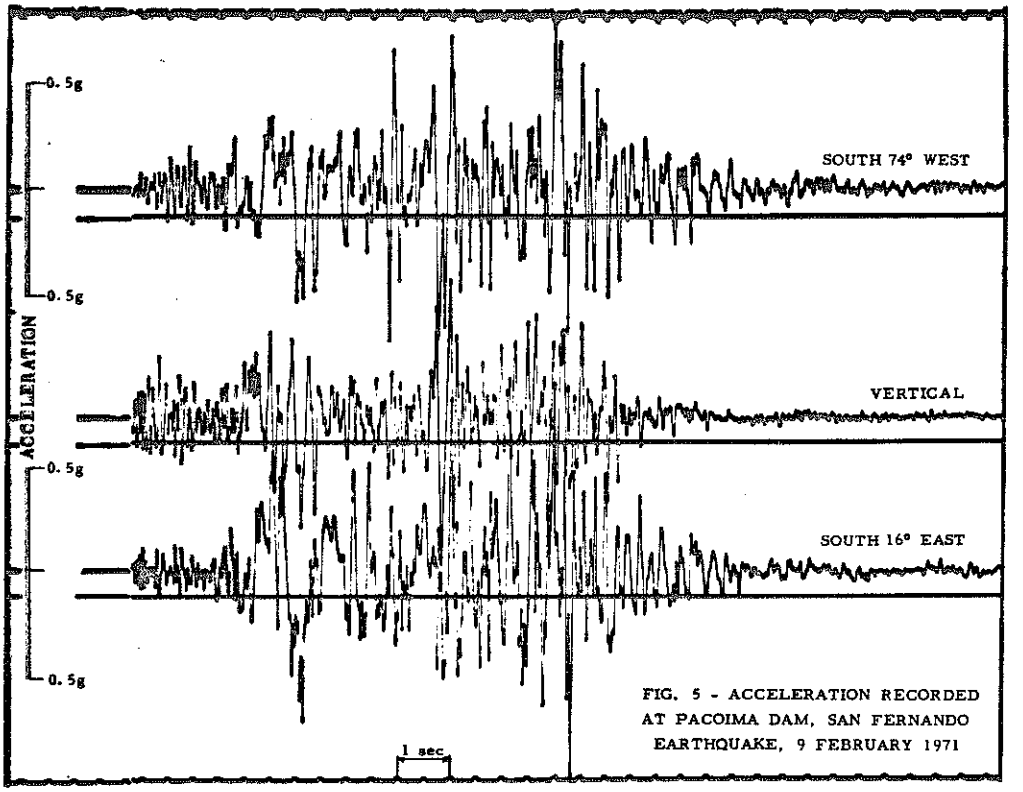

FIG. 5 - ACCELERATION RECORDED AT PACOIMA DAM, SAN FERNANDO EARTHQUAKE, 9 FEBRUARY 1971

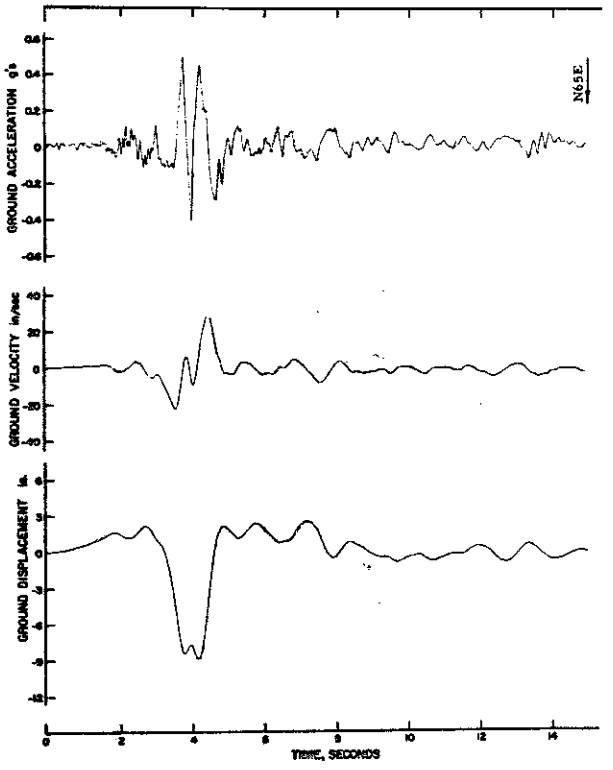

Fig. 6 - N65E accelerogram recorded 200 ft from surface trace during the Parkfield earthquake of 27 June 1966; magnitude 5.6; strike-slip fault.

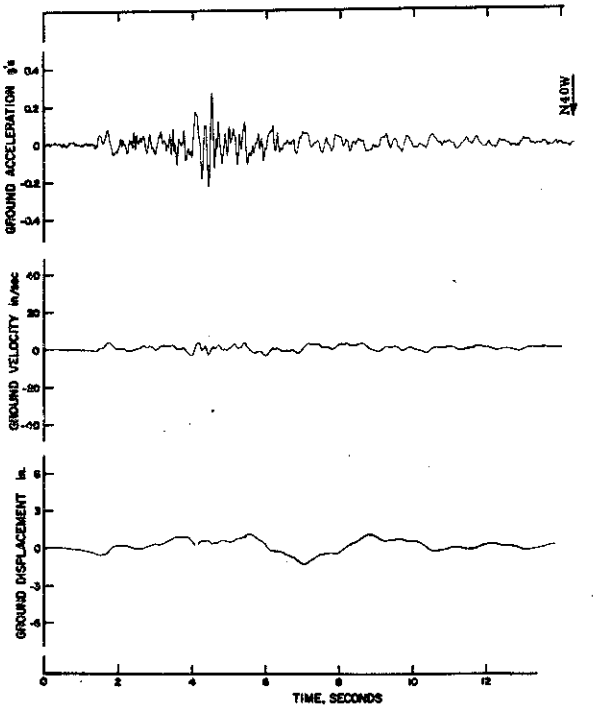

Fig. 7 - N50E accelerogram recorded 5.3 miles from the causative fault during the Parkfield earthquake. The accelerographs that recorded Figs. 6 and 7 were along a line perpendicular to the fault trace.

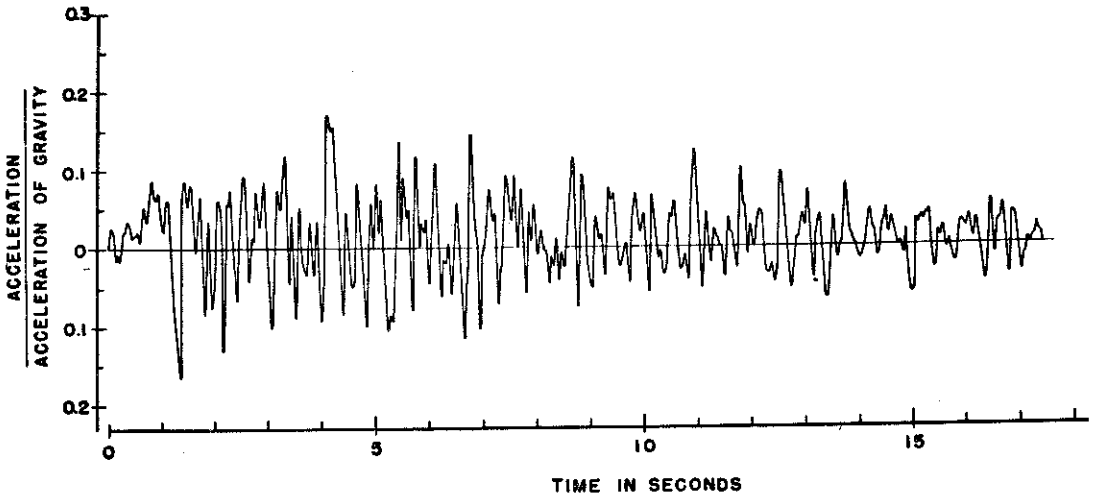

Fig. 8 - S52E accelerogram recorded at Taft, California, 25 miles from the causative fault during the Tehachapi earthquake of 21 July 1952; magnitude 7.6; compressive thrust fault.

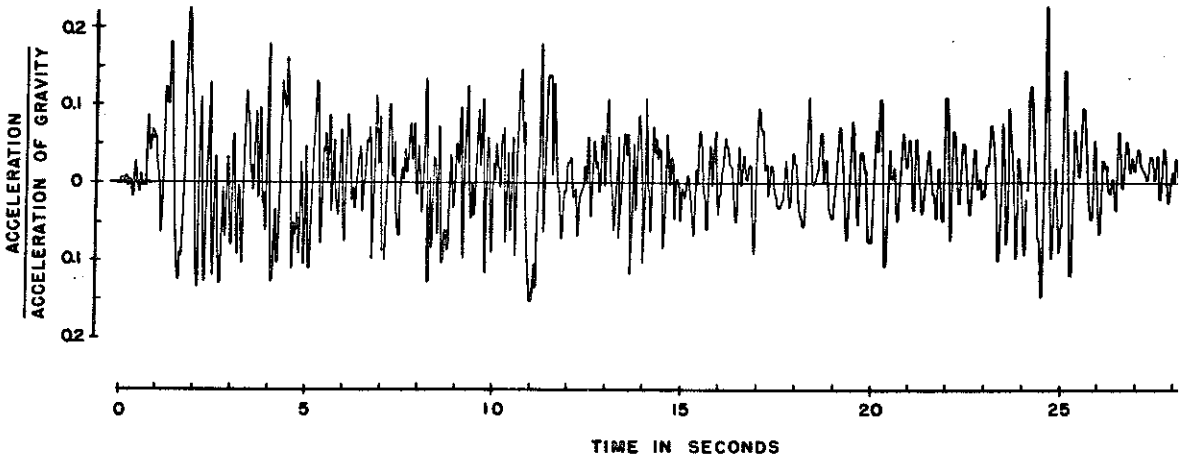

Fig. 9 - E-W accelerogram recorded 4 miles from the fault at El Centro California, during earthquake of 18 May 1940; magnitude 7.1; strike-slip fault.

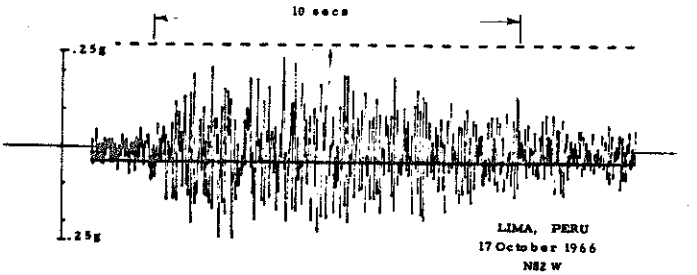

Fig. 10 - N82W accelerogram, Lima, Peru, 17 October 1966; magnitude 7.5; underthrust faulting. This motion has much higher frequencies than do California earthquakes which, presumably, reflects geological conditions.

THE SAN FERNANDO, CALIFORNIA, EARTHQUAKE OF FEBRUARY 9, 1971

by

P. C. Jennings[I] and G. W. Housner[II]

SYNOPSIS

The San Fernando earthquake of February 9, 1971 was a Magnitude 6.6 shock that killed 58 persons, injured 2400 and caused approximately 500 million dollars damage. Because of the broad scope of the earthquake's effects and the large number of consequent studies, this report is limited to a brief summary of the more important features of the earthquake, a listing of the more significant actions taken or proposed as a consequence of the shock, and a bibliography of some of the more important general reports about the effects of the earthquake.

INTRODUCTION

The Magnitude 6.6 San Fernando earthquake occurred on the northern edge of metropolitan Los Angeles shortly after 6 a.m., February 9, 1971. The shock took 58 lives, injured 2400 and caused an estimated 500 million dollars in property damage. Although only a moderate earthquake in seismological terms, the San Fernando earthquake was a major event from the engineering point of view because of the large number and variety of engineered structures and facilities that were subjected to strong ground shaking, the significant resulting damage and the excellent instrumental coverage.

It is not surprising, then, that the San Fernando earthquake is already one of the most thoroughly studied shocks in history. There are several general reports about the event as well as many detailed investigations of particular features of the earthquake, some of which are to be presented at 5WCEE. In addition, the earthquake has produced code changes, changes in standard practice, and has initiated detailed examinations and recommendations by task forces and advisory groups appointed by political bodies in the State of California.

GEOLOGIC FEATURES

Unlike the more usual California earthquake, which is generated by strike-slip faulting on an essentially vertical fault plane, the San Fernando earthquake was generated on a thrust fault which dipped approximately 45° to the north, underlying the east-west trending San Gabriel Mountains. The hypocenter lay about 8 miles deep, and the

---

[I] Professor of Applied Mechanics, California Institute of Technology, Pasadena, California.

[II] Professor of Civil Engineering and Applied Mechanics, California Institute of Technology, Pasadena, California.

east-west extent of the faulting was approximately 12 miles. At some locations the fault displacements reached the surface of the ground. In addition, a relatively large area of alluvial ground suffered deformation because of fault displacement at depth. A portion of the San Gabriel Mountains was elevated as much as 5 feet by the fault displacement. Numerous landslides were caused on the relatively steep slopes of the mountains and, in addition, there were landslides on relatively shallow sloping alluvial ground in the northern part of the San Fernando Valley.

In the general region where the fault displacement reached the surface of the ground, and to the north of this region, there was very severe ground shaking. Because of the proximity of the causative fault, this shaking of the ground would not have been more severe, it is thought, had the Magnitude of the earthquake been 8 or greater; but a much larger area would have been affected by strong shaking, and the duration of shaking would have been longer.

ACCELEROGRAPH AND SEISMOSCOPE NETWORK

Because of the requirement in Los Angeles that three accelerograp be installed in each building of ten or more stories, some 60 buildings were outfitted with three accelerographs each: one in the basement, one at midheight, and one at roof level. These code accelerographs provide good coverage in certain regions of Los Angeles city. In addition, the California Institute of Technology had 25 accelerographs and the Nationa Oceanic and Atmospheric Administration (NOAA) had 17 accelerographs installed at strategic locations. Other agencies had a smaller number o instruments located in their structures and on their grounds. Usable records were obtained from 241 accelerographs. At the time of the ear quake all of the strong-motion accelerographs were maintained by the Seismological Field Survey (NOAA).

The Los Angeles County Flood Control District had installed an accelerograph on a rock ridge adjacent to Pacoima Dam, located about tw miles north of the surface expression of the faulting, just above the apparent center of energy release. This instrument recorded the stronge ground shaking ever recorded for any earthquake, with peak horizontal accelerations exceeding 1g (75%gvertical). Approximately five miles south of the surface expression of the fault, accelerographs in the seve story Holiday Inn recorded the ground motion (28%g) and the building motion (40%g at the top). Other accelerometers and seismoscopes gave recordings on crystalline rock, sedimentary rock and alluvium.

EFFECTS ON STRUCTURES

Hazardous Old Structures. Earthquake design provisions were first incorporated in the Los Angeles building code in 1933, following the Long Beach earthquake. In the San Fernando earthquake, buildings constructed before 1933 demonstrated much less resistance than buildings constructed after 1933. Fortunately, most of the structures in the region of very strong shaking were relatively new.

New Buildings. There were 13 high-rise buildings in Los Angeles, ranging from 26 to 52 stories in height, 15 to 25 miles from the center of the earthquake. These vibrated strongly during the earthquake, but none received structural damage, although there was a certain amount of plaster cracking and damage to equipment. Numerous structures, from 10 to 25 stories in height, in Los Angeles and in the southern San Fernando Valley were 10 to 20 miles from the center of the earthquake. Some of the closer of these had moderate structural damage, such as cracking of shear walls and columns. The Holy Cross Hospital building and the Indian Hills Medical Center building, both new seven-story reinforced concrete structures, were in the region of very strong shaking. Both structures were severely cracked and damaged and, had the strong shaking lasted longer, portions of these buildings might have collapsed. A number of single-story industrial buildings were severely damaged by the ground shaking in the region near the center of the earthquake. These structures had masonry or concrete walls and wood roofs. The connections of the wood roofs to the tops of the walls were inadequate, with consequent failure of the connection and partial collapse of the structures. Joints between tilt-up wall slabs were another weak point in some buildings of this type.

Behavior of Dams. Pacoima Dam (372 feet high concrete arch, constructed in 1928) at the center of the earthquake was not damaged by ground shaking, but one rock abutment showed evidences of movement and distortion during the earthquake. There were many earth dams in the region of moderately strong to strong shaking (15%g or greater), and the dams designed and constructed during recent years withstood the earthquake very well. On the other hand, the old earth dams performed poorly. The lower San Fernando Dam, a 140 foot high hydraulic-fill earth dam, impounding the water supply for the city of Los Angeles, was in the region of very strong shaking and was severely damaged. During the earthquake the upstream face and the crest slid into the reservoir, leaving only 5 feet of freeboard against overtopping. The condition of this dam appeared so hazardous that 80,000 persons living below the dam were evacuated from their homes for four days, until the reservoir could be reduced to a safe level.

Hospitals. It was a striking fact that in the region of strong shaking, four hospitals were damaged so severely that they could not be used after the earthquake. At the Veterans Administration Hospital a pre-1933 building that had not been designed to resist earthquakes, collapsed and killed 49 persons. The Olive View Hospital, a new $30 million facility, was so severely damaged by the earthquake as to be almost a total loss.

Highway Structures. In the region of strong shaking (25%g or greater) there were 70 bridge structures forming part of the freeway system. Of these, five collapsed and forty others suffered some damage. There was no significant damage to highway bridges where the ground shaking was less than about 25%g. In the central region of the earthquake, permanent deformation of the ground contributed to the damage.

Electrical Power Facilities. The Pacific Intertie Converter Station was the southern terminus of the high voltage transmission line bringing power to southern California from the State of Oregon. This new $110 million facility suffered extensive damage from ground shaking. Although the building itself was not seriously damaged, the electrical equipment was destroyed. Several other electrical power switching stations in the region of strong shaking also received severe damage to the electrical equipment, particularly circuit breakers.

Sewers and Water Supply. Some three hundred miles of buried sewer line were in the region of strong shaking, and it has been estimated that approximately 15 miles of it had to be replaced because of damage at numerous locations resulting from ground deformation. In the same region the buried pipelines of the water distribution system were reported to have had approximately 1000 breaks, so that this region was temporarily without water for drinking or for fighting fires.

Water Treatment and Storage Facilities. A large water treatment plant under construction in the region of very strong shaking, received damag from landsliding and from ground shaking; in particular, a large underground reinforced concrete reservoir was severely damaged.

Schools. School buildings in general performed well during the earthquake if they had been constructed since 1933, when special earthquake provisions (The Field Act) were specified for their design. This contra strongly with the extremely poor performance of the school buildings during the 1933 Long Beach, California earthquake. Some of the school buildings in the northern San Fernando Valley were damaged by permanent ground displacement, a few received structural damage from grou shaking, and some received undesirable architectural damage, such as fallen light fixtures, pieces of the ceiling dropping, etc. The earthquak caused damage to a number of pre-1933 school buildings in Los Angeles and made it clear that the old masonry school buildings were very hazardous in the event of strong shaking. Following the earthquake, th City of Los Angeles demolished 90 pre-1933 school buildings and strengthened 100 others to make them safe for occupancy.

Architectural and Mechanical Damage . Many multistory buildings in the region of moderately strong to strong ground shaking survived with structural damage, but did incur costly damage to architectural finishe and to mechanical equipment. Many new buildings suffered extensive plaster cracking, because the plaster was too stiff to accommodate the interfloor deformation of the structure. Although some of the older office buildings in Los Angeles had many windows broken, the new offic buildings had very little glass breakage. (The code requires new buildi to have their windows so designed that they can accommodate interfloor deformation without shattering). Many office buildings suffered damage to the elevator systems. This was mostly a matter of the counterweigh coming out of the guides and becoming tangled so that the elevator could not function. In many libraries, the bookshelves proved to have inadeq

strength to resist the shaking and collapsed. In many buildings the air conditioning equipment jumped off its supports and furniture moved about and the less stable pieces overturned.

DISASTER RELIEF

The disaster relief operations following the earthquake were, in general, quite effective except for some breakdown in communications immediately after the earthquake. Following the earthquake, the Red Cross set up emergency shelters at five schools. Food was provided in the shelters and, in addition, two large feeding stations were set up. The Red Cross assisted over 11,000 families at a cost of over $1,100,000. Following the earthquake, the Federal Government announced that it would provide rehabilitation funds for damage to buildings and facilities owned by local city and county governments. In addition, the Federal Government made available low interest loans to individuals who had suffered damage to their homes or businesses during the earthquake. Some 7000 loans with a value of $34 million had been approved by April 30, 1971. Of this, 6800 loans worth $26 million were to repair or rebuild homes damaged in the earthquake. Repayment of the first $500 was required as well as everything above $3000, but the intervening $2500 was forgiven.

ACTIONS TAKEN AFTER THE EARTHQUAKE

As might be expected, the San Fernando earthquake prompted a number of actions for mitigating future earthquake damage that otherwise would not have been initiated. For example, the Los Angeles City building code was revised. Immediately following the earthquake, revisions were made to eliminate weaknesses that had been exposed by the disaster, such as the inadequate connections between the wood roofs and the masonry walls of one-story industrial buildings; and the poor behavior of inadequately reinforced concrete columns under the action of large strains. At present, it is required that high-rise buildings be designed on the basis of a dynamic analysis, and a completely revised earthquake design code is being developed for the City of Los Angeles.

Revisions have been made to the State Highway Department earthquake design criteria. Immediately after the earthquake, the design criteria were increased by over 100%; new and improved details were specified for new bridges; and a program of research was initiated to develop a satisfactory set of design criteria based on modern knowledge. Existing highway bridges were examined for weaknesses which had led to collapse of bridges during the San Fernando earthquake. Where these weaknesses existed, the structures are being strengthened.

A program was initiated by the State Department of Dam Safety to review all old dams from the point of view of earthquake resistance.

The electrical power companies in California initiated a study to develop better earthquake design specifications for electrical equipment. The counterpart of the severely damaged Pacific Intertie Station is

located in the State of Oregon at the other end of the transmission syste Following the earthquake a study was made of the Oregon installation to investigate its weaknesses and to determine how it should be strengthen so that it would perform satisfactorily in the event of strong ground shaking.

Following the earthquake the Los Angeles County Government appointed an earthquake investigation commission which studied the overal consequences of the earthquake and made recommendations for mitigati the effects of future earthquakes. The report of the commission listed series of recommendations and, to implement these, the County Govern ment appointed a number of task forces. The only recommendation of t commission which has not been acted upon was that which recommended that steps be taken to eliminate the hazard provided by the old pre-1933 buildings. It has been estimated that there are more than 20,000 old masonry, pre-1933 buildings in metropolitan Los Angeles, having a val of approximately 8 billion dollars. Although these pose a massive threa in the event of future strong ground shaking, the problem of eliminating strengthening them is so great that the local governments do not see hov to take action.

The San Fernando Veterans Administration Hospital suffered sever damage to many of its old buildings and the collapse of one caused the majority of the deaths in the earthquake. Following the earthquake, the Veterans Administration initiated a program for preventing similar disasters in the future. All existing Veterans Administration hospitals are being investigated to see if they are hazardous and those buildings which do pose a serious earthquake hazard are being either evacuated o strengthened. Revised earthquake design criteria have been formulated for new Veterans Administration hospital buildings. In addition, a program has been initiated for installing strong-motion accelerographs at many hospital sites in seismic regions throughout the country.

NOAA, through the Seismological Field Survey, is purchasing a large number of strong-motion accelerographs for installation throughout the country in seismic regions with an inadequate number of instruments at present.

The State of California has initiated an accelerograph installation program, which will install strong-motion accelerographs in regions of the State not at present covered. This program is financed by a small charge on building permits in cities that do not have an accelerograph installation program like that of Los Angeles.

Following the earthquake, insurance companies revised their progr in particular, they have made insurance cheaper and more convenient t purchase for the individual home owner.

PRINCIPAL CONCLUSIONS FROM THE EARTHQUAKE

The information provided by the large number of accelerographs and seismoscopes in the Los Angeles area demonstrated the value of good instrumental coverage. Countries and seismic regions that want to develop satisfactory earthquake engineering should install strong-motion accelerographs to record the shaking of the ground and the vibration of buildings during future earthquakes.

Analyses of buildings whose motions were recorded during the earthquake showed that the dynamic response of a building can be calculated with satisfactory accuracy by means of a digital computer, when the earthquake ground motion is given.

The San Fernando earthquake demonstrated again that the greatest hazard from earthquakes comes from old, weak buildings. Cities in seismic regions would be well advised to initiate programs for eliminating old, hazardous buildings or strengthening them so that they can resist future earthquakes without collapse.

The San Fernando earthquake damage emphasized the vulnerability of hospitals to earthquake ground shaking. A badly damaged hospital building must be evacuated, and even if the building itself is not damaged, the shaking may so damage the equipment and otherwise disrupt operations that the hospital is no longer functional just when hospital services are especially needed. Cities that are subject to strong ground shaking should require hospital buildings and equipment to be designed to remain functional during severe earthquakes.

Damage to new buildings by the San Fernando earthquake showed that the building code needed improvement; not only were there specific structural details that required improvement, but it appeared that the actual strength specified by the code would not be sufficient to ensure safety in the event of very strong ground shaking of prolonged duration.

The damage to the San Fernando Dam showed that old dams pose a great hazard in the event of strong shaking. All existing dams should be investigated for earthquake safety and the maximum allowable reservoir elevation under which the dam will be safe should be specified.

The damage sustained by public utilities (electrical, water, gas, sewers) demonstrated that public welfare and safety would be much enhanced if the public utilities were checked for performance during strong shaking.

Although the emergency operations following the San Fernando earthquake were adequate, the question was raised as to what would happen if a great earthquake were to shake the entire metropolitan area. It is clear that to mitigate future earthquake disasters, the local government should establish earthquake disaster programs.

REFERENCES

1. Jennings, P. C. (Ed.), "Engineering Features of the San Fernando Earthquake," Earthquake Engrg. Research Lab. Report No. 71-02, Calif. Inst. of Tech., Pasadena, June, 1971, 512pp.

2. Hudson, D. E. (Ed.), "Strong-Motion Instrumental Data on the San Fernando Earthquake of February 9, 1971," Earthquake Engrg. Research Lab., Calif. Inst. of Tech., and Seismological Field Surve National Oceanic and Atmospheric Admin. (NOAA), Pasadena, Calif. Sept. 1971, 260 pp.

3. U. S. Geological Survey and NOAA, "The San Fernando, California Earthquake of February 9, 1971," U. S. Govt. Printing Office, Wash. D. C., 1971, 254 pp.

4. Hudson, D. E., Brady, A. G., Trifunac, M. D., et al., "Strong-Motio Earthquake Accelerograms — Digitized and Plotted Data, Volume I, Uncorrected Accelerograms," Parts C, D, E, F, G, H, I, J, K, L, M, N, Accelerograms from the San Fernando Earthquake. Earthquake Eng Research Lab., Calif. Inst. of Tech., July, 1971 - June 1973.

5. Steinbrugge, K. V., Schader, E. E., Bigglestone, H. C., and C. A. Wee "San Fernando Earthquake, February 9, 1971," Pacific Fire Rating Bureau, August, 1971, 93pp.

6. Hudson, D. E., "Local Distribution of Strong Earthquake Ground Motions," Bull. Seis. Soc. of Am., Vol. 62, No. 6, Dec. 1972.

7. EERI/NOAA, "Report on the San Fernando Earthquake," NOAA, (In Press).

8. Los Angeles County Earthquake Commission, "Report of the Los Angeles County Earthquake Commission, San Fernando Earthquake, February 9, 1971," November, 1971, 45 pp.

9. Joint Panel on the San Fernando Earthquake, "The San Fernando Earthquake of February 9, 1971 — Lessons from a Moderate Earthquake on the Fringe of a Densely Populated Region," National Acad. of Sci. -National Acad. of Engrg., March, 1971, 24pp.

10. California Geology, April-May 1971, Special San Fernando Earthquake Edition.

11. "Reports of the Earthquake Task Forces," Chief Administrative Officer, County of Los Angeles, March, 1972, 8 Vols.

12. Bolt, B. A., "San Fernando Rupture Mechanism and the Pacoima Strong-Motion Record," Bull. Seis. Soc. of Am., Vol. 62, No. 4, pp. 1053-1061.

13. Lew, H. S., Leyendecker, E. V. and R. D. Dikkers, "Engineering Aspects of the 1971 San Fernando Earthquake," National Bureau of Standards Building Sciences Series 40, U. S. Govt. Printing Office, Washington, D. C., December, 1971, 412 pp.

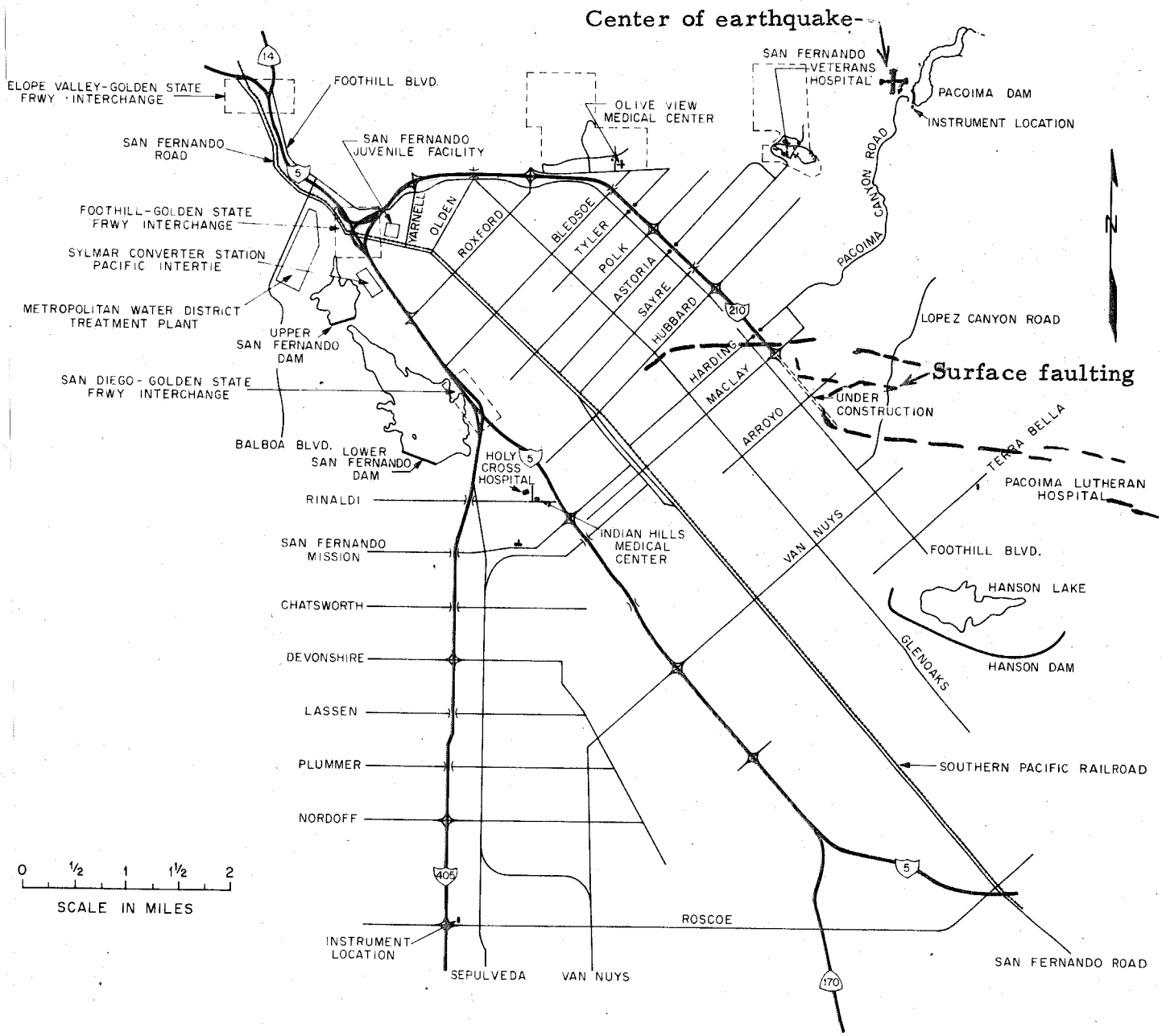

NORTHERN SAN FERNANDO VALLEY

*Figure 1 — The area of San Fernando Valley that was most seriously affected by the 9 February 1971 earthquake, and the facilities most severely damaged are shown on this map. The San Fernando Valley forms the northern part of the metropolitan Los Angeles area.

*(Because of space limitations, only a few photographs will appear in the paper as published in the Proceedings of 5WCEE. Additional photographs of damage are shown here to present a more complete picture of the event).

Figure 2 — Fractured column at Olive View Hospital.

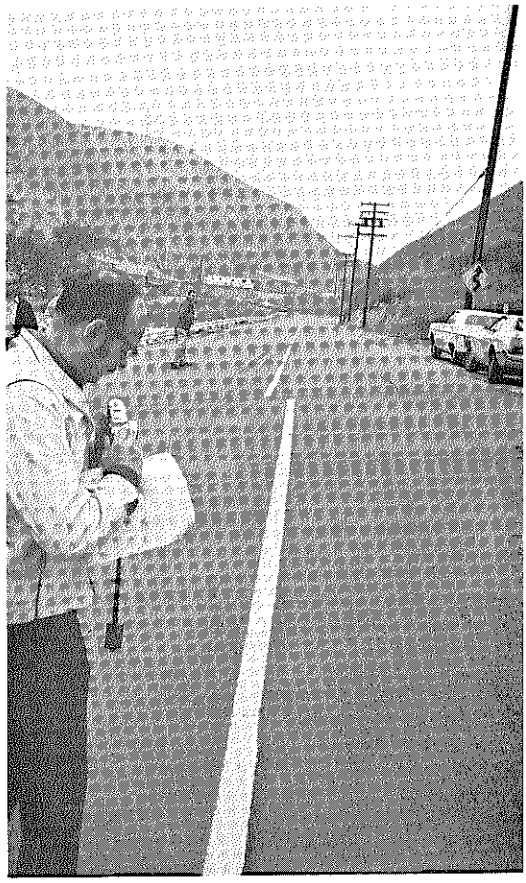

Figure 3 — White line in roadwa displaced by fault movement.

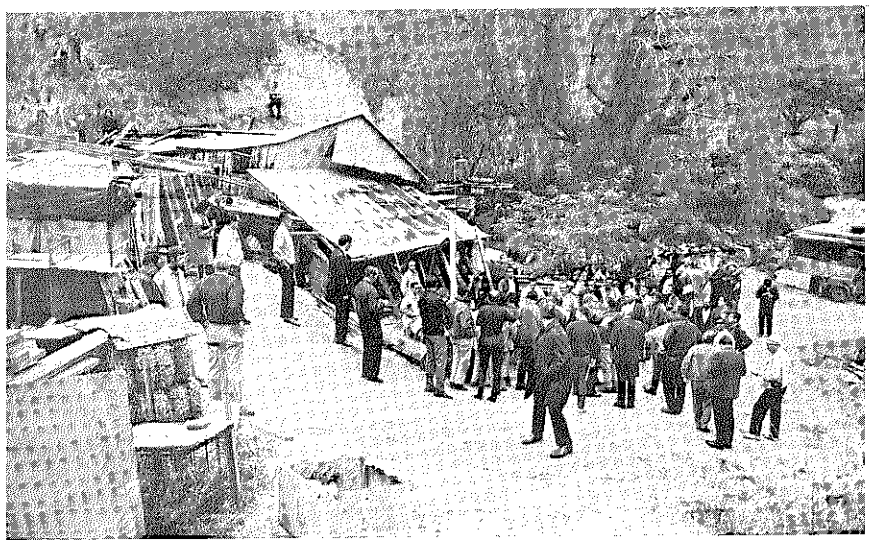

Figure 4 — Fault displacement in floor of canyon that was originally level.

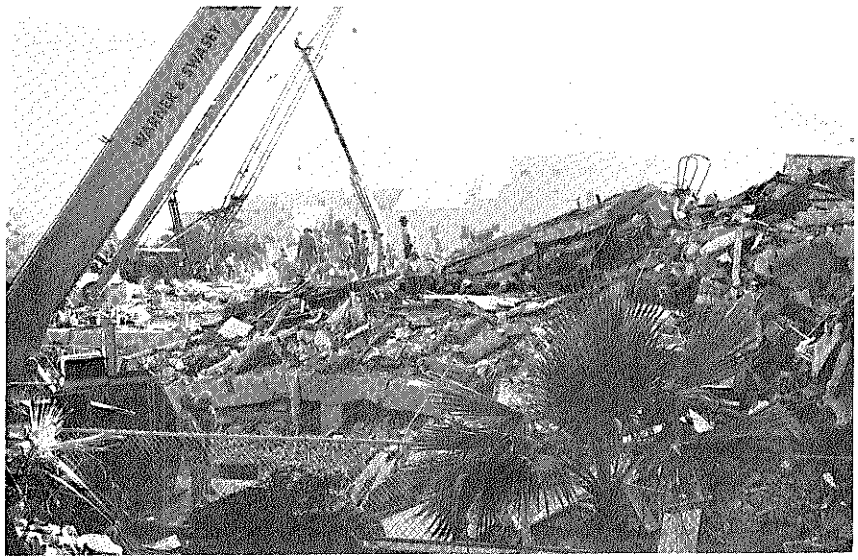

Figure 5 — Collapsed building at Veterans Administration Hospital. This building, constructed in 1928, had not been designed to resist earthquakes. Forty-nine persons lost their lives in this collapse.

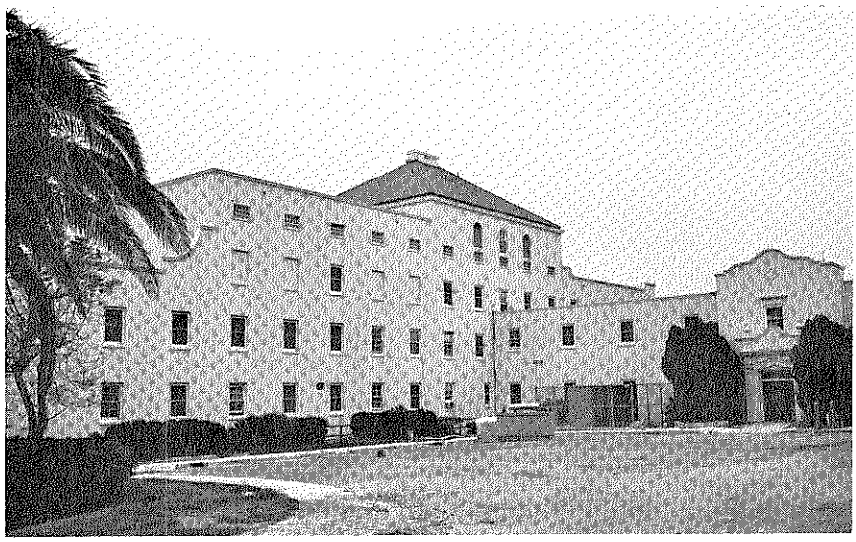

Figure 6 — Reinforced concrete building at Veterans Administration Hospital, constructed to resist earthquakes, survived the ground shaking with no significant damage.

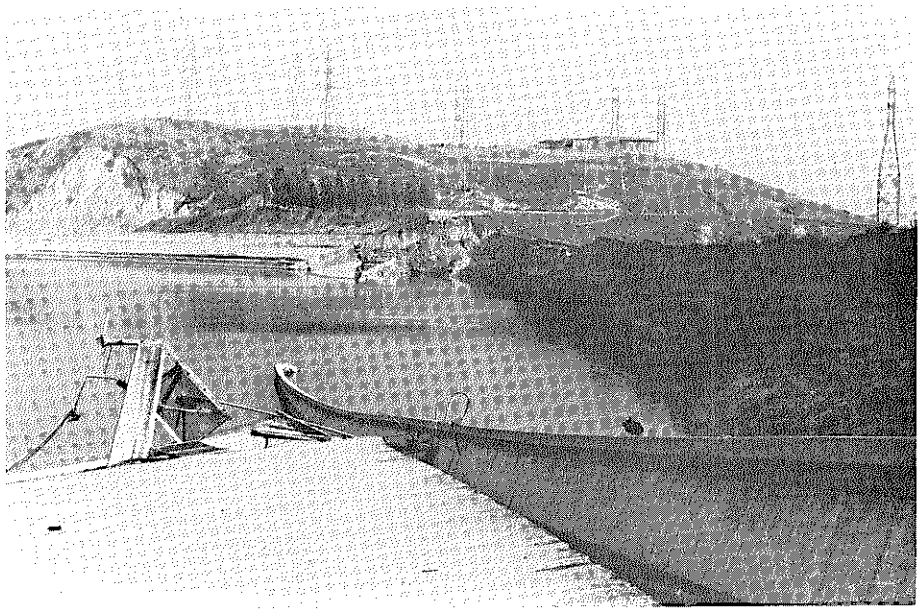

Figure 7 — Lower San Fernando Dam failed during the earthquake. The front face of the dam failed along a slip circle, but the remainder of the dam continued to retain the water.

Figure 8 — Upper San Fernando Dam started to fail during the earthquake. The crest of the dam moved downstream five feet as evidenced by the collapse of the access bridge to the intake tower.

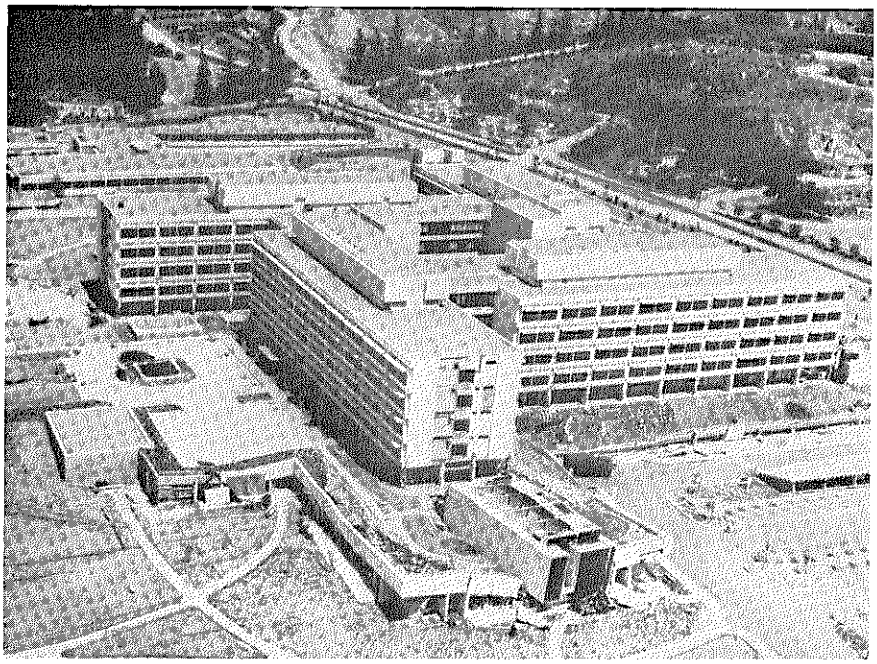

Figure 9 — New Olive View Hospital building was severely damaged by the earthquake. Three of the four independent stair towers were pushed over by the large amplitude motions of the main building.

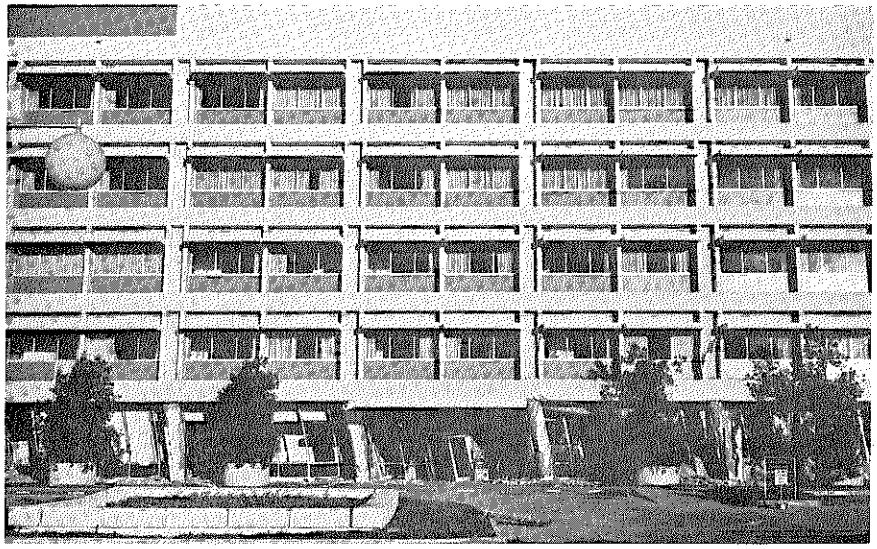

Figure 10 — West elevation of the main Olive View Hospital building.

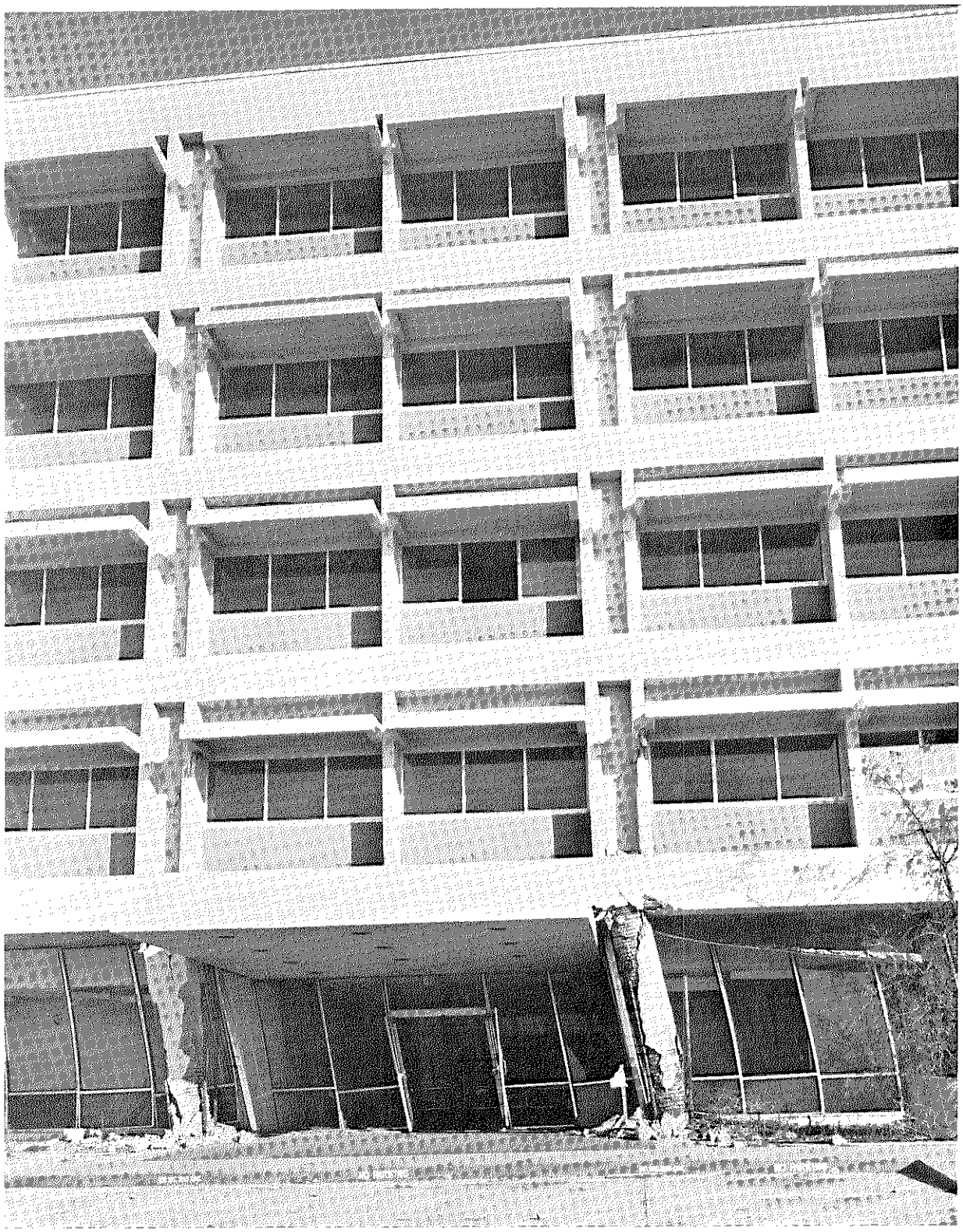

Figure 11 — West elevation of Olive View Hospital building. The spirally-reinforced concrete columns underwent large deformations but still continued to support the weight of the building.

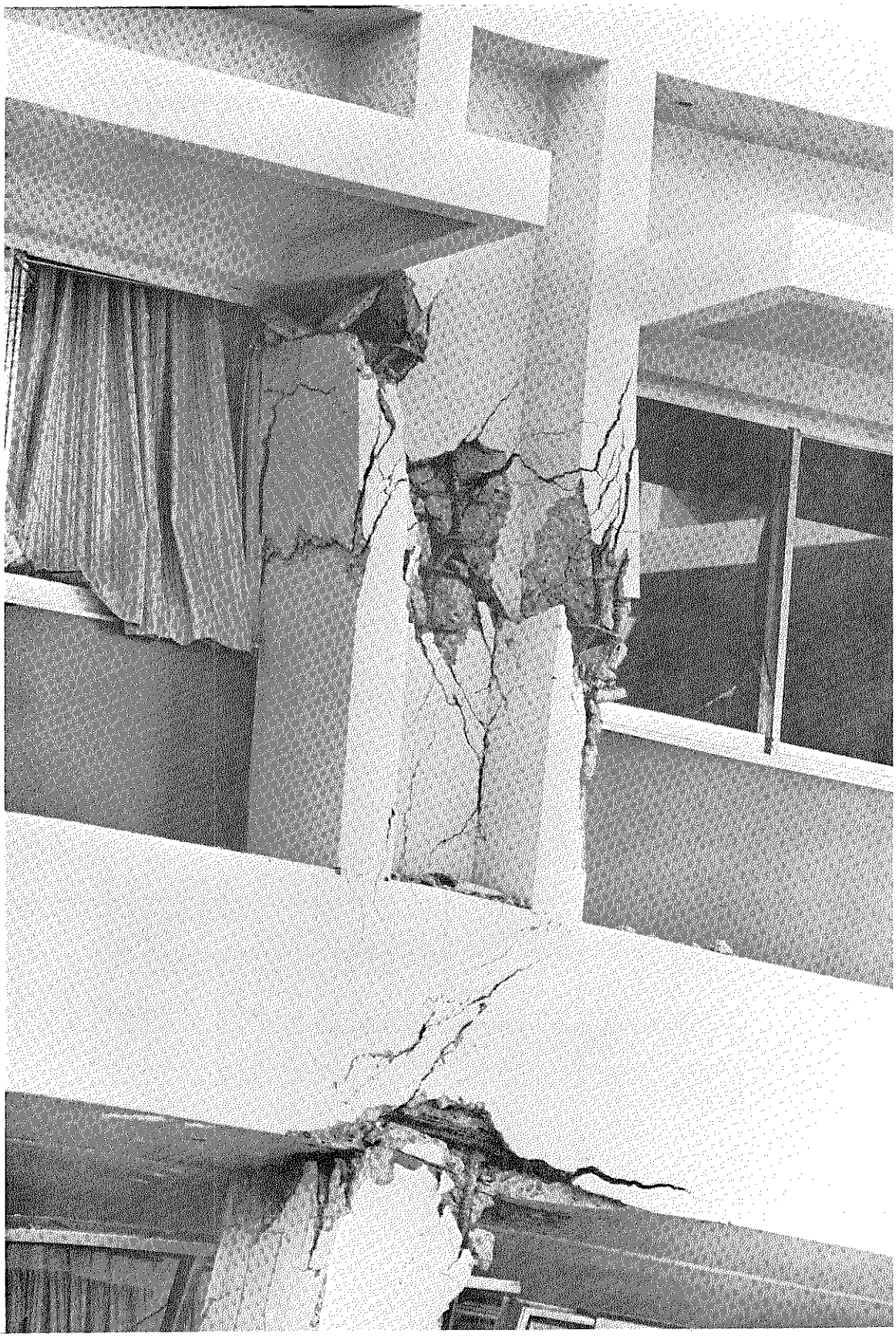

Figure 12 — Fractured second-story column of main Olive View Hospital building is evidence of large alternating shear forces during the earthquake.

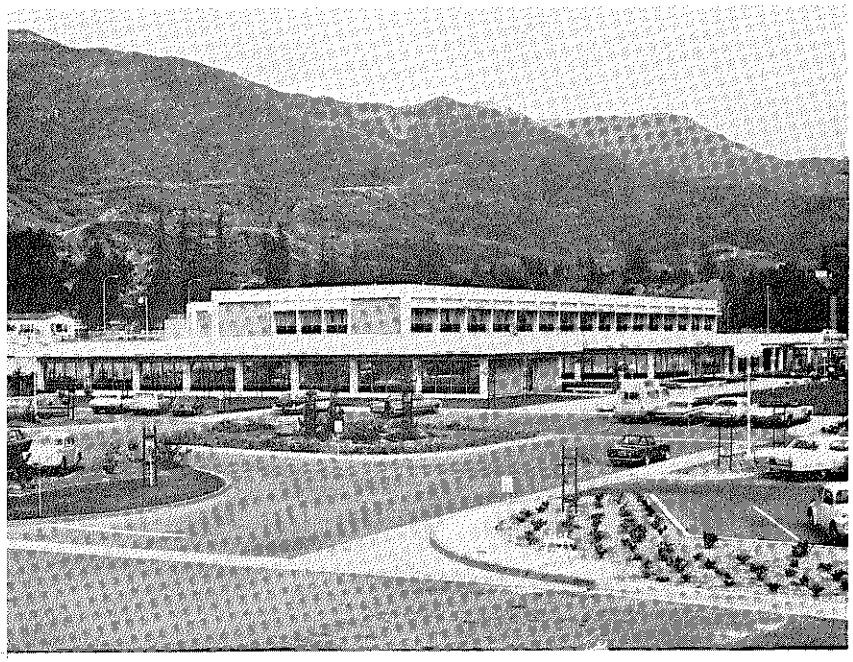

Figure 13 — Psychiatric building at Olive View Hospital before the earthquake.

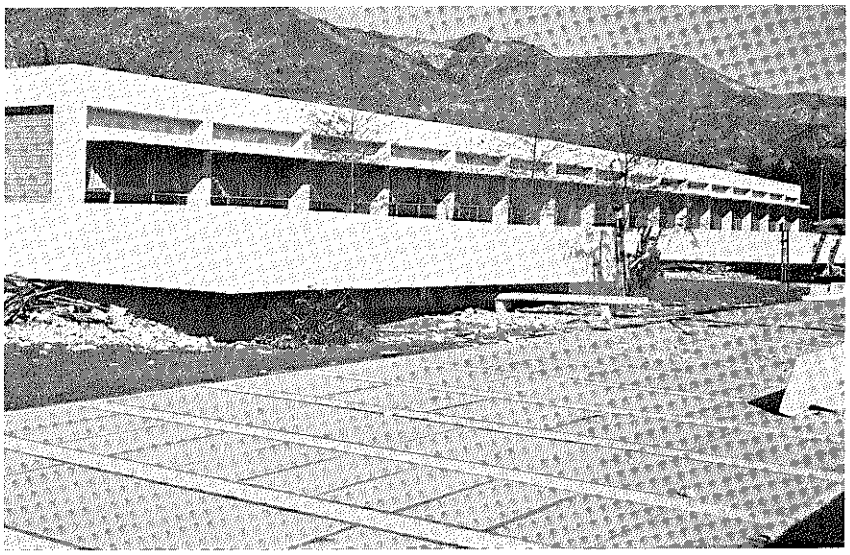

Figure 14 — Psychiatric building after the earthquake. The first story of the building collapsed completely.

Figure 15 — Old buildings, not constructed to resist earthquakes were severely damaged by the strong ground shaking.

Figure 16 — Old masonry buildings were very hazardous to passers-by as well as to those within.

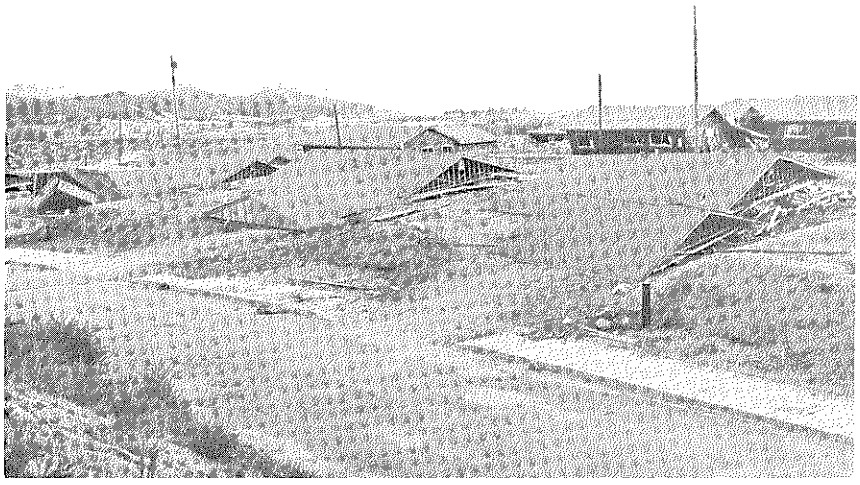

Figure 17 — Wood frame houses in various stages of construction suffered different degrees of damage during the earthquake.

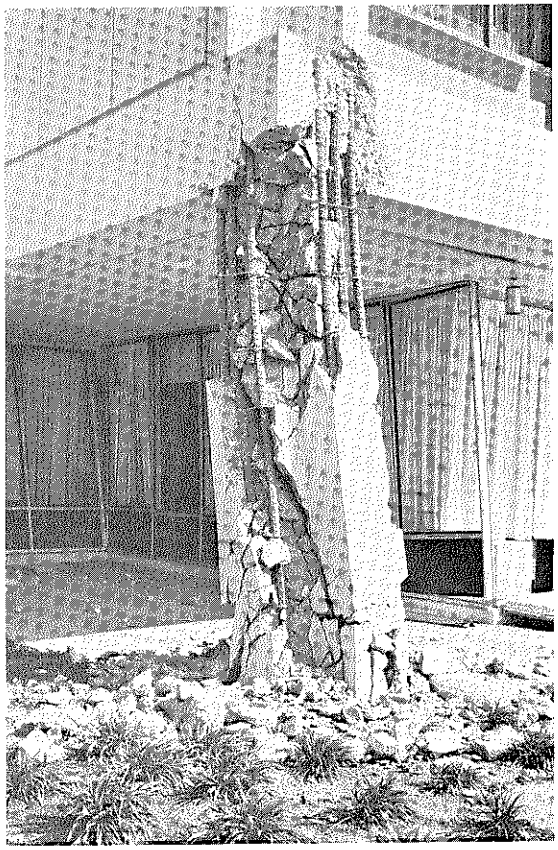

Figure 18 — Fractured corner column of main Olive View Hospital building had inadequate steel ties.

Figure 19 — Collapse of library bookshelves at California Institute of Technology.

Figure 20 — Five highway bridges in the region of very strong shaking collapsed.

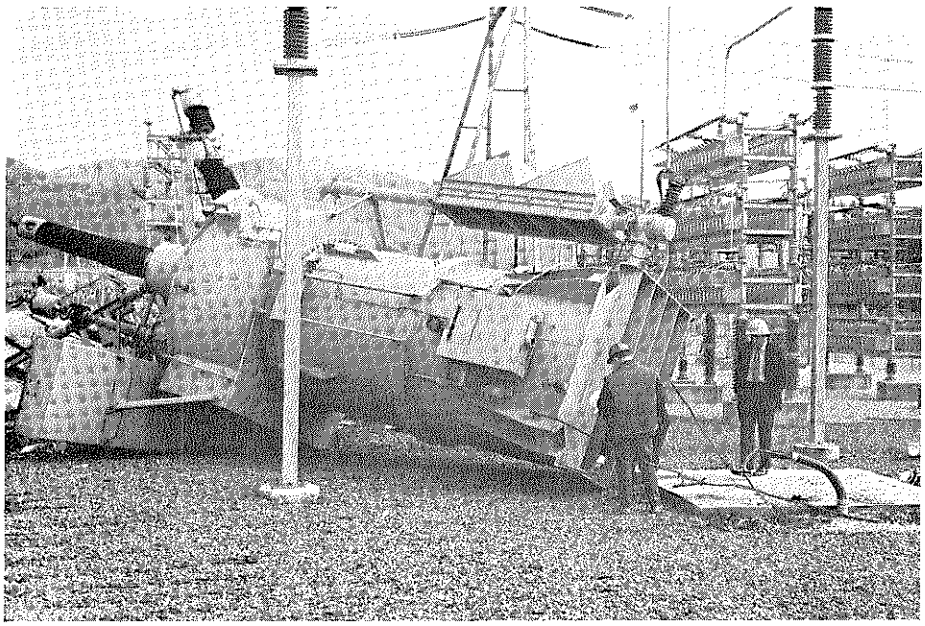

Figure 21 — Electrical transformers toppled during the earthquake because they were not anchored securely to the foundation.

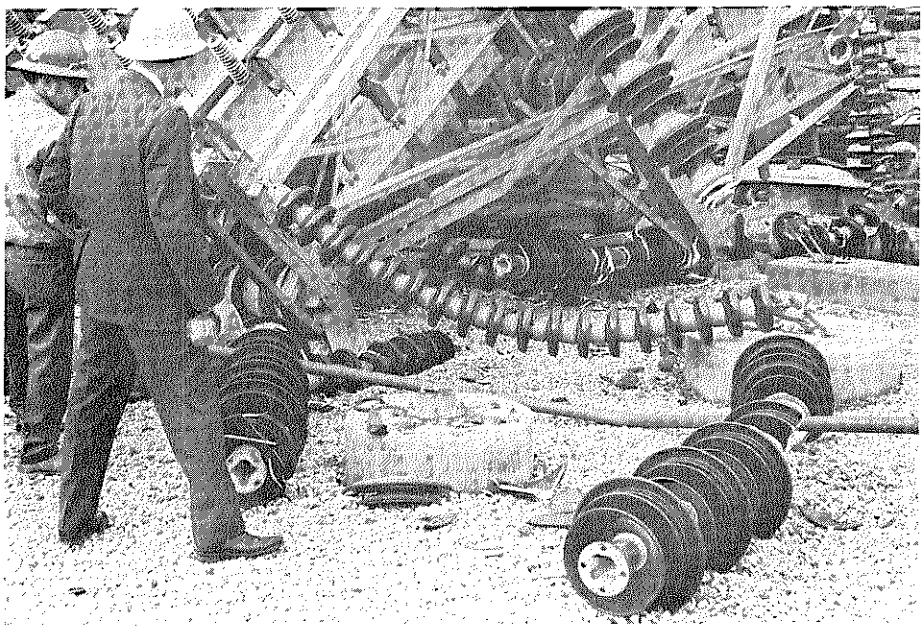

Figure 22 — Much damage was sustained by electrical equipment that had not been designed to withstand such strong vibrations.

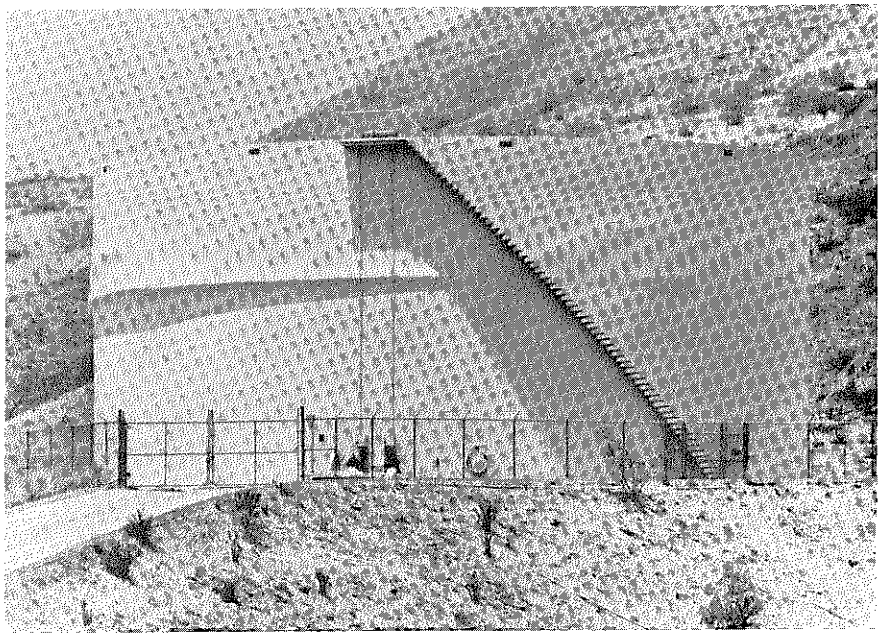

Figure 23 — The Sesnon water tank in Sylmar had been designed for earthquake forces, but sustained a buckle where there was a change in plate thickness.

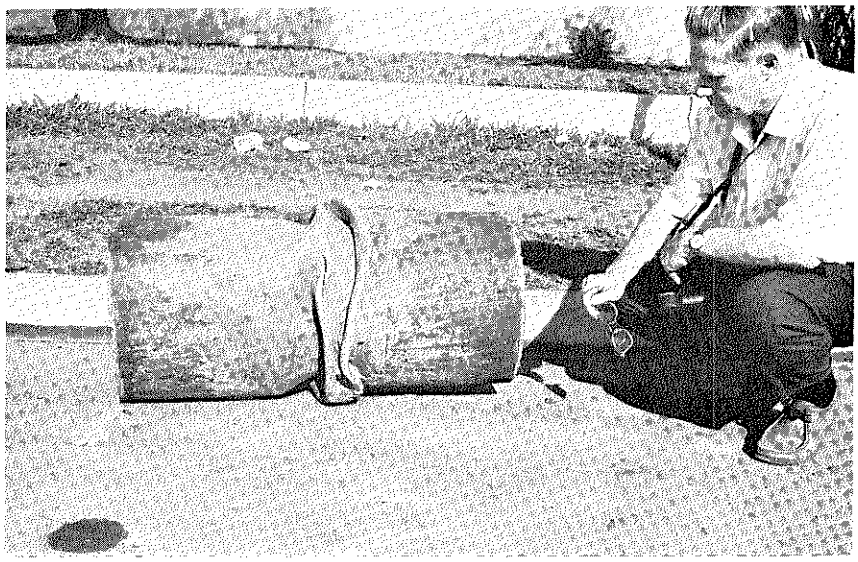

Figure 24 — Extensive ground deformation in the general region of surface faulting damaged underground pipes. The pipe shown is a 16-in. diameter, 1/4-in. thick, gas pipe that was buckled by compressive deformation. This pipe had been buried 6 ft. beneath the street.